

Anno accademico 2023/2024



UNIVERSITÀ  
DEGLI STUDI  
DI BRESCIA

UNIVERSITÀ DEGLI STUDI DI BRESCIA

Dottorato ricerca in

INGEGNERIA CIVILE, AMBIENTALE, DELLA COOPERAZIONE INTERNAZIONALE  
E DI MATEMATICA

Settore scientifico disciplinare

ICAR/03 INGEGNERIA SANITARIA -AMBIENTALE

Ciclo  
XXXVI

Titolo della tesi

Optimizing the Thermal Treatment for Sustainable Hazardous Waste Management and Soil  
Remediation

Nome del dottorato dell'ultimo anno

Roya Biabani Reshtehroudi

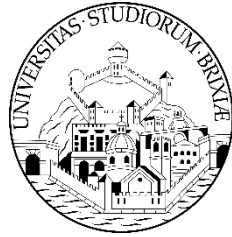
Nome del supervisore

Mentore Vaccari (Professore Associato in Ingegneria Sanitaria e Ambientale, Università degli Studi di Brescia, Dipartimento di Ingegneria Civile, Architettura, Territorio e Ambiente, Via Branze 38, 25123 Brescia, Italia)

Nome del co-supervisore

Pierro Ferrari (Senior Manager, Ricerca e Innovazione presso Brixambiente Srl, Via Molino Emili 22, Maclodio, Italia)

Academic year 2023/2024



UNIVERSITÀ  
DEGLI STUDI  
DI BRESCIA

UNIVERSITÀ DEGLI STUDI DI BRESCIA

PhD IN

CIVIL, ENVIRONMENTAL, INTERNATIONAL COOPERATION AND  
MATHEMATICAL ENGINEERING

Scientific and disciplinary sector

ICAR/03 INGEGNERIA SANITARIA -AMBIENTALE

Cycle  
XXXVI

Dissertation title

Optimizing the Thermal Treatment for Sustainable Hazardous Waste Management and Soil  
Remediation

Name of the final year PhD student

Roya Biabani Reshtehroudi

Supervisor's name

Mentore Vaccari (Associate Professor in Sanitary and Environmental Engineering, University  
of Brescia, Department of Civil Engineering, Architecture, Land and Environment, Via  
Branze 38, 25123 Brescia, Italy)

Co-supervisor's name

Piero Ferrari (Senior Manager, Research and Innovation at Brixambiente Srl, 22 Via Molino  
Emili, Maclodio, Italy)

## **DEDICATION**

This thesis is dedicated to my beloved. Without the support of you this work could not have been possible. You helped me find the strength to continue at times I thought I had none.

Thank you from the bottom of my heart.

## **ACKNOWLEDGEMENTS**

I cannot claim full credit for this project without recognizing the mentorship of Professor Mentore Vaccari. His unwavering support and patience were indispensable for the completion of this work, and I am truly grateful for the opportunity to work under his guidance.

I also want to express my appreciation to Brixambiente Srl for their continuous support and the use of their facilities during my tenure with the company. This research was funded through a grant from the company.

Roya

## **Abstract**

The escalation of industrialization and urbanization has led to a significant upsurge in solid hazardous waste production, posing intricate and costly challenges for governments, industries, and communities. These hazardous wastes, including industrial byproducts, chemicals, and materials, present grave risks to the environment and public health due to their potential for contaminating soil and groundwater. Contaminated soils are a growing environmental concern, categorized as waste due to the peril they pose. This necessitates stringent management and remediation measures to mitigate their detrimental effects. Governments and international bodies have established stringent regulations for proper waste management and soil remediation, reflecting the global shift toward resource conservation and sustainability. Thermal treatment technologies, capable of converting waste into energy or secondary raw materials, play a pivotal role in this endeavour. Advances in these technologies have made it possible to process hazardous waste and contaminated soils efficiently and safely. However, challenges like emissions control and residue management must be addressed. The efficiency of thermal treatment processes relies on a complex interplay of operating conditions and control parameters, underscoring the importance of understanding their impact on waste management and environmental remediation.

In the scope of this study, efficiency in thermal treatment processes is explored through operational parameter optimization, including heating time and temperature. Experiments involving one inorganic waste type and two organic waste types were conducted to mitigate reactivity of inorganic hazardous waste and reduce concentration of persistent organic pollutants, such as polychlorinated biphenyls and banned pesticides, in contaminated soil samples.

## **Riassunto**

L'escalation dell'industrializzazione e dell'urbanizzazione ha portato a un significativo aumento della produzione di rifiuti pericolosi solidi, presentando sfide intricate e costose per governi, industrie e comunità. Questi rifiuti pericolosi, compresi sottoprodotti industriali, sostanze chimiche e materiali, rappresentano gravi rischi per l'ambiente e la salute pubblica a causa della loro potenziale contaminazione del suolo e delle acque sotterranee. I suoli contaminati sono una crescente preoccupazione ambientale, categorizzati come rifiuti a causa del pericolo che rappresentano. Ciò richiede rigorose misure di gestione e rimedio per mitigare i loro effetti dannosi. Governi e organismi internazionali hanno stabilito rigorose normative per la corretta gestione dei rifiuti e la bonifica del suolo, riflettendo il cambiamento globale verso la conservazione delle risorse e la sostenibilità. Le tecnologie di trattamento termico, capaci di convertire i rifiuti in energia o materie prime secondarie, svolgono un ruolo centrale in questo sforzo. Gli avanzamenti in queste tecnologie hanno reso possibile trattare in modo efficiente e sicuro i rifiuti pericolosi e i suoli contaminati. Tuttavia, è necessario affrontare sfide come il controllo delle emissioni e la gestione dei residui. L'efficienza dei processi di trattamento termico si basa su una complessa interazione di condizioni operative e parametri di controllo, sottolineando l'importanza della comprensione del loro impatto sulla gestione dei rifiuti e sulla bonifica ambientale.

Nell'ambito di questo studio, l'efficienza nei processi di trattamento termico è esplorata attraverso l'ottimizzazione dei parametri operativi, compresi il tempo e la temperatura di riscaldamento. Sono stati condotti esperimenti che coinvolgono un tipo di rifiuto inorganico e due tipi di rifiuti organici per mitigare la reattività dei rifiuti pericolosi inorganici e ridurre la concentrazione di inquinanti organici persistenti, come policlorobifenili e pesticidi vietati, nei campioni di suolo contaminato.

## Table of Contents

|  |    |
|--|----|
| DEDICATION.....  | 3  |
| ACKNOWLEDGEMENTS.....  | 4  |
| Abstract.....  | 5  |
| Chapter 1: Introduction.....   | 17 |
| 1.1. European Waste Regulations and Reactive Aluminium Powders.....  | 18 |
| 1.2. Regulatory Framework and Criteria for Sites of National Interest (SIN) in Italy: SIN Brescia-Caffaro.....                         | 21 |
| 1.3. Assessment of Organochlorine Pesticides (OCPs): Ubiquitous Presence, Environmental Impact, and Regulatory Considerations.....     | 25 |
| 1.4. Research objectives and originality of the contribution.....  | 27 |
| 1.4.1. Aluminium alloy waste powders.....  | 28 |
| 1.4.2. Soils contaminated with PCBs.....   | 28 |
| 1.4.3. Soils contaminated with pesticides.....   | 28 |
| Chapter 2: Literature Review.....  | 30 |
| 2.1. Introduction.....   | 31 |
| 2.2. A Sustainable Approach to European Waste Management: Prioritizing the Waste Hierarchy and Thermal Treatment.....                  | 33 |
| 2.3. Managing Hazardous Waste in Europe: Challenges, Treatment Methods, and Environmental Impacts.....                                 | 34 |
| 2.3.1. High-temperature oxidation of Aluminium.....  | 36 |
| 2.3.2. Aluminium alloy powder waste.....   | 39 |
| 2.4. Addressing Soil Pollution: Regulatory Frameworks, Environmental Impacts, and Sustainable Remediation Strategies.....              | 42 |
| 2.4.1. Persistent organic pollutants (POPs): Regulatory Frameworks, Environmental Impacts, and Sustainable Remediation Strategies..... | 44 |
| 2.4.2. Evolution of remediation approaches.....  | 49 |
| 2.4.3. Undesirable effects of thermal desorption remediation on soil properties.....   | 50 |
| 2.5. Scope and Objectives.....   | 61 |
| Chapter 3: Materials and Methods.....  | 63 |
| Overview.....  | 64 |

|   |     |
|---|-----|
| 3.1. Aluminium alloy waste powders.....   | 65  |
| 3.1.1. Unreacted aluminium measurement.....   | 67  |
| 3.1.2. TGA test.....  | 68  |
| 3.1.3. Tubular furnace simulation experiments.....                                  | 68  |
| 3.2. Soils contaminated with persistent organic pollutants.....                     | 69  |
| 3.2.1. PCB-contaminated soil.....   | 69  |
| 3.2.2. Soil contaminated by pesticides.....   | 74  |
| Chapter 4: Results and Discussion.....  | 75  |
| 4.1. Aluminium alloy waste powders.....   | 76  |
| 4.1.1. Basic characteristics of the samples.....                                    | 76  |
| 4.1.2. Hydrogen generation capacity of the raw samples.....                         | 79  |
| 4.1.3. Thermal reaction characteristics of the tested samples.....                  | 81  |
| 4.1.4. Pre-treatment simulation experiment of the samples in a tubular furnace..... | 85  |
| 4.1.5. Suggestions for handling and storage of the samples.....                     | 94  |
| 4.2. PCB-contaminated soil.....   | 95  |
| 4.2.1. TG results.....  | 95  |
| 4.2.2. Experimental Simulation of PCB-Contaminated Soil Treatment Processes.....    | 100 |
| 4.3. Pesticides-contaminated soil.....  | 104 |
| 4.3.1. TG results.....  | 104 |
| 4.3.2. Analysis of pesticide-contaminated soil reaction kinetics.....               | 106 |
| 4.3.4. Treatment simulation experiment of pesticide-contaminated soil.....          | 111 |
| Conclusions.....  | 116 |
| Bibliography.....   | 123 |



## Table of Figures

|   |    |
|---|----|
| Figure 1. 1 Italian contaminated sites of national interest (SIN) .....   | 23 |
| Figure 1.2 Perimeter Definition of the Brescia-Caffaro Site of National Interest (DM 24 February 2003) .....  | 24 |
| Figure 2. 1 a) The evolution of remediation approaches to environmental during last decades; b) Core Elements of Green Remediation .....  | 50 |
| Figure 2. 2 Different soil organic matter (SOM) types and their decomposition temperatures and the reduction of SOM across a range of temperatures, with each panel corresponding to heating duration ( (González-Pérez, et al., 2004); (Schulten & P., 1999))..... | 55 |
| Figure 2. 3 Average temperature threshold at which the dehydroxylation occurs for different soil mineralogy ( (González-Pérez, et al., 2004); (Schulten & P., 1999)).....   | 56 |
| Figure 2. 4 Reduction of clay-sized particles vs. heating time and temperature ( (Borchardt, 1989); (Dixon, 1989); (Fanning, et al., 1989)).....  | 56 |
| Figure 2. 5. BMPs evaluation result of thermal desorption remediation techniques. ....  | 60 |
| Figure 3. 1 Schematic diagram for the experimental systems; (a) Gas volume measurement system; (b) Tubular furnace  | 69 |
| Figure 3. 2 (a) Investigations on irrigation ditch sediments: spatial trend of PCBs; (b) PCB contaminated soils downstream Caffaro S.p.A. (Caso Caffaro: La Guida al cittadino dell'Asl di Brescia, 2013) .....   | 70 |
| Figure 3. 3 Concentration of the PCB congeners; (b) Concentration of PCDD and PCDF congeners.....   | 71 |
| Figure 3. 4 The contamination level and threshold for the different pesticides listed in Italian Legislative Decree n. 152/2006.....  | 74 |
| Figure 4. 1 SEM characterization of the tested samples: (a) the S1; (b) the S2; (c) the S3; (d) the S4; (e) the S5; (f) particle size distribution of the tested samples.....   | 78 |

|   |     |
|---|-----|
| Figure 4. 2 (a) hydrogen production of different samples over an hour; (b) temperature change during the reaction of aluminium and alkaline water; (c) hydrogen generation rate during the reaction of aluminium and alkaline water .....   | 81  |
| Figure 4. 3 TGA/DTA curves of (a) the S1; (b) the S2; (c) the S3; (d) the S4; (e) the S5 .....  | 84  |
| Figure 4. 4 The ignition and combustion phenomena of the samples; a) the S1 at 500 °C; b) the S2 at 500 °C; c) the S3 with additive 1:4 (w:w) at 525 °C; d) the S4 at 500 °C; e) the S5 without additive at 500 °C; f) the S5 with additive 1:2 at 525 °C.....  | 86  |
| Figure 4. 5 The reactivity reduction and hydrogen production of pre-treated products vs. heating time at different set temperatures; (a and b) the S1; (c and d) the S2; (e and f) the S3; (g and h) the S4; (i and j) the S5 .....   | 91  |
| Figure 4. 6 Typical XRD result for the investigated powders; (a) the S1; (b) the S2; (c) the S3; (d) the S4; (e) the S5 .....   | 92  |
| Figure 4. 7 The SEM images of the pre-treated samples in the furnace; (a) the S1 treated at 475°C for 4 min; (b) the S2 treated at 475°C for 4 min; (c) the S3 with additive (1:4) treated at 525 °C for 5 min; (d) the S4 treated at 525°C for 5 min; (e) the S5 with additive (1:2) treated at 525 °C for 10 min..... | 93  |
| Figure 4. 8 TGA/DTA curves under (a) air; (b) nitrogen .....  | 95  |
| Figure 4. 9 Verification of First-Order Reaction Assumption: Controlling Curve Analysis; a) aerobic condition; b) anaerobic condition.....  | 98  |
| Figure 4. 10 Calculation of reaction rate constant $k(T)$ .....   | 98  |
| Figure 4. 11 Removal efficiencies of PCBs for raw and thermally treated soil.....   | 100 |
| Figure 4. 12 Composition of PCB isomer groups in both untreated and thermally treated soil at 500°C for 20 min.....   | 102 |
| Figure 4. 13 Concentration of different PCDD/Fs congeners in the raw sample and the treated sample at 500°C for 20 min .....  | 103 |
| Figure 4. 14 Molecular geometry of a) Dieldrin; b) Aldrin; c) DDT; d) DDE; e) DDD .....   | 105 |
| Figure 4. 15 a) thermogravimetry and b) differential scanning calorimetry analysis of aldrin, dieldrin and DDT (liquid state).....  | 105 |
| Figure 4. 16 TGA/DTA curves of the tested sample (a) under air atmosphere; (b) under nitrogen atmosphere .....  | 106 |
| Figure 4. 17 Effect of heating rate on thermal behaviour of PCB-contaminated soil.....  | 109 |
| Figure 4. 18 Verification of first-order reaction assumption: controlling curve analysis; a) aerobic condition; b) anaerobic condition.....   | 109 |
| Figure 4. 19 Calculation of reaction rate constant $k(T)$ .....   | 110 |

Figure 4. 20 Removal Efficiency of Different Pesticides from Soil Samples at Various Temperatures and Residence Times (a) 5 min, (b) 10 min, (c) 15 min.....112

Figure 4. 21 Mass Spectrometry analysis of pesticide-contaminated soil; a) anaerobic conditions at 300 °C for 10 min; b) anaerobic conditions at 350 °C for 10 min; c) aerobic conditions at 300 °C for 10 min; d) aerobic conditions at 350 °C for 10 min .....114

## Table of Tables

|   |    |
|---|----|
| Table 2. 1 Substances currently listed in the relevant annexes to the POPs Regulation (European Chemical Agency, 2023).....   | 48 |
| Table 2. 2. Thermal treatment studies applied to contaminated soils separated based on contaminant.....   | 51 |
| Table 3. 1 Physicochemical properties of contaminated soil.....   | 72 |
| Figure 4. 1 SEM characterization of the tested samples: (a) the S1; (b) the S2; (c) the S3; (d) the S4; (e) the S5; (f) particle size distribution of the tested samples.....   | 78 |
| Figure 4. 2 (a) hydrogen production of different samples over an hour; (b) temperature change during the reaction of aluminium and alkaline water; (c) hydrogen generation rate during the reaction of aluminium and alkaline water.....  | 81 |
| Figure 4. 3 TGA/DTA curves of (a) the S1; (b) the S2; (c) the S3; (d) the S4; (e) the S5.....   | 84 |
| Figure 4. 4 The ignition and combustion phenomena of the samples; a) the S1 at 500 °C; b) the S2 at 500 °C; c) the S3 with additive 1:4 (w:w) at 525 °C; d) the S4 at 500 °C; e) the S5 without additive at 500 °C; f) the S5 with additive 1:2 at 525 °C.....  | 86 |
| Figure 4. 5 The reactivity reduction and hydrogen production of pre-treated products vs. heating time at different set temperatures; (a and b) the S1; (c and d) the S2; (e and f) the S3; (g and h) the S4; (i and j) the S5.....  | 91 |
| Figure 4. 6 Typical XRD result for the investigated powders; (a) the S1; (b) the S2; (c) the S3; (d) the S4; (e) the S5.....  | 92 |
| Figure 4. 7 The SEM images of the pre-treated samples in the furnace; (a) the S1 treated at 475°C for 4 min; (b) the S2 treated at 475°C for 4 min; (c) the S3 with additive (1:4) treated at 525 °C for 5 min; (d) the S4 treated at 525°C for 5 min; (e) the S5 with additive (1:2) treated at 525 °C for 10 min..... | 93 |
| Figure 4. 8 TGA/DTA curves under (a) air; (b) nitrogen.....   | 95 |
| Figure 4. 9 Verification of First-Order Reaction Assumption: Controlling Curve Analysis; a) aerobic condition; b) anaerobic condition.....  | 98 |
| Figure 4. 10 Calculation of reaction rate constant $k(T)$ .....   | 98 |

|   |     |
|---|-----|
| Figure 4. 11 Removal efficiencies of PCBs for raw and thermally treated soil.....   | 100 |
| Figure 4. 12 Composition of PCB isomer groups in both untreated and thermally treated soil at 500°C for 20 min.....   | 102 |
| Figure 4. 13 Concentration of different PCDD/Fs congeners in the raw sample and the treated sample at 500°C for 20 min.....   | 103 |
| Figure 4. 14 Molecular geometry of a) Dieldrin; b) Aldrin; c) DDT; d) DDE; e) DDD.....  | 105 |
| Figure 4. 15 a) thermogravimetry and b) differential scanning calorimetry analysis of aldrin, dieldrin and DDT (liquid state).....  | 105 |
| Figure 4. 16 TGA/DTA curves of the tested sample (a) under air atmosphere; (b) under nitrogen atmosphere.....   | 106 |
| Figure 4. 17 Effect of heating rate on thermal behaviour of PCB-contaminated soil.....  | 109 |
| Figure 4. 18 Verification of first-order reaction assumption: controlling curve analysis; a) aerobic condition; b) anaerobic condition.....   | 109 |
| Figure 4. 19 Calculation of reaction rate constant $k(T)$ .....   | 110 |
| Figure 4. 20 Removal Efficiency of Different Pesticides from Soil Samples at Various Temperatures and Residence Times (a) 5 min, (b) 10 min, (c) 15 min.....  | 112 |
| Figure 4. 21 Mass Spectrometry analysis of pesticide-contaminated soil; a) anaerobic conditions at 300 °C for 10 min; b) anaerobic conditions at 350 °C for 10 min; c) aerobic conditions at 300 °C for 10 min; d) aerobic conditions at 350 °C for 10 min..... | 114 |

## Table of Equations

|   |               |
|---|---------------|
| $2Al + 6H_2O \rightarrow 2Al(OH)_3 + 3H_2 + \text{Heat}$  | Equation 2. 1 |
| .....   | 40            |
| $2Al + 4H_2O \rightarrow 2AlO(OH) + 3H_2 + \text{Heat}$   | Equation 2. 2 |
| .....   | 40            |
| $2Al + 3H_2O \rightarrow Al_2O_3 + 3H_2 + \text{Heat}$  | Equation 2. 3 |
| .....   | 40            |
| Hot $H_2 + O_2(\text{air}) + \text{combustibles} \rightarrow \text{fire}$   | Equation 2. 4 |
| .....   | 40            |
| $Al(\text{Metal}) + (OH)(AQ)^{-1} + 3H_2O(\text{Liquid}) \rightarrow Al(OH)^{-1}_4(AQ)^{-1} + 3/2H_2(\text{Gas}) + \text{Heat}$ |               |
| Equation 2. 5 .....   | 40            |
| SOM Reduction = $1 - (\text{SOM}_{\text{Final}}/\text{SOM}_{\text{Initial}})$   | Equation      |
| 2. 6.....   | 54            |
| $2NaOH + 2Al + 2H_2O \rightarrow 2NaAlO_2 + 3H_2$   | Equation 3. 1 |
| .....   | 67            |
| $n_{H_2} = V/22400$   | Equation 3.   |
| 2.....  | 67            |
| $n_{Al} = n_{H_2}/1.5$  | Equation      |
| 3. 3.....   | 67            |
| $WAIS = 26.98(\text{gmol}) \times n_{Al}$   | Equation      |
| 3. 4.....   | 67            |
| $WAIP = WAIS \times WP/WS$  | Equation      |
| 3. 5.....   | 67            |
| $\eta = (WAI - WAIP)/WAI \times 100$  | Equation      |
| 3. 6.....   | 67            |
| $t_d = t_i - t_0$   | Equation 3. 7 |
| .....   | 69            |
| $2Al + N_2 \Delta 2AlN$   | Equation 4.   |
| 1.....  | 82            |

|   |             |
|---|-------------|
| $2\text{Al} + 3\text{ZnO} \rightarrow 3\text{Zn} + \text{Al}_2\text{O}_3$ | Equation 4. |
| 2.....  | 87          |
| $\frac{dx}{dt} = kTf(x)$  | Equation    |
| 4. 3.....   | 96          |
| $x = w_i - wt w_i - wf$   | Equation    |
| 4. 4.....   | 96          |
| $kT = A \exp(-E_a/RT)$  | Equation    |
| 4. 5.....   | 96          |
| $\frac{dx}{dt} = A \exp(-E_a/RT)f(x)$                                     | Equation    |
| 4. 6.....   | 96          |
| $\beta = dT/dt$   | Equation    |
| 4. 7.....   | 96          |
| $\beta = dT/dx \times dx/dt$  | Equation    |
| 4. 8.....   | 96          |
| $\frac{dx}{dT} = 1/\beta \frac{dx}{dt}$                                   | Equation    |
| 4. 9.....   | 96          |

|   |                |
|---|----------------|
| $\frac{dx}{dT} = A\beta \exp(-E_a/RT) x$                              | Equation       |
| 4. 10.....  | 96             |
| $\frac{dx}{x} = A\beta \exp(-E_a/RT) dT$                              | Equation       |
| 4. 11.....  | 97             |
| $G_x = 0 \Rightarrow \frac{dx}{x} f(x) = A\beta 0 T \exp(-E_a/RT) dT$ | Equation       |
| 4. 12.....  | 97             |
| $\ln(-\ln(1-x)) = \ln A R \beta E_a - \frac{2R T E_a - E_a}{R T}$     | Equation 4. 13 |
| .....   | 97             |
| $\ln(-\ln(1-x)) = -\frac{E_a}{R T} + \ln A R \beta E_a$               | Equation 4. 14 |
| .....   | 97             |
| $t_{1/2} = 0.693 k(T)$  | Equation       |
| 4. 15.....  | 98             |
| $E_a = \text{Slope} \times R$   | Equation       |
| 4. 16.....  | 99             |
| $A = \beta E_a R T^2 \exp(\text{Intercep of Eq. 4. 14})$              | Equation       |
| 4. 17.....  | 99             |
| $\Delta s = R \ln(A_h M T)$   | Equation 4.    |
| 18.....   | 99             |
| $\Delta H = E_a - RT$   | Equation 4. 19 |
| .....   | 99             |
| $\Delta G = \Delta H - T \Delta s$                                    | Equation 4. 20 |
| .....   | 99             |



# **Chapter 1: Introduction**

### **1.1. European Waste Regulations and Reactive Aluminium Powders**

The European Union's waste management policy is outlined in the Community Strategy for Waste Management and is enshrined in the Waste Framework Directive (75/442/EEC) (EC, 1975) and the accompanying Hazardous Waste Directive (91/689/EEC) (EC, 1991), along with a regulation on waste shipments (93/259/EEC) (EC, 1993). The Waste Framework Directive and the Hazardous Waste Directive have historically established a framework for waste management, comprising two sets of daughter directives: one addressing specific types of wastes and the other outlining requirements for permitting and operating waste disposal facilities. Another group of legal instruments focuses on the shipment of waste within, into, and out of the EU (EC, 2003).

While there are various approaches to classifying waste, it can be categorized by its origin (e.g., industrial, medical, nuclear waste), composition (e.g., glass, plastic, organic waste), the level of danger it poses (e.g., hazardous, non-hazardous, radioactive), or the way it is managed and treated (e.g., municipal, urban, landfilled waste). Each of these approaches results in a list of wastes, and often these definitions overlap, complicating the collection and

interpretation of waste data (UNEP, 2006). Article 3 of the Waste Framework Directive 2008/98/EEC (EC, 2008) defines waste as "any substance or object which the holder discards or intends or is required to discard." Article 2 specifies exclusions from the directive's scope, including gaseous effluents emitted into the atmosphere, wastewater, radioactive waste, and solid waste such as land (in situ), including unexcavated contaminated soil, uncontaminated soil, naturally occurring material from construction activities, decommissioned explosives, faecal matter, animal by-products, carcasses of animals, and waste resulting from extractive industries.

During the initial phase, a crucial task involves identifying the sources, types, and quantities of wastes generated in the designated area. While the European Waste Catalogue provides essential definitions for waste types, integral for various functions such as waste management regulation and control, its specificity renders it unsuitable for direct application in strategy development. Hence, it is imperative to employ a method that broadly groups and categorizes wastes. The Handbook on the Implementation of EC Environmental Legislation (EC, 2003) suggests the following waste categories for strategy development:

- Municipal solid waste (MSW): Encompasses household waste, waste similar to household waste from commercial premises, institutional wastes (schools, government offices, etc.), market wastes, and street/drain cleaning wastes.
- Garden and bulky waste.
- Hazardous wastes: Special wastes that, due to their toxic, infectious, irritant, explosive, flammable, or carcinogenic, teratogenic, or mutagenic effects, are or may be harmful to human health or the environment.
- Other industrial wastes: Wastes of industrial origin not requiring special methods of handling, treatment, and disposal. Many industrial wastes fall under this category, e.g., most construction wastes.
- Special wastes: Those requiring special methods of handling, treatment, and disposal due to their nature or quantity, driven by economic and/or environmental reasons in particular.
- Healthcare (hospital and clinical) wastes: A specific type of special waste, some of which must be considered obnoxious or potentially hazardous.

- Ash and slag from combustion processes: Typically associated with ash or slag from solid fuel-fired processes used for steam-raising and/or power production, some of which (e.g., fly-ash from waste incineration plants) may be potentially hazardous.
- Agricultural wastes: Particularly those originating from intensive cropping and livestock production.
- Sludge: Mainly from water and wastewater treatment.
- Mining wastes.

In EU legislation, the categorization of waste into hazardous and non-hazardous is grounded in the system for classifying and labelling dangerous substances and preparations. Initially, the characteristics defining waste as hazardous were established in Directive 91/689/EEC (EC, 1991) and were subsequently detailed in the Waste List Decision 2000/532/EEC (EC, 2000). As part of the ongoing evolution, Directive 91/689/EEC has been superseded by the latest Waste Framework Directive 2008/98/EC (EC, 2008). The term "hazardous waste" now refers to waste exhibiting one or more of the hazardous properties outlined in Annex III of the Waste Framework Directive 2008/98/EC.

According to the European Waste Catalogue adopted by Decisions (EU) N° 995/2014 and 1357/2014 of 18 December 2014 of the Council of the European Community, as amended by Decisions 2000/532/EC, machining sludges containing dangerous substances with 12 01 14\* code and waste blasting material containing dangerous substances with 12 01 16\* are classified as hazardous waste ( (EC, 2014a), (EC, 2014b)). Machining sludge and residues from blasting processes are by-products of metal finishing techniques, such as brushing, polishing, and sandblasting, applied to aluminium products to enhance their performance and longevity.

The reaction between aluminium and humidity or water has the potential to generate explosive hydrogen gas at high temperatures. The Centre for Chemical Process Safety of the American Institute of Chemical Engineers (Board, 2005) reported that 19% of explosion accidents, mainly involving aluminium powder explosions, are attributed to metal oxidation. Micron and nano-aluminium powders are commonly produced as by-products in various industries. The high reactivity and burn rates of aluminium powder can lead to fatal and devastating explosion accidents without adequate precautions. (Li, et al., 2016) systematically analysed the aluminium powder explosion accident in Kunshan on August 2, 2014. The incident resulted in significant damages, including 75 deaths, 185 injuries, and a direct

economic loss of 3.51 billion Yuan. This accident not only heightened public awareness of the risks associated with aluminium powder explosions but also spurred research on such explosions under special circumstances.

Aluminium particle exhibits a characteristic core-shell structure, featuring active Al surrounded by a dense Al<sub>2</sub>O<sub>3</sub> layer. Consequently, the oxidation of the Al particle involves the evolution of the oxidant, the alumina shell, and the active Al within. Moreover, the Al oxidation process is significantly influenced by factors such as the diffusion of the oxidant, the growth and rupture of the alumina shell, and the melting and gasification of the internal active Al.

The study aims to determine the applicability of the thermal desorption process for pretreatment of reactive Aluminium alloy powders and to define the optimal treatment time and temperature to reduce the reactivity of metallic powders. For this, the experimental tests were conducted at the laboratory of university of Brescia in Maclodia on a laboratory scale. The experimental tests utilized samples of reactive powders collected from industrial sites in northern Italy. The tests involved sample characterization, thermogravimetric analysis in nitrogen and air, and thermo-desorption tests under an air atmosphere.

## **1.2. Regulatory Framework and Criteria for Sites of National Interest (SIN) in Italy:**

### **SIN Brescia-Caffaro**

In Italy, the issue of contaminated sites was first addressed at a regulatory level with 'Ronchi Decree' n. 22 of 1997 (D.lgs. n. 22, 1997). Subsequently, the laws that defined the majority of Sites of National Interest (SINs) were 'Law No. 426 of 09/12/1998' and 'Law No. 179 of 31/07/2002.' Today, the reference directive is Legislative Decree 152/2006 (D.lgs. n. 152, 2006).

Sites of National Interest (SIN) represent areas that can be identified based on the characteristics of the site, the quantities and dangers of the pollutants present, the impact on the surrounding environment in terms of health and ecological risk, as well as damage to cultural and environmental property. These areas are defined by a specific decree of the Ministry of the Environment and Protection of Land and Sea (MATTM, now the Ministry of Ecological Transition, MiTE) on the basis of the criteria established by Article 252 of Legislative Decree 152/2006 (D.lgs. n. 152, 2006). They are characterized by particular

complexity and specific environmental and/or health problems, the procedures for which are the responsibility of the Ministry itself.

Legislative Decree 22/1997 (D.lgs. n. 22, 1997) (Ronchi Decree) was the first regulatory act that addressed this issue in Article 17, titled "Reclamation and Environmental Restoration of Polluted Sites," explored in detail in Ministerial Decree 471/1999 (D.M. n. 471, 1999) and fully incorporated in Legislative Decree 152/2006, under Article 252, titled "Sites of National Interest." The SINs, in their complexity, depict very large, contaminated areas classified as dangerous by the Italian State, requiring remediation of the soil, subsoil, and/or surface and underground waters to avoid damage to the environment and human health, as well as the risk to assets of historical and cultural interest and significant socio-economic impact.

Legislative Decree 152/2006, known as the "Consolidated Environmental Law," outlines the technical criteria and administrative procedures for contaminated sites in its article and the five annexes to Part IV, Title V. Article 252, titled "Sites of National Interest," in paragraphs 1, 2, and 3, delineates the classification criteria for a site of national interest, as follows:

1. Sites of national interest, for remediation purposes, can be identified based on the characteristics of the site, the quantities and dangers of pollutants present, the impact on the surrounding environment in terms of health and ecological risk, as well as damage to cultural and environmental assets.
2. Sites of national interest are identified by a decree of the Minister of the Environment and Protection of Land and Sea, in agreement with the involved Regions, according to the following guiding principles and criteria:
  - a. Reclamation interventions must concern areas and territories, including water bodies, of particular environmental value.
  - b. Reclamation must involve areas and territories protected pursuant to Legislative Decree 01/22/2004, number 42.
  - c. Health and environmental risks due to the detected exceeding of risk threshold concentrations must be particularly high, considering population density or the extension of the affected area.
  - d. The socio-economic impact caused by pollution in the area must be significant.

e. Contamination must constitute a risk for assets of historical and cultural interest of national importance.

f. Interventions should concern sites within the territory of multiple regions.

f-bis. The presence, current or past, of refinery activities, integrated chemical plants, or steel mills.

2-bis. In any case, sites affected by asbestos production and extraction activities are identified as sites of national interest for remediation purposes.

3. For the determination of the site's perimeter, encompassing various environmental matrices, including surface water bodies and related sediments, consultation occurs with Municipalities, Provinces, Regions, and other local bodies. This process ensures the participation of those responsible, as well as the owners of the areas to be reclaimed if different from the responsible subjects. The site-specific intervention values of the environmental matrices in marine areas, which define contamination levels necessitating intervention measures, are identified through a non-regulatory decree of the Ministry of Ecological Transition. This occurs upon the proposal of the Higher Institute for Environmental Protection and Research (ISPRA) (Art b37, paragraph 1, letter (h), of Law Number 108 of 2021).

With these criteria and procedures, MATTM identified 57 sites throughout the national territory (Figure 1. 1), of which 28 concern the coastal strip. The first regulations that identified most SINs were issued from 1998 with Law 426 of 09/12/1998 (D.lgs. n. 426, 1998) until 2002 with Law number 179 of 31/07/2002 (D.lgs. n. 179, 2002).

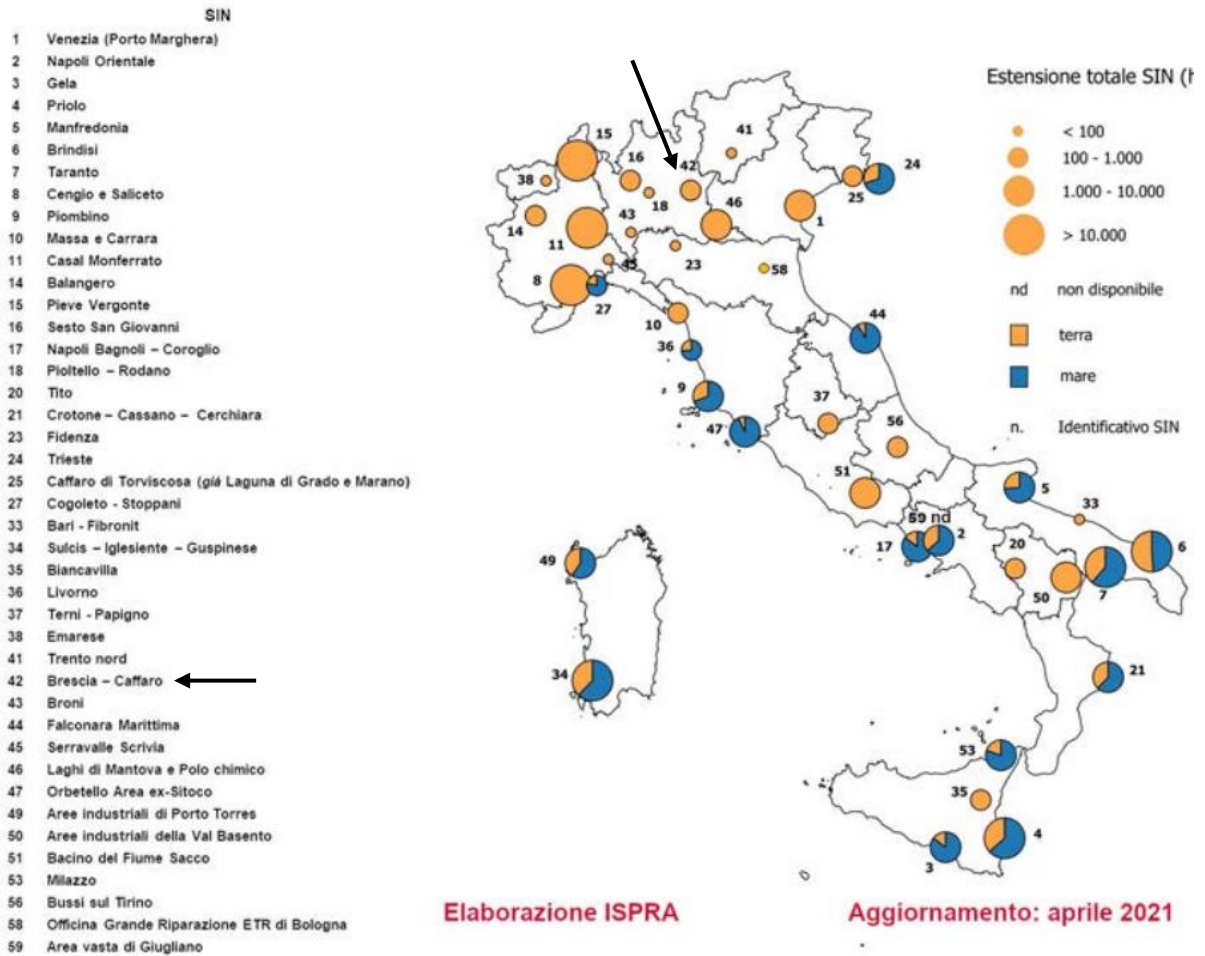


Figure 1. 1 Italian contaminated sites of national interest (SIN)

Legislative Decree number 179/2002 (D.lgs. n. 179, 2002) identified the Site of National Interest (SIN) 'Brescia – Caffaro (industrial areas and related landfills to be reclaimed)' as a remediation intervention of national interest. This designation was due to the high environmental risk conditions resulting from past industrial activities in the Caffaro factory area.

The SIN was delineated by Ministerial Decree on 24 February 2003 and establishes distinct perimeters for the land (approximately 262 hectares), including the canals (comprising a system of natural and artificial canals throughout the SIN area with a linear development of a few tens of kilometres), and for groundwater (approximately 2100 hectares) (Figure 1. 2). In cases where areas fall within the SIN perimeter for the groundwater matrix only, the responsibility for the remediation process concerning the soil/subsoil environmental matrix lies with the Municipality of Brescia.



The waters of the canals served as one of the mediums for the spread of pollution in the 'Brescia – Caffaro' Site of National Interest. The primary pollutants present, such as PCBs and PCDD/F dioxins, exhibit low solubility, and consequently, they were transported in the solid phase within the sediments. The initial characterization of the canals was carried out by the authorities (Municipality of Brescia - ARPA). Subsequently, the Caffaro company conducted further characterization through an agreement with the Municipality of Brescia.

Over time, farmers have engaged in cleaning the canals using manual shovels, depositing the removed material from the canal bottom onto the banks. This practice inadvertently facilitated the spread of contamination.

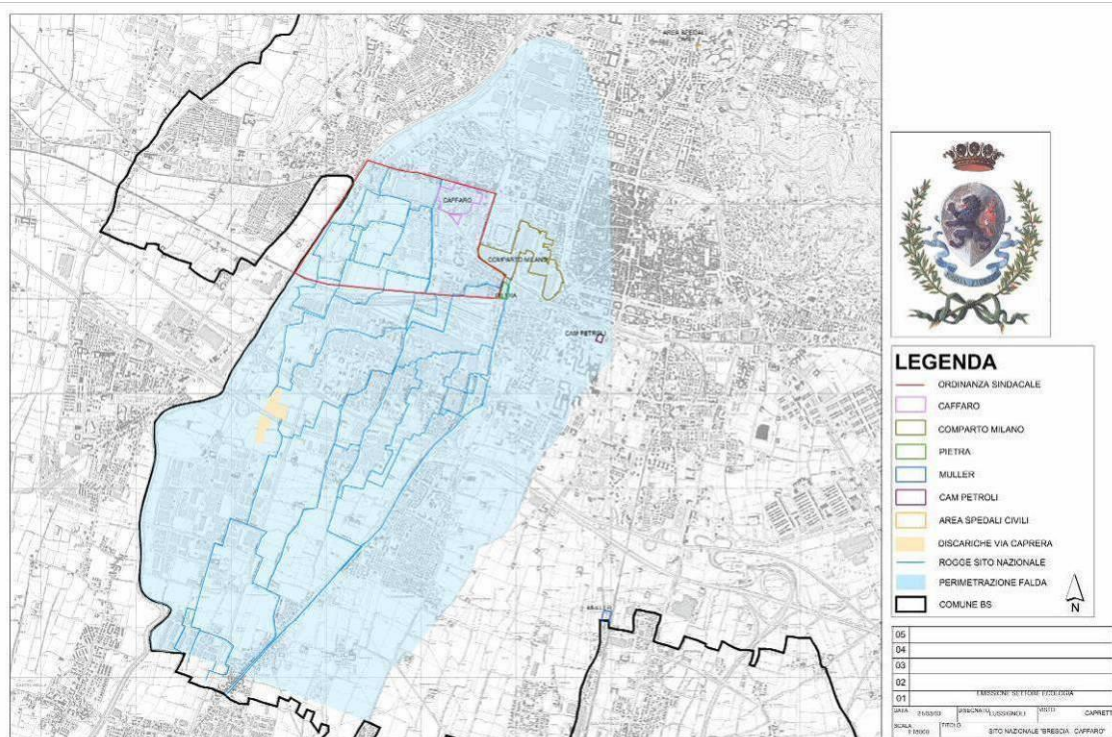


Figure 1.2 Perimeter Definition of the Brescia-Caffaro Site of National Interest (DECRETO 24 FEBBRAIO, 2003)

The various characterization campaigns of the canals were conducted with the aim of assessing the extent and depth of contamination. The numerous data acquired require specific evaluation, which is still underway by the competent authorities. However, the following general conclusions can be drawn:

- Brescia is dealing with a situation of widespread contamination distributed variably along the many kilometres of these waterways.
- Contamination is present both upstream and downstream of the Caffaro area, with downstream contamination values being significantly higher.
- Notably, this difference is evident for three contaminants analysed: mercury, polychlorinated biphenyls (PCBs), and PCDD/PCDF. Mercury values downstream are about an order of magnitude higher than upstream, for dioxins, this ratio rises to two orders of magnitude, while for PCBs, it can even reach three to four orders of magnitude.
- At greater depths (100-150 cm), this ratio tends to decrease, particularly concerning PCBs, until it reaches an average of two orders of magnitude.
- The extent and depth of pollution result in the presence of considerable contaminated volumes, making remediation and/or safety activities significantly challenging.

A more detailed analysis of the results can be obtained by referring to both the specific technical reports at the competent sector of the Municipality of Brescia and the results of the new investigations conducted by ARPA.

To address concerns regarding contaminated soils with persistent organic pollutants (e.g., PCBs and PCDD/Fs) in Brescia, this study aims to demonstrate the applicability of the thermal desorption process for eliminating these pollutants from the contaminated soil.

### **1.3. Assessment of Organochlorine Pesticides (OCPs): Ubiquitous Presence, Environmental Impact, and Regulatory Considerations**

The ethical quandary surrounding soil contamination and remediation initiatives has become increasingly notable in Italy since the 1990s, particularly in the wake of numerous industrial site disposals and the resulting implications tied to alterations in land use. Contamination frequently transcends industrial zones, infiltrating inhabited areas due to the diverse composition of the soil matrix and the transport of contaminants via water. This may lead to the migration of pollution to deeper subsoil layers or beyond the original boundaries of the contaminated site.

The study of organochlorine pesticides (OCPs) has recently gained attention due to their widespread presence, persistence, and tendency to accumulate in the environment, along with

their significant toxicity to both humans and non-target organisms (Jiang, et al., 2009.). These pesticides are typically divided into two categories based on their raw materials: those synthesized with benzene and those with cyclopentadiene. Aldrin, chlordane, dieldrin, endrin, and heptachlor, belonging to the class of chlorinated cyclodiene pesticides, were designated as part of the "dirty dozen" persistent organic pollutants (POPs) in the 2004 Stockholm Convention. Subsequently, technical endosulfan and its related isomers were added to the convention in May 2011. Hexachlorobenzene (HCB), DDT, and Lindane (g-HCH), the earliest and most widely used chlorobenzene pesticides, were successively classified as POPs by the Conference of the Parties of the Stockholm Convention on POPs (Zhang, et al., 2012). Although Italy has signed but not yet ratified the Stockholm Convention, and despite the ban on most OCPs' agricultural use in the 1970s, these agrochemicals persist in the soil, sediments, water, atmosphere, and organisms ( (Ferrante, et al., 2010) (Montuori, et al., 2014); (Pozo, et al., 2016); (Qu, et al., 2016)).

OCPs typically undergo degradation in the environment over time; however, owing to their persistent nature and attraction to organic matter, a significant amount of these chemicals may persist in soils (Zhang, et al., 2012). These OCPs have a tendency to accumulate in organisms and undergo biomagnification along the food chain (Naso, et al., 2003). The soil then becomes a source of reemission as the OCPs are released into the atmosphere (Tao, et al., 2008). Agricultural soils with a substantial OCP presence can be transported into surface water through farm drainage and runoff, and into groundwater through irrigation with sewage from farmlands (Montuori, et al., 2014). The environmental fate of OCPs in soils is influenced by various factors, with the physicochemical characteristics of agrochemicals (e.g., vapor pressure, water solubility), land use type, application history, and agricultural practices (e.g., flood irrigation, superphosphate application, and tilling), soil properties (e.g., organic carbon, pH, texture, and moisture content), as well as meteorological variables (e.g., temperature, wind direction) being perhaps the most crucial ( (Yu, et al., 2013); (Zhang, et al., 2011)). Consequently, soil plays a pivotal role in the circulation of these substances across different environmental sectors, but the behaviour and fate of OCPs in soils on a regional scale represent a complex process.

Therefore, this study aims to demonstrate the effectiveness of the ex-situ thermal desorption process for remediating soil contaminated with organochlorine pesticides. For this, sampling was conducted from a Northern Italian chemical company, specializing in the formulation of various agricultural products such as herbicides, fungicides, insecticides, fertilizers,

biological products, and biocides, that has been officially designated as a contaminated site. Prior to the prohibition of Organochlorine pesticides in Italy, this company produced pesticides and discharged contaminated wastewater into an industrial area, leading to soil contamination extending to a depth of 5 meters.

#### **1.4. Research objectives and originality of the contribution**

In the previous sections, we have discussed the challenges associated with the reactive aluminium powders and contaminated soils, particularly those contaminated with persistent organic pollutants (POPs) such as polychlorinated biphenyls (PCBs) and banned pesticides. Reactive aluminium powders lead many workspace risks specially in the aluminium surface treatment factories. Moreover, persistent organic pollutants pose significant risks to human health and the environment due to their persistence, bioaccumulation, and toxicity. In light of these challenges, thermal treatment processes have emerged as a promising alternative for the treatment of reactive metal powders and remediation of contaminated soils. This study focuses on the application of thermal process for the treatment of reactive aluminium powder and the remediation of contaminated soils containing PCBs and banned pesticides, using a lab-scale thermal treatment process.

In contrast to previous studies, this research did not involve testing pure aluminium powders; instead, we utilized authentic aluminium alloy powder samples sourced from companies specializing in aluminium surface treatment. Regarding the study on the effect of thermal treatment on contaminated soils with the mentioned POPs contaminants, the state of the art showed that previous studies reported the efficiency of thermal treatment only for one or two specific heating times and temperatures. Therefore, for a better understanding of the remediation process, a comprehensive study covering a wide range of heating times and temperatures' effects on remediation efficiency is needed. Last but not least, it is necessary to mention that this thesis project is an industry-based study, so the research goals were defined according to the priority and interests of the company. For this, this study employs a series of laboratory experiments, using a lab-scale furnace, to evaluate the effectiveness of thermal desorption under different conditions, including varying temperatures and treatment durations and different atmospheres. This approach allows for a thorough assessment of the optimal treatment conditions for reducing the concentration of the target contaminants in contaminated soils and for reducing the reactivity of the aluminium alloy powders.

The main research objectives are listed as follows:

#### **1.4.1. Aluminium alloy waste powders**

To the best of our knowledge, this study represents the first investigation into the efficacy of thermal desorption in mitigating the reactivity of reactive Aluminium alloy powders, which are considered waste. Here are the primary research objectives that we pursued in our study.

- To determine the optimal treatment time and temperature for thermal oxidation to achieve the desired reduction in reactivity.
- To analyse the changes in the physical and chemical properties of the metallic powders before and after thermal processes.
- To assess the impact of thermal treatment process on the mechanical properties and microstructure of the Aluminium alloy powders.

#### **1.4.2. Soils contaminated with PCBs**

By understanding the applicability and effectiveness of thermal desorption for the treatment of contaminated soils, this study aims to contribute to the development of innovative and efficient soil remediation technologies. Therefore, the objective of this study is to evaluate the effectiveness of thermal desorption in reducing the concentration of PCBs in the contaminated soils and to determine the optimal treatment conditions.

- To investigate the effectiveness of thermal treatment in reducing the concentration of polychlorinated biphenyls (PCBs) in contaminated soil.
- To determine the optimal temperature and duration of thermal treatment for achieving the desired reduction in PCB concentration.
- To assess the fate and transport of PCBs in soil during and after thermal treatment, including the potential for PCB re-release or transformation into more toxic compounds such as polychlorinated-p-dioxins (PCDDs) and the related furans (PCDFs).

#### **1.4.3. Soils contaminated with pesticides**

Soil contamination by banned pesticides poses significant environmental and health risks, necessitating effective remediation methods. Thermal desorption has emerged as a promising technology for reducing pesticide concentrations in contaminated soils. This study aims to evaluate the effectiveness of thermal desorption in reducing the concentration of banned pesticides in contaminated soils and to determine the optimal treatment conditions.

- To assess the efficacy of thermal desorption in reducing the concentration of banned pesticides in contaminated soils.
- To identify the optimal temperature and duration of thermal desorption for achieving the desired reduction in pesticide concentration.
- To investigate the fate and transport of pesticides in soil during and after thermal desorption, including the potential for pesticide re-release or transformation into more toxic compounds.

# **Chapter 2: Literature Review**

## **2.1. Introduction**

With industrialization and urbanization, the generation of solid hazardous wastes has increased significantly. Managing and treating these wastes have become complex and costly challenges for governments, industries, and communities. Solid hazardous wastes, which include various industrial byproducts, chemicals, and materials, pose a substantial risk to the environment and public health. These materials may contain toxic compounds, heavy metals, and other contaminants that can leach into the soil and groundwater, leading to long-term environmental degradation and potential health hazards. Moreover, contaminated soils are an increasingly pressing environmental concern, drawing attention due to their potential for adverse impacts on ecosystems and human health. These soils are categorized as waste primarily because they pose a significant threat to the environment and public well-being. Contamination can result from various sources, including industrial activities, agriculture, and improper disposal of hazardous substances. When soil becomes tainted with pollutants such as heavy metals, pesticides, or toxic chemicals, it can no longer perform its vital functions effectively, such as supporting plant growth or filtering water. Instead, it becomes a potential source of harm. This necessitates the classification of contaminated soils as waste, triggering specific management and remediation measures to mitigate their detrimental effects and safeguard our environment.

Over the years, governments and international organizations have developed strict regulations and guidelines for the proper management and disposal of hazardous wastes and remediation of contaminated soils. Compliance with these regulations is essential to prevent pollution and mitigate the risks associated with these types of wastes. In addition, the global push for resource conservation and sustainability has emphasized the importance of recovering valuable resources from waste materials. Thermal treatment technologies can play a role in achieving a circular economy by converting waste into usable energy or secondary raw materials. Advances in thermal treatment technologies have made it possible to efficiently and safely process solid hazardous wastes and contaminated soils. Thermal treatment processes can yield energy in the form of heat or electricity, which can offset energy consumption and reduce greenhouse gas emissions. This dual benefit of waste treatment and energy production is a key driver in the adoption of these technologies.

While thermal treatment offers several advantages, it is not without challenges. Emissions control, residue management, and the potential release of harmful pollutants are concerns that must be addressed for safe and sustainable waste treatment. The efficiency of thermal



treatment processes in waste management and environmental remediation is profoundly influenced by a complex interplay of operating conditions and control parameters. Thermal treatment methods, such as incineration, pyrolysis, and thermal desorption, have become integral in addressing the challenges of waste disposal and soil remediation, given their potential to effectively reduce the volume of waste, destroy hazardous compounds, and mitigate environmental contamination. However, achieving optimal efficiency in these processes is far from straightforward. It hinges on a delicate balance of factors like temperature, residence time, feedstock composition, and air flow rates, among others. Understanding how operating conditions and control parameters impact the efficiency of thermal treatment is not only essential for maximizing resource recovery and minimizing environmental impacts but also for ensuring the safety of these processes. In this context, this introduction delves into the critical role that operating conditions and control parameters play in shaping the outcomes of thermal treatment methods, highlighting their significance in achieving sustainable waste management and environmental remediation objectives.

The scope of this study encompasses the evaluation and enhancement of efficiency in thermal treatment processes through the optimization of operational parameters including heating time and temperature. To achieve this goal, thermal experiments were conducted using one inorganic waste type and two organic waste types. The inorganic waste comprises five samples obtained from the aluminium surface finishing industries. These samples have been categorized as hazardous waste under the EWC codes 12 01 14\* and 12 01 16\*, as defined in the European Waste Catalogue, as per Decisions (EU) N° 995/2014 and 1357/2014 issued on December 18, 2014, by the Council of the European Community, with modifications introduced by Decisions. This objective seeks to alleviate the reactivity of the samples, given that their reactivity can potentially result in the liberation of energy, such as in combustion or even explosions within a workspace.

On the flip side, through the application of elevated temperatures and controlled conditions, this research endeavours to attain a meaningful reduction, elimination, or alteration of organic persistent pollutants (e.g., polychlorinated biphenyls and banded pesticides) in contaminated soil samples.

## **2.2. A Sustainable Approach to European Waste Management: Prioritizing the Waste Hierarchy and Thermal Treatment**

The European waste management strategy emphasizes a prioritized waste hierarchy, which encompasses prevention, preparing for reuse, recycling, other forms of recovery (such as energy recovery), and, as a last resort, disposal (EC, 2008). Consequently, landfills should primarily receive pre-treated waste that is neither biologically active nor containing mobile hazardous substances. Reuse and recycling are the primary strategies for efficient material recovery. In cases where material recovery is not practically achievable, energy recovery becomes a viable option. Moreover, the waste hierarchy allows for flexibility in decision-making to select options that yield the best overall environmental outcomes, guided by life-cycle thinking (EC, 2008). Thus, an effective integrated waste management system necessitates the integration of various treatment processes. This includes recycling processes for material recovery, biological treatments for specific waste streams, and thermal treatments for energy recovery. Additionally, the system should incorporate service landfills for the disposal of residues generated by these treatment methods.

In this context, the term "thermal treatment" refers to any thermochemical conversion process occurring at elevated temperatures, leading to alterations in the chemical structure of the processed material. In recent decades, the main interests toward thermal treatments were due to their ability to significantly reduce the solid waste in mass (about 70–80%) and in volume (about 80–90%), allowing preserving landfill space, as well as to eliminate the tendency of waste to putrefy giving place to sanitary problems (this last aspect being especially important in the past) (Gohlke & Martin, 2007).

Combustion procedures, commonly referred to as incineration, are the prevailing thermal techniques utilized for various waste categories. These include Municipal Solid Waste (MSW), which represents unsorted residual waste (i.e., the waste remaining after separate collection), and Industrial Hazardous Waste (IHW). Typically, waste incineration is linked with the reclamation of energy, resulting in the generation of electricity and/or heat. Application of incineration in Municipal Solid Waste (MSW) and Industrial Hazardous Waste (IHW) management are described below.

### **2.3. Managing Hazardous Waste in Europe: Challenges, Treatment Methods, and Environmental Impacts**

Hazardous waste has emerged as a significant challenge for Europe. In 2020, Europe generated a total of 2538 million tons of waste consist of construction with a 36.4% of the total, mining and quarrying (25.3%), manufacturing (10.3%), waste and water services (10.0%), and households (8.5%). The remaining 9.5% were wastes generated from other various economic activities, mainly services (4.6%) and energy (3.1%) (Eurostat, 2020). Within the EU-28, there was a total of 100.7 million tons of hazardous waste (HW), constituting 4.0% of the overall waste volume. This hazardous waste originates from diverse sources, encompassing industrial manufacturing processes, e-wastes, and various others. These hazardous waste materials can manifest in different physical states, including liquids, solids, and sludges. The US Environmental Protection Agency (EPA) characterizes hazardous waste (HW) as "waste with properties that render it perilous or potentially harmful to human health or the environment" (EPA, 2020). Annex III of Directive 2008/98/EC (EC, 2008) outlines the characteristics, such as the presence of heavy metals, dioxins, or other harmful substances, that classify a waste stream as hazardous. Further elaborating on this, Decision 2000/532/EC (EC, 2008) defines hazardous waste as encompassing liquids, solids, gases, or sludge that present actual or potential risks to public health or the environment. This category can encompass various materials, including discarded commercial products like cleaning solutions or pesticides, as well as by-products from industrial processes. While many forms of hazardous waste can be effectively recycled, others necessitate treatment or disposal methods like landfilling or incineration in hazardous waste incinerators (HWIs). In 2016, within the EU-28, 51% of hazardous waste was sent to landfills, 6% was incinerated without energy recovery, and energy recovery was the method employed for 8% of all hazardous waste materials. A total of 35% of hazardous waste was recovered through recycling or backfilling, equivalent to 53 kilograms per inhabitant (Eurostat, 2020).

It's worth noting that a portion of the hazardous waste sent to landfills may, in some cases, require recycling or recovery to comply with new regulations. For example, waste may be hazardous due to the presence of toxic components like heavy metals or PCBs, it might be unfeasible to attain the required level of material purity for recycling. However, recycling could be excessively energy-intensive, or the costs of recycling may be prohibitively high (Vandecasteele, et al., 2014). In such cases, thermal treatment with energy recovery can serve as a cost-effective and sustainable treatment option. As stated by (Oppelt, 1987), "of all the

treatment technologies, properly designed incineration systems have the highest overall capacity for the destruction and control of a wide range of hazardous waste streams." While the primary objective of hazardous waste incineration (HWI) is indeed the destruction of hazardous waste and the concentration of non-destructible hazardous components. However, modern waste incinerators also pursue other goals, such as recovering energy, materials, and chemicals from waste, as well as reducing waste volume and mass (BREF, 2006). This aligns the HWI process with the principles of Cleaner Production, or more recently, with the principles of (Resource Efficient and Cleaner Production, 2014).

The term Cleaner Production, introduced by UNEP in 1990, is defined as "the continuous application of an integrated environmental strategy to processes, products, and services to increase efficiency and reduce risks to humans and the environment." Resource Efficiency and Cleaner Production specifically advance:

- Production Efficiency through optimizing the use of natural resources (raw materials/resources, energy, water).
- Environmental Management by minimizing the adverse impacts of industrial production systems on nature and the environment (air, water, and soil).
- Human development by reducing risks to individuals and communities while supporting their development.

Even though in contemporary facilities, hazardous waste incineration (HWI) with energy recovery predominantly adheres to the tenets of RECP, it continues to be perceived by the general public as posing risks to air quality and public health. Throughout history, incineration facilities have been linked to the release of harmful substances into the environment. These include notably polychlorinated dibenzo-p-dioxins and dibenzofurans (PCDD/Fs) and metallic elements with high atomic weights ( (Cheng & Hu, 2010); (Vehlow, 2015); (Vilavert, et al., 2015); (Rovira, et al., 2018)).

In 1997, the International Agency for Research on Cancer (IARC) categorized 2,3,7,8-tetrachlorodibenzo-p-dioxin (TCDD), the most potent PCDD/F congener, as a Group 1 carcinogen. This classification was established on the basis of limited human evidence, sufficient evidence from studies on experimental animals, and a wealth of mechanistic information. IARC specified that TCDD exerts its effects through a mechanism that involves the aryl hydrocarbon receptor (AhR), a receptor found in both humans and animals.

Subsequent research findings have provided additional support for the initial IARC classification made in 1997 (IARC, 1997).

Subsequently, the World Health Organization (WHO) established toxic equivalency factors (TEFs) for polychlorinated dibenzo-p-dioxins (PCDDs), dibenzofurans (PCDFs), and dioxin-like polychlorinated biphenyls (PCBs) (Van den Berg, et al., 1998). These TEFs are instrumental in assessing risks to humans, fish, and wildlife. In 2005, the WHO-TEFs underwent a reevaluation (Van den Berg, et al., 2006) and are currently employed for the risk assessment of PCDD/Fs. Notably, it's not just PCDD/Fs that raise concerns; heavy metals also feature prominently among the pollutants released from waste incinerator stack emissions. These metals are persistent and have a propensity to accumulate in the environment and enter the food chain ( (Bocio, et al., 2005); (González, et al., 2019)). Furthermore, various metals and metalloids exhibit toxic properties, even at relatively low exposure levels, and have been linked to numerous health issues, including skin lesions, neurological disorders, learning disabilities, and adverse respiratory effects ( (Jan, et al., 2015); (Menon, et al., 2016); (Hartwig & Jahnke, 2012); (Weiss & Carver, 2018)). Some toxic metals like Arsenic (As), Cadmium (Cd), Mercury (Hg), and Lead (Pb) also carry potential for carcinogenic, mutagenic, and teratogenic effects ( (Domingo, 1994); (Lansdown, 2014)).

In waste incineration, metals are primarily found in bottom and fly ash, with only limited amounts of these elements released from the stack in particulate or vapor form (Peng, et al., 2020). Nonetheless, the atmospheric emission of metals remains a concern because the presence of heavy metals in soils and the broader environment can directly impact public health. Accumulating evidence suggests that human exposure to toxic metals results in the buildup of these substances in tissues, which may subsequently lead to adverse health effects (Ma, et al., 2018). While most incinerators worldwide are dedicated to municipal solid waste incineration (MSWIs), the number of hazardous waste incinerators (HWIs) and medical waste incinerators (MWIs) is considerably lower. Despite their lower numbers, HWIs warrant particular attention due to the potentially high risks associated with the waste they handle.

### **2.3.1. High-temperature oxidation of Aluminium**

Aluminium (Al) has been recognized as an effective combustion agent due to its numerous benefits, including low oxidant consumption, a high combustion calorific value of 31,070 J/g, and a high measured specific impulse ( (Maggi, et al., 2012); (Deluca, et al., 2017)). When

exposed to air, Al forms a dense alumina ( $\text{Al}_2\text{O}_3$ ) shell with a high melting point of approximately  $2000\text{ }^\circ\text{C}$ , which enhances the safety of aluminum powder during production, storage, transportation, and usage ( (Joshi, et al., 2018); (Jin, et al., 2020)). However, the oxidation process of Al is directly influenced by the presence of the  $\text{Al}_2\text{O}_3$  shell, which hinders the contact between the active Al and oxidation components ( (Tang, et al., 2017); (Wu, et al., 2019)). Consequently, the ignition and combustion reaction activity of Al are restricted by this shell. Moreover, the combustion product  $\text{Al}_2\text{O}_3$  tends to re-coat the surface of the active Al, further impeding the combustion chemical reaction ( (Braconnier, et al., 2020); (Liang, et al., 2020); (Liang, et al., 2019)). This results in incomplete combustion of Al and reduced energy release efficiency (Braconnier, et al., 2020).

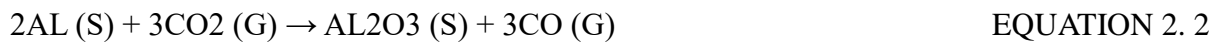
The presence of an  $\text{Al}_2\text{O}_3$  shell on the surface of aluminum (Al) significantly influences the oxidation process of Al. (Trunov, et al., 2006) examined the simultaneous growth and phase transformation of  $\text{Al}_2\text{O}_3$  during the oxidation of Al particles (mechanism of  $\text{Al}_2\text{O}_3$  crystal transformation). The oxidation process of Al can be divided into four stages. Initially, the amorphous  $\text{Al}_2\text{O}_3$  on the Al surface gradually thickens, and the reaction rate is controlled by the outward diffusion of Al cations (Jeurgens, et al., 2002). Subsequently, the amorphous  $\text{Al}_2\text{O}_3$  on the Al surface transforms into  $\gamma\text{-Al}_2\text{O}_3$  when the critical thickness is reached, or when the temperature reaches a certain level ( (Jeurgens, et al., 2000); (Jeurgens, et al., 2002)). As the density of  $\gamma\text{-Al}_2\text{O}_3$  is higher than that of amorphous  $\text{Al}_2\text{O}_3$ , the  $\text{Al}_2\text{O}_3$  shell on the Al surface ruptures. This allows the internal active Al to come into contact with the oxide, significantly increasing the reaction rate. As the  $\gamma\text{-Al}_2\text{O}_3$  shell grows and heals, the reaction rate decreases significantly. Eventually, a regular polycrystalline layer of  $\gamma\text{-Al}_2\text{O}_3$  forms by the end of the second stage. In the third stage, the growth of  $\gamma\text{-Al}_2\text{O}_3$  continues. At the same time,  $\gamma\text{-Al}_2\text{O}_3$  transforms the crystal phase into  $\delta\text{-Al}_2\text{O}_3$  or  $\theta\text{-Al}_2\text{O}_3$ . Due to the similar density of  $\delta\text{-Al}_2\text{O}_3$  and  $\theta\text{-Al}_2\text{O}_3$  to that of  $\gamma\text{-Al}_2\text{O}_3$ , the  $\text{Al}_2\text{O}_3$  shell does not rupture, and the reaction does not change significantly. Additionally, the reaction rate is limited by the inward grain boundary diffusion of oxidant anions in the third stage (Ruano, et al., 2003). When the stable and denser  $\alpha\text{-Al}_2\text{O}_3$  forms due to increased temperature, the third stage ends. The fourth stage begins when  $\text{Al}_2\text{O}_3$  is completely transformed into  $\alpha\text{-Al}_2\text{O}_3$ . In the third stage, the thickness of the  $\gamma\text{-Al}_2\text{O}_3$  layer decreases, and the oxidation rate momentarily increases. Once most of the oxide layer is transformed into coarse and dense  $\alpha\text{-Al}_2\text{O}_3$ , the contact between the internal active aluminum and the oxidized components is completely blocked, and the reaction rate rapidly decreases.

The oxidation of high-purity aluminium sheet or powders in various atmospheres, including dry oxygen, moist oxygen, carbon dioxide, and carbon monoxide, has been a subject of research interest due to its relevance in various industrial applications. Oxidation is a chemical reaction in which a substance combines with oxygen to form an oxide. In the case of aluminium, the oxide formed is aluminium oxide (Al<sub>2</sub>O<sub>3</sub>), commonly known as alumina. In dry oxygen, the oxidation of aluminium proceeds according to the following chemical reaction:



This reaction results in the formation of a dense and adherent layer of alumina on the surface of the aluminium, which acts as a protective barrier against further oxidation. However, in moist oxygen, the presence of water vapor can lead to the formation of aluminium hydroxide (Al(OH)<sub>3</sub>) in addition to alumina. This can result in the formation of a less protective and more porous oxide layer, which may lead to increased rates of oxidation.

In carbon dioxide, the oxidation of aluminium can also occur, but the reaction is less vigorous compared to that in oxygen. The reaction proceeds as follows:



This reaction results in the formation of alumina and carbon monoxide gas. The presence of carbon monoxide can further react with the aluminium oxide to form aluminium carbide (Al<sub>4</sub>C<sub>3</sub>), which is a hard and abrasive material.

In carbon monoxide, the oxidation of aluminium is also less vigorous compared to that in oxygen. The reaction proceeds as follows:



This reaction results in the formation of alumina and carbon. The presence of carbon can further react with the aluminium oxide to form aluminium carbide.

Therefore, the alumina coating surrounding the Al particles is fundamental for preventing the oxidation of Al particles with water and air humidity. In this study, we explore the use of thermal treatment as a means of preventing the generation of explosive gases during the creation of alumina around Al particles of aluminium waste powders. We investigate the mechanisms of Al particle oxidation with water and the role of the alumina coating in protecting the Al particles from oxidation. We also examine the effectiveness of thermal

treatment in preventing the generation of explosive gases and enhancing the protective properties of the alumina coating. The findings of this study have important implications for the development of new materials and processes for various industrial applications.

### **2.3.2. Aluminium alloy powder waste**

Due to worldwide industrialization and fast economic growth, industrial solid waste production has constantly increased over the decades. Among metals, aluminium as the second-most used metal globally has been used in a remarkably wide range of commercial goods in modern society due to its unique combination of characteristics such as softness, lightness, strength, excellent electrical and heat conductivity, low density, and low melting point (Tsakiridis, et al., 2013). The most notable wastes generated in the aluminium production cycle are red mud, dross, grinding filter powder, furnace gas filter powder, skimming, and salt cake (Gil, 2005). Types of metallic wastes and their amounts vary depending on the raw materials used, operating conditions, the type of technology, and furnace technology used (Yoshimura, et al., 2008). Aluminium's natural tendency to corrosion leaves it looking dull through an aluminium oxide layer that forms over the metal to protect it. Towards increasing performance and service life of aluminium products, proper surface treatment technologies allow aluminium surfaces to remain pristine and prevent them from becoming tarnished or showing any signs of rusting. Metal surface technologies, such as brushing, polishing, and sandblasting, generally imply phases that produce grinding filter powder, mainly as a by-product (Gil, 2005). The expansions of aluminium dust during the processing, storage, and transportation of bulk materials and powders have been characterized as an environmental hazard with the potential to cause harms to metal working area, waste transport and disposal systems (EC, 2000). Apart from the difficulties in managing the risk of dust explosions in metal working industries, the potential hazards of aluminium wastes disposal area have been studied by many researchers ( (Amer, 2002); (Australian Gov. Dept. of the Environment and Water, 2007); (Lucheva, et al., 2005); (Miškufová, et al., 2006); (Shinzato & Hypolito, 2005)).

At present, the traditional disposal methods (e.g., storing and landfilling) are greatly limited for the hazardous aluminium wastes. Aluminium waste dusts cannot be transferred to landfills because they will likely react amphotericly with water in the presence of hydroxyl ions and lead to inadvertent generation of hydrogen (Calder & Stark, 2010) (Calder & Stark, 2010). A study by (Arm & Lindeberg, 2006) reported hydrogen explosions that occurred in landfills, rock caverns, old oil wells containing wet fly ashes caused by aluminium-water reactions.

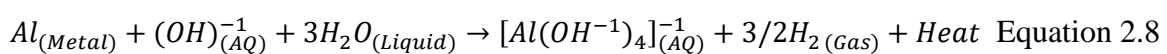


The overall reactions responsible for hydrogen generation in water-aluminium reaction are as follows (Petrovic & Thomas, 2008):



On exposure to oxidative atmospheres and temperature, an oxide film forms rapidly on aluminium particles surface, providing stability ( (Campbell, et al., 1999); (Emsley, 1991) (Emsley, 1991)). According to (Trunov, et al., 2005a) and (Trunov, et al., 2005b), oxidation of pure aluminium, that is caused by a sequence of polymorphic phase transitions, occurring during the growth of the oxide film, can be divided to four main stages between 300 and 1500 °C. While the thickness of the natural amorphous alumina layer increases slowly in the initial stage (300 °C < T < 550 °C), this layer transforms into  $\gamma$ -Al<sub>2</sub>O<sub>3</sub> around 550 °C and this leads to a stepwise mass increase (the second stage). When pure Al reaches its melting point at ~660°C, the transformation of  $\gamma$ -Al<sub>2</sub>O<sub>3</sub> layer into  $\theta$ -Al<sub>2</sub>O<sub>3</sub> polymorph occurs (the third stage). Finally, as a result of the fourth stage, the  $\alpha$ -Al<sub>2</sub>O<sub>3</sub> is formed at temperatures above 1100°C. Thus, the most probable aluminium-water reaction at room temperature is Equation 2. 14.

(Shmelev, et al., 2016) and (Rosenband & Gany, 2010) reported that the presence of a small fraction of activators enables a spontaneous reaction of activated aluminium particles even with cool water, which typically would not react with oxide or hydroxide surface layers. (Nithiya, et al., 2018) confirmed the alkaline compounds in aluminium wastes. In a landfill, a highly exothermic reaction, which occurs when the water in contact with aluminium wastes become alkaline, between hydroxyl ions and aluminium metal inadvertently releases large amounts of flammable or toxic gases (e.g., hydrogen, acetylene, ammonia, carbon monoxide, and benzene) (Stark, et al., 2012). Hydrogen gas from the amphoteric reaction of aluminium-water in the presence of hydroxyl ions is believed to be (Stark, et al., 2012):



The consequences of the amphoteric reaction of aluminium within landfills are discussed by (Stark, et al., 2012). Their report showed that aluminium-water reaction may cause: (1)

changes in leachate composition and quality; (2) undesirable increase in waste temperatures; (3) changes in gas composition and pressure with decreasing methane production and with increasing the generation of combustible and toxic gases; (4) microbial activity that would be considered desirable in anaerobic environments decreases; and consequently (5) the nuisance odors increase as a symptom surrounding the landfills.

Furthermore, fine particles of aluminium powder cannot be stored without specific safety precautions and considerations because they can readily disperse as a cloud in air due to their low masses. Upon dispersion in the air, which allows the particles to mix with oxygen, the burning occurs quickly so that an explosion results. Many studies have investigated the flammability of aluminium waste dusts produced by different metal industrial processes and the dust properties that contribute to explosions ( (Marmo, et al., 2004), (Marmo, et al., 2015), (Marmo, 2017)), (Cavallero, et al., 2004), (Lembo, et al., 2001), (Miao, et al., 2016), (Keown, 2016)). According to prevention and mitigation of dusts explosion with the concept of inherent safety, avoidance of dust cloud formation or control it below the minimum explosible concentration is fundamental (Amyotte & Eckhoff, 2010). Managing the risk of explosions in storages is not an easy task and lead to difficulties especially in small companies that often have limited resources.

Moreover, with increasingly attentions to the renewable high calorie fuel such as hydrogen, there is a tendency to use aluminium and its alloys as the suitable metal source for hydrogen production. Therefore, disposal, utilization, and explosion control of this materials are receiving increasing attention in the future. According to the above concerns regarding the disposal of aluminium waste powders, it does not appear that any of the disposal methods alone would be effective in reducing the hazardous consequences that exist when aluminium explosible dust is present in quantities above its minimum explosive concentration. Therefore, reducing aluminium waste powders' reactivity as much as possible through thermal pre-treatment or thermal oxidation (not higher than 600 °C) may be the most promising approach, and then to determine the appropriate disposal (such as landfills) or utilization (such as direction used in the formulation of porous concrete (Kumar, et al., 2015), fingerprint detection compounds (Sodhi & Kaur, 2001), coatings and inks ( (Karlsson, et al., 2008); (Sverak, et al., 2013)) and hydrogen generation devices ( (Nie, et al., 2012); (Shimamura, et al., 2014)) according to the risk assessment of residual reactivity level.

The utilization of low-medium temperature thermal treatment for waste disposal has increased due to its effectiveness and lower energy usage in recent years. Thus, in this study the efficiency of medium temperature pre-treatment of different aluminium waste powders from surface treatment industries, which applied a variety of processes to treat aluminium surfaces (e.g., shot blasting and polishing), was investigated.

#### **2.4. Addressing Soil Pollution: Regulatory Frameworks, Environmental Impacts, and Sustainable Remediation Strategies**

There has been widespread degradation of soil due to several anthropic activities (e.g., mineral resource extraction, high agricultural inputs, warfare, and military training) which have polluted the soil over the past several decades ( (Fayiga & Saha, 2016); (Jiang, et al., 2018)). Any chemical or substance that is out of place or present at a higher than normal concentration in the soil can cause soil pollution. The Waste Framework Directive (EC, 2008) enforces a legal requirement to classify waste soils for disposal, and those who do not act in accordance with the guidance, run the potential risk of being prosecuted. Contaminated soils are categorized as wastes for several compelling reasons:

**Environmental Risks:** Contaminated soils often contain hazardous substances, such as heavy metals, volatile organic compounds, and persistent organic pollutants. These contaminants can leach into groundwater, endangering both the environment and human health (Wuana & Okieimen, 2011). As a result, treating contaminated soils as waste is seen as a protective measure against potential pollution.

**Regulatory Requirements:** Environmental regulations in many regions require the proper management of contaminated soils to prevent adverse impacts. Categorizing them as wastes allows for adherence to legal requirements, ensuring responsible disposal, and minimizing the risks associated with contamination (Ramón & Lull, 2019).

- **Land Reuse and Redevelopment:** In many cases, contaminated sites need to be remediated before they can be safely reused or redeveloped (Sun, et al., 2022). By categorizing contaminated soils as wastes, it becomes possible to employ appropriate cleanup methods and ensure that the land meets environmental standards.
- **Accountability and Liability:** Treating contaminated soils as wastes clarifies liability issues, making it easier to assign responsibility for their management, cleanup, and potential long-term monitoring (Ostad-Ali-Askari, 2022).

- **Public Health and Safety:** Recognizing contaminated soils as wastes underscores the importance of safeguarding public health and safety. It promotes the use of proper disposal methods, containment, and monitoring, reducing the risk of exposure to harmful contaminants (Adipah, 2019).
- **International Agreements:** International agreements and conventions, such as the Basel Convention, govern the transboundary movement of hazardous wastes. Contaminated soils may fall under the purview of these agreements, reinforcing their classification as wastes for responsible handling (Adipah, 2019).

Soil pollution is an emerging threat to food security, ecosystem, and human health (FAO and UNEP, 2021). Food security can be impacted by soil pollution both by reducing crop yields due to toxic levels of contaminants and by rendering crops produced from polluted soils unsafe to consume. The pollutants also negatively affect soil microorganisms and larger soil-dwelling organisms, reducing soil biodiversity and affecting the services provided by the organisms. Based on scientific evidence, carcinogens such as arsenic, chromium VI, benzene, vinyl chloride, dichloromethane, hexachlorocyclohexanes, dichloromethane, polychlorinated biphenyls (PCBs), polycyclic aromatic hydrocarbons (PAHs), and pharmaceuticals such as antibiotics may pose health risks to humans ( (Anning & Akoto, 2018); (Baars, et al., 2001); (Crettaz, et al., 2002); (Dardouri & Sghaier, 2018); (Gabarrón, et al., 2018); (Gan, et al., 2017); (Lü, et al., 2018); (Spadaro & Rabl, 2004); (Zabaleta, et al., 2018)). In addition, contaminated surface water and groundwater problems, resulting from transferring the pollutants from soil to water, lead enormous environmental hazard through eutrophication and direct human health issues because of contaminated drinking water (Rodríguez-Eugenio, et al., 2018). Apart from the mentioned issues due to contaminated soils, unequal distribution of the burden of cost attributed to the contaminated sites leads to other socio-economic aspects, such as low real state benefits and perceptions. The effects of land pollution are not only seen on the contaminated site, but also on surrounding land by affecting the surrounding house prices. The remediation of contaminated sites increases surrounding property values and tax revenues, enhances land utilization in this region, propels regional development, and encourages private investment (Li, et al., 2015). Therefore, to respond to the concerns about contaminated soils, FAO's revised World Soil Charter recommends that national governments should systematically control pollution, improve soil environmental quality, and ensure soil ecosystem stability and safety in order to promote significant developments in soil remediation (FAO, 2015a). Moreover, in new environmental policies and strategies

(European Green Deal and Agenda 2030), soil conservation, prevention, and remediation are the key goals, which aim at transforming major production, consumption, and trade systems in a comprehensive and sustainable manner ( (UN—United Nations;, 2015); (EC—European Commission , 2019); (EC—European Commission, 2021)).

Various soil remediation techniques have been successfully employed to reduce the risks associated with different pollutions (Lim, et al., 2016), including biological, physicochemical, thermal, and integrated strategies. The main aim of these conventional remediation techniques in soil remediation plants is to remove or reduce the contaminant levels to an acceptable level in a short period of time at low cost without considering the side effects of their implementation. There has been widespread concern about soil resource sustainability since the Food and Agriculture Organization (FAO, 2015b) report of "The State of the World's Soil Resources" was published in 2015. Sustainable or green approaches are imperative throughout the remediation process as they address environmental, social, and economic aspects. In a sustainable remediation strategy, the objective is to minimize the negative impacts of remediation projects, maximize their long-term benefits, and achieve an overall net benefit for society, the economy, and the environment (Cundy, et al., 2013). The economic and environmental impacts of the soil remediation projects can be assessed through some methods, such as life cycle assessment ( (Chen, et al., 2009); (Liang, et al., 2023)), risk reduction methods (Sakaguchi, et al., 2014), environmental merit and cost assessments (Wan, et al., 2020), carbon footprint predictions (Ferdos & Rosen, 2013). For the purposes of modelling End-of-Life (EoL) of remediated soil in these methods, it is necessary to evaluate the quality of remediated soil. End-of-Life (EoL) refers to a product whose quality is such that its use does not harm human health or environment ( (JRC, 2008), (JRC, 2009), (JRC, 2010); (EC, 2008)). Therefore, for a successful remediation project, it is essential to evaluate the negative effects of remediation processes on soil physical, chemical, and biological properties because the extreme impacts may impair certain post-treatment land uses.

#### **2.4.1. Persistent organic pollutants (POPs): Regulatory Frameworks, Environmental Impacts, and Sustainable Remediation Strategies**

Persistent organic pollutants (POPs) are harmful substances characterized by their chemical stability, resistance to environmental degradation, and the tendency to accumulate and magnify within the food chain. Exposure to POPs poses severe risks to human health,

including issues such as cancer, neurological damage, birth defects, sterility, and suppression of the immune system. Stringent regulations and prohibitions on the use of POPs have led to the accumulation of large quantities of unusable materials containing these chemicals on a global scale. Furthermore, the degradation of storage facilities, improper storage practices, and historical production and usage of POPs have resulted in widespread soil contamination worldwide. The Food and Agricultural Organization (FAO) of the United Nations, through its Programme on the Prevention and Disposal of Obsolete Pesticides, is actively compiling an inventory of obsolete pesticide stockpiles present across the globe.

The global community has addressed the health risks associated with obsolete POPs stockpiles by establishing treaties and organizations dedicated to managing POPs chemicals and waste. The Stockholm Convention (Stockholm Convention, 2001) on POPs, adopted in 2001 and enacted in 2004, binds parties to diminish or eradicate the production, utilization, and release of the 12 most concerning POPs worldwide, initially identified by the Intergovernmental Forum on Chemical Safety and the International Programme on Chemical Safety Table 2. 1. Another international treaty governing POPs is the Basel Convention on the Control of Transboundary Movements of Hazardous Wastes and their Disposal, adopted in 1989 and in force since 1992. To comply with Stockholm Convention provisions regarding collaboration with the Basel Convention on POPs waste matters, the Basel Convention has issued guidance on the environmentally sound management of POPs waste. In 2004, the Basel Convention invited Stockholm Convention signatories to consider its recommendations on the environmentally sound management of POPs wastes .

The POPs Review Committee (POPRC ), a subsidiary body of the Stockholm Convention, comprises environmental experts responsible for assessing proposals to include new chemicals in the Convention. The POPRC evaluates a chemical's characteristics, as well as its impacts on human health and the environment, using criteria outlined in Annex D of the Convention. If the chemical aligns with the Convention's screening criteria, the POPRC formulates a risk profile in accordance with Annex E (of the Convention) and, if deemed necessary, conducts a risk management evaluation as outlined in Annex F (of the Convention). Following the risk management evaluation, the POPRC recommends to the Conference of the Parties (COP) whether to include the chemical in one or more of the Convention's annexes (Annexes A, B, and/or C). Additionally, the listing process aims to contribute to the development of a plan for reducing the chemical's use in current and future environmental applications.

Historically, combustion systems employing high-temperature incineration have been extensively used for treating soil and stockpiles contaminated with POPs to eliminate the contaminants. This approach is favoured due to the capability of high-temperature incinerators to handle large quantities of contaminated material and effectively treat various contaminants. Modern incinerators, with precise combustion environments, can achieve a high Destruction and Removal Efficiency (DRE) for POP contaminants, reaching DREs as high as 99.9999%, especially for incinerators addressing non-liquid PCBs in the US. The US EPA has sanctioned the use of incinerators for treating PCB-contaminated material with concentrations exceeding 50 parts per million.

However, relying solely on incineration for POPs waste treatment has certain limitations. Incinerators cannot eliminate inorganic constituents (metals) in waste streams, and these may either be released in air emissions or retained in solid residues. Consequently, waste containing both POPs and specific metals might not be suitable for incineration in certain cases. Some heavy metals, like lead, cadmium, mercury, and arsenic, may partially vaporize during combustion and exit the incinerator with the flue gases, necessitating additional off-gas treatment systems for their removal (Chuai, et al., 2022). Incinerators handling waste streams contaminated with heavy metals may generate bottom ash with elevated metal concentrations, requiring characterization to determine if it qualifies as Resource Conservation and Recovery Act (RCRA) hazardous waste, necessitating stabilization and appropriate disposal (Kleinhans, et al., 2018).

Moreover, concerns about potential environmental and health effects associated with POPs combustion have been expressed by site owners, operators, remedial project managers, and other stakeholders. The combustion of POPs can create polychlorinated dibenzo-p-dioxins (dioxins) and polychlorinated dibenzo-p-furans (furans) (Reinmann, et al., 2010).

Also, most POPs-containing stockpiles are located in developing countries where incinerators generally do not achieve high DREs. Consequently, these countries often have to transport obsolete POPs stockpiles to developed nations for treatment and disposal. Stringent international regulations on transporting contaminated material make the transportation of obsolete POPs from developing to developed countries cost-prohibitive. Due to health and environmental concerns associated with waste incineration, some countries, such as Australia and the Philippines, have adopted non-incineration policies ( (Budnik, et al., 2014); (Okoh, 2015)).

The utilization of the incineration method in soil remediation, while acknowledged for its efficacy, presents drawbacks, particularly in terms of cost efficiency. The elevated expenses associated with incineration surpass the essential requirements for soil treatment, thereby deviating from the principles of sustainability. This incongruence raises concerns about the compatibility of the incineration approach with the need for a more targeted and economically sustainable strategy in the realm of soil remediation. Therefore, in the subsequent discussion, there is a call for a reevaluation of thermal treatment of soil to better conform to sustainable principles, with a focus on optimizing cost-effectiveness and prioritizing environmental impacts.



Table 2. 1 Substances currently listed in the relevant annexes to the POPs Regulation (EUROPEAN CHEMICAL AGENCY, 2023)

| <b>Substance name</b>  | <b>Date of inclusion in the POPs Regulation</b> | <b>POPs Regulation Annex</b> |
|--|---|------------------------------|
| Endosulfan and its isomers   | 19-giu-2012                                     | I, part A# IV                |
| Heptabromodiphenyl ether (Group)                                     | 24-ago-2010                                     | I, part A# IV                |
| Hexabromocyclododecane (HBCDD)                                       | 01-mar-2016                                     | I, part A# IV                |
| Hexabromodiphenyl ether (group)                                      | 24-ago-2010                                     | I, part A# IV                |
| Pentabromodiphenyl ether (group)                                     | 24-ago-2010                                     | I, part A# IV                |
| Pentachlorophenol and its salts and esters                           | 20-giu-2019                                     | I, part A# IV                |
| Perfluorohexane-1-sulphonic acid, its salts and related substances   | 29-dic-2022                                     | I, part A# IV                |
| Perfluorooctane sulfonates (PFOS)                                    | 24-ago-2010                                     | I, part A# IV                |
| Perfluorooctanoic acid (PFOA), its salts and PFOA-related substances | 15-giu-2020                                     | I, part A# IV                |
| Polychlorinated Biphenyls (PCB)                                      | 29-apr-2004                                     | I, part A# III, part A# IV   |
| Polychlorinated dibenzo-p-dioxins and dibenzofurans (PCDD/PCDF)      | 29-apr-2004                                     | I, part A# III, part A# IV   |
| Polychlorinated naphthalenes   | 19-giu-2012                                     | I, part A# III, part A# IV   |
| Naphthalene, chloro derivs.  | 19-giu-2012                                     | I, part A# III, part A# IV   |
| Polycyclic aromatic hydrocarbons (PAHs)                              | 29-apr-2004                                     | I, part A# III, part A# IV   |
| Dicofol  | 18-ago-2020                                     | I, part A# III, part A# IV   |
| Bis(pentabromophenyl) ether  | 20-giu-2019                                     | I, part A# III, part A# IV   |
| Hexachlorobenzene  | 29-apr-2004                                     | I, part A# III, part A# IV   |
| Chlordecone  | 29-apr-2004                                     | I, part A# IV                |
| Dodecachloropentacyclo[5.2.1.02,6.03,9.05,8]decane                   | 29-apr-2004                                     | I, part A# IV                |
| Aldrin   | 29-apr-2004                                     | I, part A# IV                |
| Hexabromo-1,1'-biphenyl  | 29-apr-2004                                     | I, part A# IV                |
| Clofenotane  | 29-apr-2004                                     | I, part A# IV                |
| Chlordane , pur  | 29-apr-2004                                     | I, part A# IV                |
| Dieldrin   | 29-apr-2004                                     | I, part A# IV                |
| Pentachlorobenzene   | 24-ago-2010                                     | I, part A# III, part B# IV   |
| Endrin   | 29-apr-2004                                     | I, part A# IV                |
| Heptachlor   | 29-apr-2004                                     | I, part A# IV                |
| Toxaphene  | 29-apr-2004                                     | I, part A# IV                |
| Alkanes, C10-13, chloro  | 19-giu-2012                                     | I, part A# IV                |
| Hexachlorobuta-1,3-diene   | 19-giu-2012                                     | I, part A# III, part A# IV   |

Annex I to the regulation are subject to prohibition (with specific exemptions) on manufacturing, placing on the market and use;  
Annex II to the regulation are subject to restriction on manufacturing, placing on the market and use;  
Annex III to the regulation are subject to release reduction provisions; and  
Annex IV to the regulation are subject to waste management provisions.

#### **2.4.2. Evolution of remediation approaches**

As shown in Figure 2. 1 (a), in response to new international environmental policies and the challenges facing soil remediation, remediation approaches for exploring innovative solutions are constantly evolving ( (EPA, 2008); (EPA, 2009); (GSR-1, 2011)). In the second half of the 20th century, contaminated soils were classified as wastes. Lack of remediation technologies and low landfilling implementation costs led to soils being disposed of directly in landfills without considering the environmental impacts. Despite landfill still being a common solution in undeveloped countries, the evolution of remediation approaches led to the traditional remediation strategy in developed countries between 1990 and 2000 (Idowu, et al., 2019). In traditional remediation, the primary impacts, which associated with the characteristics of contaminated sites and the type of contaminants, were aimed without considering the impacts of the remediation process on economic growth and environmental sustainability.

A greater emphasis by international institutions on environmental issues in the new century has led to the development of a new approach to diminishing the environmental impacts of contamination itself and remediation methods (secondary impacts). Secondary impacts refer to those associated with remediation activities, including energy use and materials consumption, and remediation monitoring. In addition to achieving the main goal of remediation, which is to clean up soil, green remediation minimizes the environmental footprint associated with remediation actions (tertiary impacts). Instead of reviewing the environmental impact only during remediation implementation, Green Sustainable Remediation (GSR) takes a step further by assessing the impact throughout the life cycle of the project (GSR-1, 2011). Therefore, the tertiary impacts also include those that result from post-remediation consequences (Hou, et al., 2018). The objective of this approach is to increase the long-term benefits of remediation projects in terms of reducing the negative effects of remediation projects on society, economy, and environment (Holland, 2011). Accordingly, it is imperative that all planning, activities, and resources dedicated to remediating a site align with the desired end or future use to meet the GSR frameworks requirements. This vision of remediation emphasizes the identification of best management practices (BMPs) for minimizing the environmental footprint of remediation activities (Simon, 2020). Suitable BMPs ensure that the chosen technology capable sustainably to overcome the undesirable side effects within a life cycle. Figure 2. 1 (b) shows the core

elements which a best management practices of green remediation must balance in a cleanup project.

The best management practices emphasize minimally invasive in situ methods and use passive energy technologies as primary remedies or finishing steps. In addition, this approach addresses to reduce the potential negative impacts on soil and habitat (EPA, 2008). The selection of the most appropriate remediation technology with the least unfavourable impacts on soil properties can be achieved by identifying the effects of remediation technologies on soil characteristics.

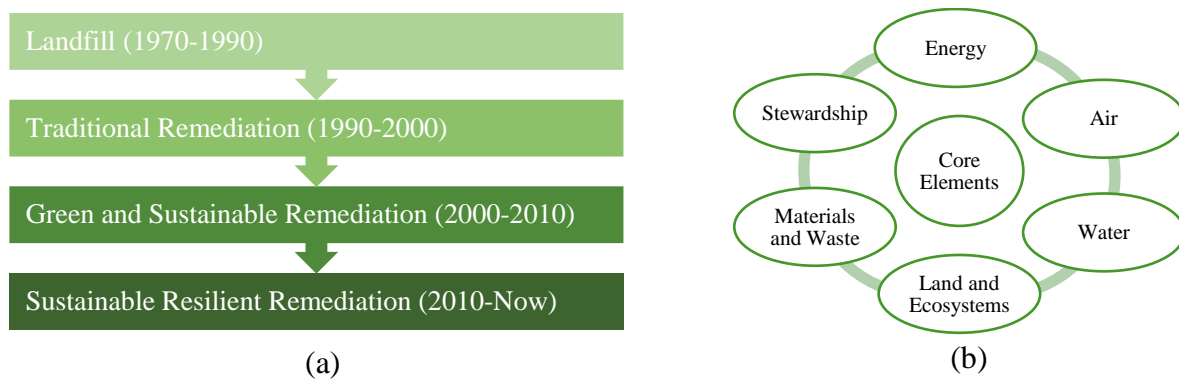


Figure 2. 1 a) The evolution of remediation approaches to environmental during last decades; b) Core Elements of Green Remediation

### 2.4.3. Undesirable effects of thermal desorption remediation on soil properties

World is experiencing a serious agricultural crisis caused by climate change, global warming, soil degradation, reduced agricultural lands, and food shortages (Nellemann, et al., 2009). Consequently, it is important to recognize and utilize remediated soils as valuable resources and to develop strategies for reusing in different purpose of applications. Researchers have been studying the effective utilization of remediated soils for a range of purposes ( (Vaccari, et al., 2012); (Ambaye, et al., 2022); (Wang, et al., 2022a)). For reusing remediated soil, it is vital to pay attention to the efficiency of remediation and more importantly to the effects on soil properties during the processes. However, most studies have only demonstrated the efficacy of different remediation technologies for specific pollutants.

Thermal desorption (TD) involves the application of heat to volatilize the contaminants into gaseous state and separates them from the solid material. From the operating temperature point of view, TD can be divided into low-temperature thermal desorption (LTTD, 100–

300°C) and high-temperature thermal desorption (HTTD, 300–550°C) (Vidonish, et al., 2016b); (Kristanti, et al., 2022)). In these ranges of temperature, different types of organic contaminants can be removed by thermal facilities. Volatile organic compounds (VOCs) such as solvents and gasoline evaporate easily when heated and some semi-volatile organic compounds (SVOCs) include diesel fuel, creosote (a wood preservative), coal tar, and several pesticides that require higher temperatures to volatilize. Moreover, metals like mercury and arsenic, which evaporate at temperatures sometimes reached during thermal desorption, can be partially removed by thermal desorption (EPA, 2012). As a result of its high efficiency, safety, and little secondary pollution production, TD is widely used for processing a variety of pollutants (Stegemeier & Vinegar, 2001). While thermal desorption is efficient and permanent method of removing pollutants from contaminated soils due to its ability to meet clean-up standards quickly and reliably, it can be in conflict of the principles proposed by the sustainable remediation goals due to its energy intensive and adversely effects on soil properties (Vidonish, et al., 2016b). As long as the soil is heated to the right temperature and for a sufficient amount of time, the contaminants can be removed and may ensure to prevent incomplete remediation or the creation of hazardous compounds. Table 2. 2 listed the key parameters of thermal treatment studies applied to different types of contaminated soil.

Thermal conductivity of soil affects thermal remediation operating conditions and is influenced by site-specific characteristics, such as soil texture, mineralogy, and soil water content (Abu-Hamdeh & Reeder, 2000). Regardless of energy consumption and off-gas emissions, TDs used for desorption of contaminants can impair soil's physical, chemical, and biological health (Sierra, et al., 2016). Therefore, to assure contaminant reduction practice aligns with sustainable remediation goals, continuous monitoring of ongoing remediation projects and energy consumption evaluation are essential.

Table 2.2. Thermal treatment studies applied to contaminated soils separated based on contaminant.

| <b>Contaminant</b> | <b>Author</b> | <b>Concentration<br/>(mg/kg)</b> | <b>Additives</b> | <b>Time<br/>(min)</b> | <b>Temperature<br/>(°C)</b> | <b>Carrier<br/>gas<br/>(ml/min)</b> | <b>Max<br/>reduc<br/>tion<br/>(%)</b> |
|--------------------|---------------|----------------------------------|------------------|-----------------------|-----------------------------|-------------------------------------|---------------------------------------|
|--------------------|---------------|----------------------------------|------------------|-----------------------|-----------------------------|-------------------------------------|---------------------------------------|

|   |                      |                         |                                 |            |  |  |   |
|---|----------------------|-------------------------|---------------------------------|------------|--|--|---|
| <b>Polychlorinated biphenyls</b>  | (Liu, et al., 2015a) | 500                     | NaOH;<br>0.1, 0.5, and<br>1 %   | 60         | 300, 400, 500,<br>and 600              | N <sub>2</sub> ; 400   | 99.0  |
|   | (Liu, et al., 2015b) | 6000                    | -                               | 60         | 500                                    | N <sub>2</sub> (99.99<br>vol.%); air<br>(21 vol.%<br>O <sub>2</sub> ); 5<br>vol.% O <sub>2</sub><br>and 95<br>vol.% N <sub>2</sub> ;<br>pure O <sub>2</sub> ;<br>400 | 93.8-<br>95.5                                       |
|   | (Qi, et al., 2014)   | 500                     | -                               | 60         | 300, 400, 450,<br>500, 550, and<br>600 | Nitrogen;<br>400   | 98.0<br>%   |
|   | (Liu, et al., 2014)  | 500                     | nZVI;<br>20, 40, 100,<br>200 mg | 60         | 400 and 600                            | Nitrogen;<br>400   | 94.2<br>% and<br>98.35<br>%                         |
|   | (Liu, et al., 2019)  | -                       | Ca(OH) <sub>2</sub> ;<br>0.1 %  | 30         | 300-600                                | Nitrogen;<br>8333  | 94.0%   |
|   | (Zhao, et al., 2012) | 8.2                     |                                 |            | 5                                      | 450  | O <sub>2</sub> /N <sub>2</sub> :<br>10%/90%<br>1000 |
| <b>Petroleum hydrocarbons, including polycyclic aromatic hydrocarbons</b> | (Lee, et al., 1998)  | Petroleum<br>1-10 (wt%) | -                               | 30-<br>180 | 120-355                                | Nitrogen<br>7.5 (cm/s)   | 99-<br>100  |

|                   |                             |                     |                   |                |  |                     |                         |
|-------------------|-----------------------------|---------------------|-------------------|----------------|--|---------------------|-------------------------|
|                   | (Bulmau, et al., 2014)      | PAHs<br>0.989 (ppm) | -                 | 30, 60         | 350-650                                    | Nitrogen<br>100-200 | 5% -<br>80%             |
|                   |                             |                     |                   |                | 225  |                     | 50-74                   |
|                   | (Wang, et al., 2010)        | 8200                |                   | 10-90          | 325<br>400<br>500                          |                     | 54-94<br>76-99<br>95-99 |
|                   | (McAlexander, et al., 2014) | 40867               |                   | 60             | 340-430                                    |                     | 98-99                   |
|                   | (Vidonish, et al., 2016a)   | 15000<br>19000      |                   | 180            | 420-650                                    |                     | 99                      |
|                   | (Merino & Bucala, 2007)     | Hexadecane<br>12000 |                   | 30             | Adiabatic<br>electric oven<br>150-800      | Helium<br>56        | 99.6-0                  |
| <b>Pesticides</b> | (Yuan, et al., 2006)        | HCB<br>55.8         | NaOH              | 10             | MW radiation<br>750 W<br>2.45 GHz          |                     | 98%                     |
|                   |                             |                     |                   |                | 225  |                     | 75-38                   |
|                   | (Gao, et al., 2013)         | BHC/DDT:<br>3116    |                   | 10-90<br>10-30 | 325<br>400<br>500                          |                     | 75-38<br>70-99<br>94-99 |
| <b>Mercury</b>    | (He, et al., 2014)          | 50                  | FeCl <sub>3</sub> | 10-90          | Rotating<br>electric<br>furnace<br>200-500 |                     | 64-98                   |
|                   | (Ma, et al., 2015)          | 134                 | Citric acid       | 60             | Laboratory-<br>scale rotary<br>kiln<br>400 |                     | 99                      |
|                   | (Sierra, et al., 2016)      | 35<br>10497         |                   | 60             | 60-750                                     |                     | 23-99<br>29-99          |

#### 2.4.3.1. Effects on soil physical properties

As the largest terrestrial source of organic carbon, soil organic matter (SOM) is not only crucial for soil health due to its strong influence on soil properties and function but also affects soil trafficability and hydraulic conductivity (Jackson, et al., 2017). During TD remediation, SOM is inevitably affected by volatilization (distillation), transformation

(charring), and oxidation (combustion) (Certinini, 2005). Depending on the composition of SOM, these mechanisms interact differently with each component (Kiersch, et al., 2012). In Figure 2. 2, different SOMs are listed in accordance with their decomposition temperature ranges. The SOM reduction depends on the temperature and time of heating, in addition to the type of SOM (Figure 2. 2). Data related to soil organic matter before and after thermal desorption were extracted from several studies, incorporating both contaminated and non-contaminated soils, and the SOM reduction is calculated using Equation 2. 9.

$$\text{SOM Reduction} = 1 - \left( \frac{\text{SOM}_{\text{Final}}}{\text{SOM}_{\text{Initial}}} \right) \quad \text{Equation 2. 1}$$

According to available data, low-temperature thermal desorption (LTTD) does not significantly reduce SOM levels ( (Pape, et al., 2015); (Yi, et al., 2016); (Bone, et al., 2010)). At high-temperature treatment conditions, however, SOM reduction can increase from 40 to 99% depending on how long the heat is applied ( (Ma, et al., 2014); (Tatano, et al., 2013); (Huang, et al., 2011); (Sierra, et al., 2016)). Review of studies found that when heating at 350 °C for longer than 20 minutes, SOM was reduced by greater than 50% in 88% of the reviewed cases.

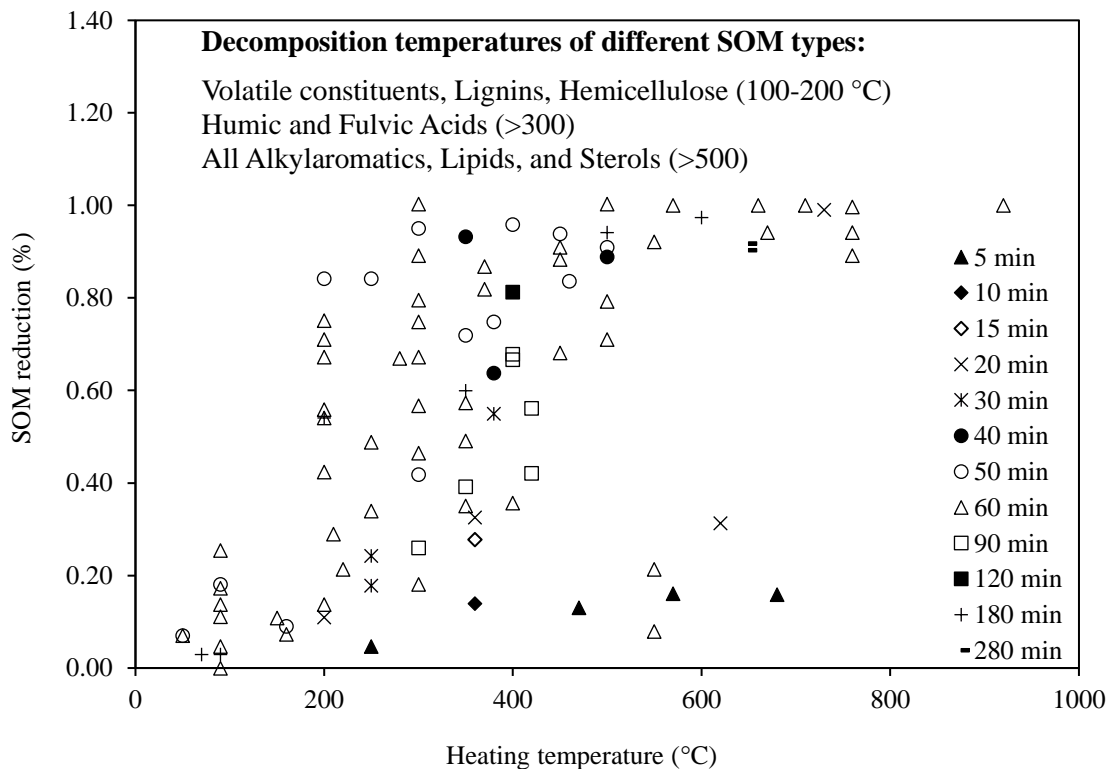


Figure 2.2. Different soil organic matter (SOM) types and their decomposition temperatures and the reduction of SOM across a range of temperatures, with each panel corresponding to heating duration ( (González-Pérez, et al., 2004); (Schulten & P., 1999))

Another important soil physical characterise which can be affected by TD is soil texture and mineralogy. As shown in Figure 2. 3, depending on the soil mineralogy, the dehydroxylation occurs at a different temperature. During thermal processes, mineral clay is dehydrolized and decomposed (Bonnard, et al., 2010) and as a result, amorphous clay-size particles are cemented together by Fe- and Al-hydroxides released by SOM combustion (Ketterings, et al., 2000). Therefore, the formation of large soil particles with poor water and nutrient retention capacity increases the vulnerability of the soil to erosion (Sierra, et al., 2016). Despite the variation in temperature thresholds for soil minerals, Figure 2. 4 shows some trends based on clay-sized particle reductions captured from nine soil heating studies. According to Figure 2. 3 and Figure 2. 4, the clay mineralogy changes with HTTD (particularly at heating temperatures over 400°C), while LTTD has no significant effect on clay mineralogy.

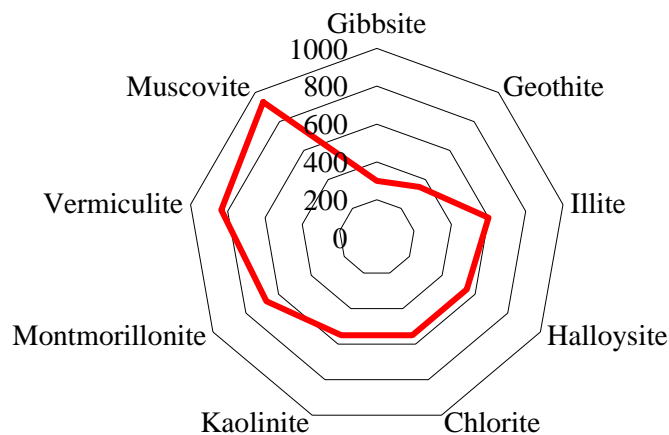


Figure 2.3. Average temperature threshold at which the dehydroxylation occurs for different soil mineralogy ( (GONZÁLEZ-PÉREZ, ET AL., 2004); (SCHULTEN & P., 1999))



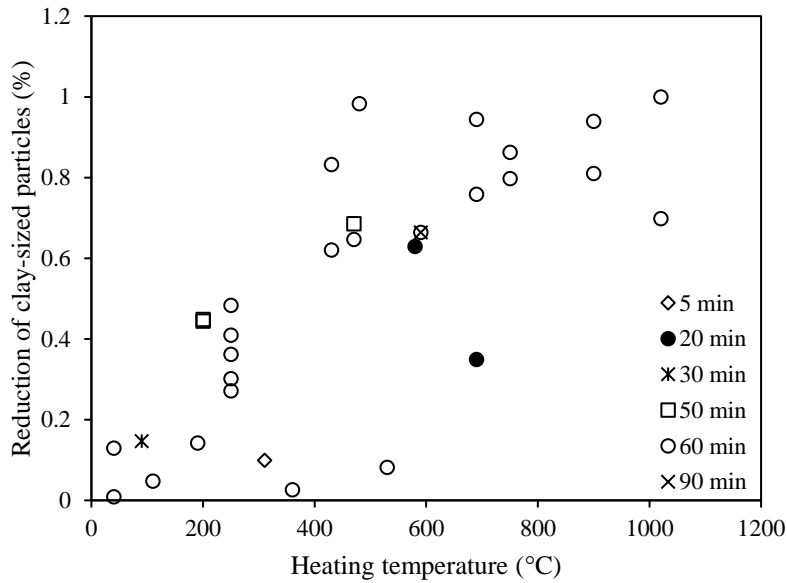


FIGURE 2. 4 Reduction of clay-sized particles vs. heating time and temperature ( (BORCHARDT, 1989); (DIXON, 1989); (FANNING, ET AL., 1989))

#### 2.4.3.2. Effects on soil chemical properties

Soil pH as an important indicator affects the amount of nutrients and chemicals that are soluble in soil water, and therefore the amount of nutrients available to plants. As a result of the decrease in soil organic matters (SOMs) following thermal treatment, soil pH changes depending on the heating time and temperature. Sodium carbonate ( $\text{CaCO}_3$ ) buffers pH changes and requires high temperatures before decomposing. Therefore, the lower the decomposition of SOMs and the higher  $\text{CaCO}_3$  contents in the soil, the lower the pH change. At LTDD condition, due to oxidative reactions and the formation of  $\text{HCO}_3^-$  during soil mineralization associated with soil heating the soil pH remains constant or decreases slowly. ( (Sierra, et al., 2016); (Ma, et al., 2014); (Badia & Marti, 2003); (Roh, et al., 2000)). In contrast, at HTDD conditions, soil pH is affected by removing acidifying influences from soil solutions ( (Pape, et al., 2015); (Terefe, et al., 2008)) and displaces  $\text{H}^+$  with alkali cations ( (Sierra, et al., 2016); (Terefe, et al., 2008); (Badia & Marti, 2003)).

Some nutrients are more available under acid conditions while others are more available under alkaline conditions. Thus, pH level directly and SOMs indirectly affect the plant available nutrients and elements in remediated soil. Nitrogen (N) and Phosphorus (P) are two key elements in plant growth. Under LTDD conditions (especially below  $220^\circ\text{C}$ ), organic N is mineralized to  $\text{NO}_3^-$  and  $\text{NH}_4^+$ , while total N remains constant (Glass, et al., 2008). However, remediated soil total N decreases by 27% and 68% at  $350^\circ\text{C}$  and  $600^\circ\text{C}$ , respectively. In

comparison with SOM and N, soil phosphorus is less sensitive to heat. Following soil heating, the concentration of P can remain constant even as the total soil mass decreases, thereby increasing the total P concentration ( (Yi, et al., 2016); (Galang, et al., 2010)). However, thermal treatment almost entirely depletes total N and P of the soil after incineration at 650 °C ( (Vidonish, et al., 2016a); (Pape, et al., 2015)). Moreover, thermal treatment impacts inorganic contaminants differently depending on the element. For example, soil pH increases following thermal treatment, as well as oxyanions of arsenic (As) and chromium (Cr) mobility, while copper leaching decreases ( (Marani, et al., 2003); (Nordmark, et al., 2011)). Therefore, the pH level of remediated soil should be carefully monitored to avoid these radical changes.

#### **2.4.3.3. Effects on soil biological properties**

Biological Properties represent the direct and indirect influence of the living organisms inhabiting a particular soil. Biological properties are the indicator to assess soil health which lead to evaluate soil functionality such as efficient filtration, soil structure, nutrient, and water cycling. Although studies demonstrated that soil microorganisms eliminated at relatively low heating temperatures (e.g., 50°C -120°C) ( (Lobmann, et al., 2016); (Van der Voort, et al., 2016)), a study by (Pape, et al., 2015) revealed that when temperature was raised from 105°C to 1000°C, the number of functional genes involved in nitrogen cycling remained stable. Soil microorganisms can recolonize remediated soils, and the recovery is dependent on pristine microbial communities and heating temperatures (Mataix-Solera, et al., 2009). In spite of the fact that soil microbial biomass is destroyed at temperatures up to 200 °C (Acea & Carballas, 1999), vegetation can play a regenerative role in restoring soil microbial biomass ( (Certinini, 2005); (Cébron, et al., 2009)). For temperatures less than 300 °C, soil organisms recover rapidly, but for temperatures higher than 300 °C, it may take more than 100 days or even 270 days for recovery to take place. However, at temperatures above 500 °C, soil management, such as fertilizer or organic amendments, may be necessary to recover microbial activity.

Existing chemicals or shifts in microbial community also influence the activity of soil enzymes to temperature (Yi, et al., 2016). It has been shown that low-temperature heating increases enzyme activity, but high-temperature heating destroys these enzymes. (Pape, et al., 2015) was shown that the low-temperature heating releases nutrients and causes cell lysis, but this is often accompanied by the addition.

#### **2.4.3.4. Best management practices (BMPs) approach for TD**

Similar to a coin, the effect of soil remediation techniques on contaminant removal and soil quality had two sides. On the one hand, reducing the level of soil dangerous contaminants to the allowable ranges. On the other hand, the adverse effects of remediation techniques on the physicochemical and biological properties of soil (e.g. pH, SOM, texture, enzyme activities and microbial diversity). Through the use of green and sustainable remediation (GSR), environmental footprints and undesirable effects may be minimized, and remediation may be optimized ( (Sheldon, 2014); (Yasutaka, et al., 2016)). Integrated into site management decisions, GSR aims to achieve a balance of economic, ecological, and social impacts. The mission of the cleanup is to protect environment and human health by utilizing best management practices (BMPs) of green remediation to minimize environmental footprints while maintaining the day-to-day objectives of the cleanup. BMP provided by US EPA can specify daily operations that meet the goals of green remediation (EPA, 2008). A site-specific plan can be developed to reduce air emissions and energy use, to preserve water quality and conserve resources, to establish near-term ecosystem improvements that can carry forward into site revitalization, to reduce material consumption, and reduce waste generation.

For instance, in TD remediation techniques, energy efficiency and soil quality are crucial indicators of sustainability. Several approaches to improving energy efficiency are available, such as: renewable energy-based technologies, energy-efficient technologies, and the application of coupled technologies. Solar energy as a free and promising source of energy for thermal remediation has been applied to the treatment of organic and inorganic contaminated soil ex situ in conjunction with soil vapor extraction and vitrification ( (Nakamura, et al., 2000); (Navarro, et al., 2009); (Navarro, et al., 2014); (Sierra, et al., 2016); (Navarro, et al., 2013)). Interfacial solar steam technique as a green and sustainable technology utilizes sustainable solar energy source to drive water evaporation is recently developed for soil remediation. The studies demonstrated the significant potential of interfacial solar evaporation technologies for being use in soil remediation ( (Wu, et al., 2022); (Liu, et al., 2022)). For in situ thermal remediation projects, the underground thermal energy storage (UTES) can increase efficiency of thermal bioremediation (Wang, et al., 2022b). The Drake Landing Solar Community as the first community-scale borehole thermal energy storage system in North America showed the great potential of solar energy in soil treatment (Catolico, et al., 2016).

As discussed, thermal treatment can damage the soil properties that is against the principles proposed by the Sustainable Remediation Forums (Ellis & Hadley, 2009). Recent studies showed that LTTD is a more sustainable method to improve energy efficiency and to diminish damage caused to soil properties (Ren, et al., 2020); (Ding, et al., 2019)). LTTD not only is a quick and efficient remediation contaminated soils, but also improves soil reusability by preserving the SOC, pH, and water holding capacity and increasing the NO<sub>3</sub>--N and NH<sub>4</sub>+--N content (Ren, et al., 2020). Therefore, BMPs approaches contribute to mitigating climate change and achieving carbon neutrality by using LTTD, as well as providing a robust and sustainable approach to remediating organic contaminated soils. Waste heat recovery unit of several industries has potential to be used as a source to provide the required heat for the LTTD. (Thekdi & Nimbalkar, 2015) reported that the melting compartments of secondary aluminium industries and thermal oxidizers of chemicals and petroleum refining industries with producing exhaust gases with temperature of 790–1090°C and 760–980°C, respectively, are some of them. The main evaluation steps of BMPs for TD processes are shown in Figure 2. 5.

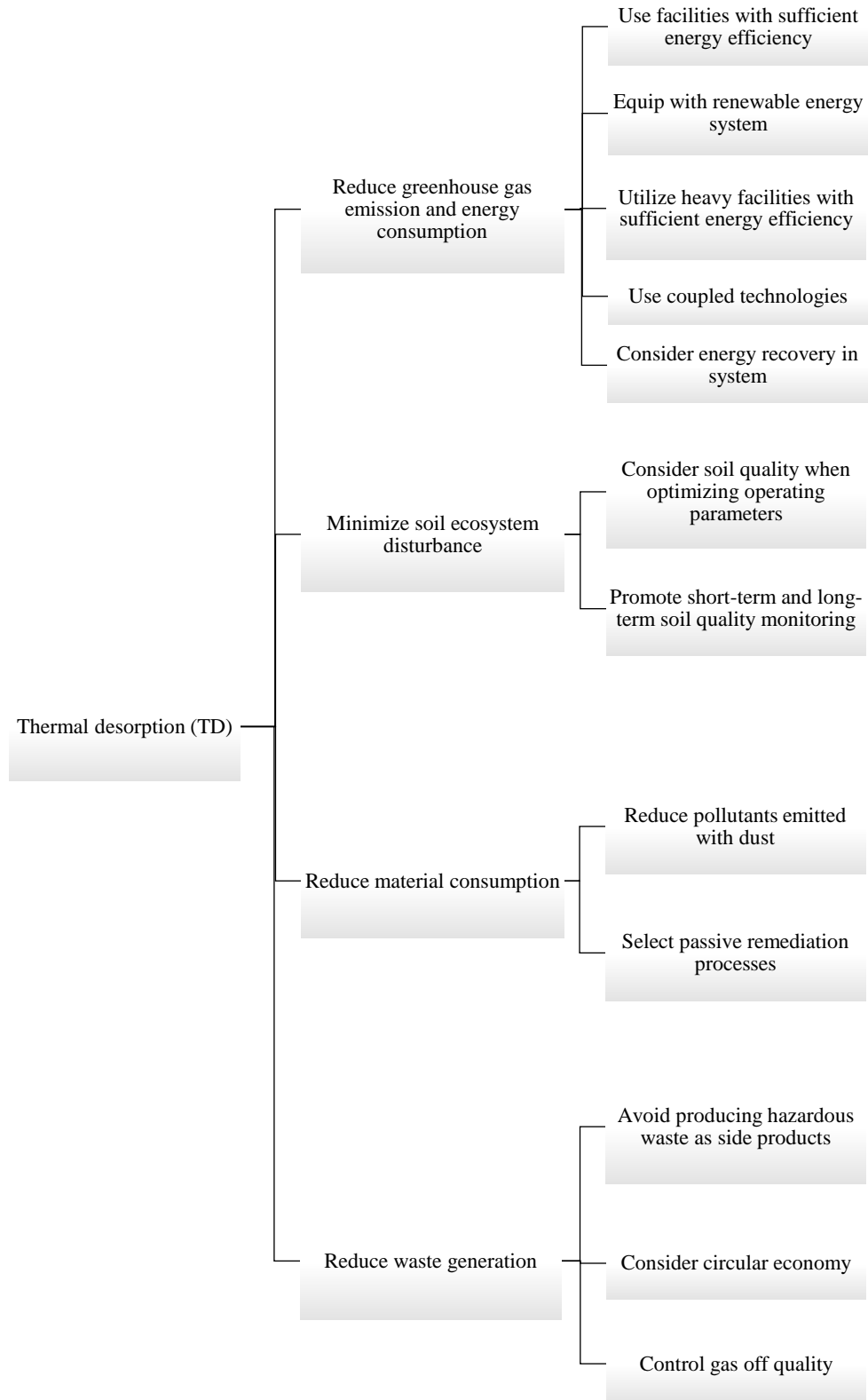


Figure 2.5. BMPs evaluation result of thermal desorption remediation techniques.

## 2.5. Scope and Objectives

In contrast to prior investigations, this study did not assess pure aluminum powders; instead, we employed genuine aluminum alloy powder samples obtained from firms specializing in aluminum surface treatment. Concerning the examination of thermal treatment's impact on soils contaminated with the aforementioned POPs contaminants, the existing literature revealed that prior studies only evaluated the efficacy of thermal treatment for specific heating durations and temperatures. Hence, to gain a more comprehensive understanding of the remediation process, a thorough investigation encompassing a broad spectrum of heating durations and temperatures' effects on remediation efficiency is essential. It is also crucial to note that this thesis project is industry-driven, thus the research objectives were determined based on the company's priorities and interests. To achieve this, a series of laboratory experiments were conducted using a lab-scale furnace to assess the efficacy of thermal desorption under varying conditions, including different temperatures, treatment durations, and atmospheres. This methodology enables a comprehensive evaluation of the optimal treatment conditions for reducing the concentration of the target contaminants in contaminated soils and mitigating the reactivity of the aluminum alloy powders.

For this, a series of experimental tests were conducted to evaluate the effectiveness of a lab-scale thermal treatment furnace in reducing the reactivity of aluminium alloy powders and remediating contaminated soils. Various tests and analyses were employed to assess the thermal processes. For instance, 360 thermal tests were conducted on aluminium powder to examine the impact of different heating times and temperatures on the reduction of aluminium-alloy powder reactivity. Additionally, 12 tests were performed to measure the ignition delay of various samples, while 20 thermogravimetric analyses (TGA) were carried out to characterize the behaviour of the samples under increasing furnace temperatures. Furthermore, 5 X-ray crystallography tests provided detailed information about the crystallographic structure and chemical composition of the samples, and 10 scanning electron microscope tests helped to determine the effects of heating time and temperature on the physical and especially surface properties of the samples. To evaluate the effectiveness of thermal remediation for soil samples contaminated with PCBs and banned pesticides, 12 TGA tests were conducted to observe the behavior of the samples as the furnace temperature increased. For PCB-contaminated soil, 27 lab-scale thermal furnace tests were performed at various furnace temperatures and heating times. The number of tests for pesticide-

contaminated soil was 45. Additionally, 12 TGA tests were conducted to study the kinetics of the samples.

The primary goals of this study can be summarized as follows:

4. **Efficient Waste Management and Resource Recovery:** The research aims to improve the efficiency of thermal treatment processes for solid hazardous wastes, with a specific focus on optimizing operational parameters such as heating time and temperature. By doing so, the study intends to facilitate the recovery of valuable resources from these wastes and contribute to the principles of a circular economy.
5. **Minimization of Environmental Contamination:** The research seeks to reduce, eliminate, or alter organic persistent pollutants, such as polychlorinated biphenyls and banned pesticides, in contaminated soil samples. This objective is crucial for mitigating the environmental degradation caused by these pollutants and safeguarding the environment and public health.
6. **Safety and Reactivity Mitigation:** For inorganic waste types, the research aims to alleviate the reactivity of hazardous waste samples. This is significant in preventing potential energy release, such as combustion or explosions, within the workspace, thereby enhancing safety measures.
7. **Optimization of Thermal Treatment Processes:** The study will delve into the critical role of operating conditions and control parameters in shaping the outcomes of thermal treatment methods. Understanding this complex interplay is essential not only for maximizing resource recovery but also for minimizing environmental impacts and ensuring the safety of these processes.

In summary, the overarching purpose of this research is to advance the field of hazardous waste treatment and soil remediation by improving the efficiency of thermal treatment processes, addressing contamination issues, and contributing to resource conservation and sustainability.

# **Chapter 3: Materials and Methods**



## **Overview**

This section provides a detailed account of the tools, materials, and procedures employed in this study, enabling other researchers to replicate the experiment and verify its validity. It is within this chapter that the author outlines the methodology, addressing the key question of how they pursued answers to their research questions.

In the following section, I will delve into a comprehensive description of the materials used, both in terms of the equipment and the specimens under study. Additionally, I will elucidate the procedures undertaken in conducting the research, including the experimental design, data collection, and data analysis techniques employed. By outlining these essential aspects, the "Materials and Methods" chapter serves to offer transparency and reproducibility, facilitating a critical assessment of the research's reliability and validity. Moreover, it offers a roadmap to the reader, guiding them through the journey of the research and explaining the choices made by the researchers in their quest for knowledge. This chapter has been thoughtfully subdivided into two distinct sections, each dedicated to a specific facet of our research.

The first section of the "Materials and Methods" chapter is intricately linked to our exploration of aluminium reactive powders—a crucial component in various industrial applications, with a particular emphasis on its reactivity and potential for controlled combustion. Our rigorous investigation into these reactive powders necessitates a thorough examination of the materials involved, as well as the methodologies employed to elucidate their behaviour. Through this section, we aim to provide a clear and detailed account of the tools, procedures, and experimental designs tailored to uncover the intricacies of aluminium reactive powders.

In parallel, our research extends its focus to the second section of the "Materials and Methods" chapter, which is dedicated to the examination of soil contaminated with persistent organic pollutants. Here, we will outline our approach in analysing and remediating contaminated soil, ensuring a meticulous account of the equipment, techniques, and processes used to address this issue.

By categorizing our "Materials and Methods" chapter into two distinct sections, we aim to provide clarity, transparency, and precision in our research approach. This division not only assists in streamlining the comprehension of our study but also offers a tailored perspective on the specific domains under investigation.

A series of experimental tests were carried out to assess the efficacy of a lab-scale thermal treatment furnace in mitigating the reactivity of aluminum alloy powders and remediating contaminated soils. Diverse tests and analyses were employed to evaluate the thermal processes. For example, 360 thermal tests were conducted on aluminum powder to investigate the impact of different heating times and temperatures on reducing the reactivity of aluminum-alloy powder. Furthermore, 12 tests were conducted to measure the ignition delay of various samples, and 20 thermogravimetric analyses (TGA) were performed to characterize the behavior of the samples under increasing furnace temperatures. Additionally, 5 X-ray crystallography tests provided detailed information about the crystallographic structure and chemical composition of the samples, and 10 scanning electron microscope tests helped to determine the effects of heating time and temperature on the physical and surface properties of the samples. To evaluate the effectiveness of thermal remediation for soil samples contaminated with PCBs and banned pesticides, 12 TGA tests were conducted to observe the behavior of the samples as the furnace temperature increased. For PCB-contaminated soil, 27 lab-scale thermal furnace tests were performed at various furnace temperatures and heating times. The number of tests for pesticide-contaminated soil was 45. Additionally, 12 TGA tests were conducted to study the kinetics of the samples.

This study evaluated the presence of microplastics (MPs) in contaminated soils using the density separation method with zinc chloride. Soil samples contaminated with banned pesticides were collected from an industrial area, and the concentration of MPs was found to be negligible. However, the separation tests on the PCB-contaminated soils revealed a significant number of MPs in the samples. As a result, the methodology and results of the tests related to MPs were presented in the section on PCB-contaminated soil.

### **3.1. Aluminium alloy waste powders**

The characteristics of the aluminium powders as a by-products of metal working processes vary depending on the production techniques. A total of five aluminium waste samples was collected from different surface treatment industries. Surface treatment companies in Northern Italy use a variety of processes to treat aluminium surfaces, including shot blasting and polishing. In blasting, different blasting media are sprayed at high velocity onto the metal surface for the purpose of treating the metal surface. Blasting is mainly used to remove contaminants from the surface of castings, in preparation for subsequent finishing treatments, such as painting, enamel coating, or mechanical treatment. Shot blasting is typically performed with rotating blade machines in which a stream of cleaning agents (steel grains or

iron shots) is emitted, bombarding the casting's surface (Pathak & Dodkar, 2020). Instead, mechanical polishing process involves using abrasive media, flat wheels, sandpaper, wool berets, polishing sponges to remove scratches, nicks, and other surface defects created during the machining process. Polishing is a technique for improving the appearance and shine of the surface either manually or mechanically, thereby achieving the desired surface structure (Hou, et al., 2022).

For this study, in three blasting factories that performed blasting on aluminium surface, dusts captured through drawholes and sent to a cyclone followed by a bag filter. Thus, three samples were collected from different grinding filter powders. In addition, two samples were collected from factories where polishing operations were conducted on aluminium products. According to the European Waste Catalogue adopted by Decisions (EU) N° 995/2014 and 1357/2014 of 18 December 2014 of the Council of the European Community, as amended by Decisions 2000/532/EC, all the samples found in this study are classified as hazardous waste according to the EWC 12 01 14\* and 12 01 16\* ( (EC, 2014a), (EC, 2014b)). Note that the purpose of this study is neither to assess the hazards associated with the samples nor to control their coding. In this study, the effect of ZnO alloy powder as an additive on the ignition and oxidation properties of the S3 and S5 was investigated. To prevent using raw materials, a zinc oxide alloy powder, which was produced as a waste in a metal industry, was utilized as an additive for decreasing the aluminium ignition delay time. The chemical composition of ZnO alloy powder is listed in Table 1. The mass fraction of the S3 and S5 to the ZnO alloy powder mixture was 1:1, 1:2, and 1:4 (w:w).

For decelerating the aging of aluminium particles, fresh aluminium waste powders were rapidly stored in vacuum bags. The particle-size distribution of the dust was realized on dry samples of about 50 g using a Ro-Tap Tyler mechanical sieve equipped with Tyler mesh sieves. A balance with  $\pm 0.0001$  g sensitivity performed for weighing operations. The morphology of the samples was determined using a scanning electron microscope (SEM) with a Zeiss EVO MA10 (Carl Zeiss, Oberkochen, Germany). The X-ray diffraction (XRD) pattern was characterized on a D2 Advance powder X-ray diffractometer (Bruker, Karlsruhe, Germany). The elemental composition of the samples was determined through an acid digestion of 0.5 g waste with 15 ml of 37% hydrochloric acid and 5 ml of 65% nitric acid in a DigiBlock with 95 °C for 2 hours. The cold digested samples were filtered on a Whatman grade 542 filters. Then, metal contents determination was performed by means of an ICP Agilent Plasma Spectrometer.

### 3.1.1. Unreacted aluminium measurement

In this study, free aluminium content was indirectly determined by measuring the volume of gas released following the reaction between aluminium waste and NaOH solutions of 30 wt%. Due to strong alkalinity of NaOH solutions, aluminium-water reaction is quick (Alviani, et al., 2019). As suggested by (Zhu, et al., 2019) and (Shi, et al., 2021), the efficiencies of the medium temperature thermal pre-treatment of aluminium waste samples can be obtained by measuring the content of the unreacted Al in the sample after thermal pre-treatment. To determine unreacted aluminium in a sample, previous studies utilized volumetric techniques using hydroxide promoters such as NaOH, Ca(OH)<sub>2</sub>, CaO, and salt promoters such as NaCl (Cai, et al., 2022). Adding these components disrupts the aluminium oxide layer on aluminium particles and releases hydrogen gas.

The schematic of the hydrogen generation and alkaline water-aluminium reaction temperature systems used in the experiment were shown in Figure 3. 1(a). Equation 3. 1 shows the water-aluminium reaction in the presence of NaOH as a hydroxide promoter (Xiao, et al., 2018).



Here are the equations that can be used to calculate the unreacted Al content in thermal pre-treated products ( (Zhou, et al., 2017); (Xiao, et al., 2018)):

$$n_{\text{Al}} = n_{\text{H}_2}/1.5 \quad \text{Equation 3. 2}$$

$$W_{\text{Al}}^{\text{S}} = 26.98 \left( \frac{\text{g}}{\text{mol}} \right) \times n_{\text{Al}} \quad \text{Equation 3. 3}$$

$$W_{\text{Al}}^{\text{S}} = 26.98 \left( \frac{\text{g}}{\text{mol}} \right) \times n_{\text{Al}} \quad \text{Equation 3. 4}$$

$$W_{\text{Al}}^{\text{P}} = W_{\text{Al}}^{\text{S}} \times W_{\text{P}}/W_{\text{S}} \quad \text{Equation 3. 5}$$

$$\eta = (W_{\text{Al}} - W_{\text{Al}}^{\text{P}})/W_{\text{Al}} \times 100 \quad \text{Equation 3. 6}$$

where  $V$  refers the volume of hydrogen produced by the reaction of unreacted aluminium with NaOH-water ( $ml$ );  $W_{\text{Al}}^{\text{S}}$  is the mass of aluminium in the tested sample ( $g$ );  $W_{\text{S}}$ ,  $W_{\text{P}}$  and  $W_{\text{Al}}$  are the mass of tested sample ( $g$ ), the total mass of the thermal pre-treated product ( $g$ ) and the total mass of Al in the original sample, respectively;  $W_{\text{Al}}^{\text{P}}$  is the total mass of aluminium in the thermal pre-treated product. Moreover,  $\eta$  refers to the thermal pre-treatment efficiency.

### 3.1.2. TGA test

The determination of the parameters of non-isothermal oxidation under the standard conditions of programmed heating in an atmosphere of air can be utilized to compare the reactivity of the powders (Esposit, et al., 2020). Parameters for an evaluation of the reactivity of powders, including temperature of intensive oxidation onset ( $T_{on}$ , °C), the mass gain at the first oxidation step ( $\alpha I$ , mass %), and the total mass gain at the end of the oxidation process ( $\alpha T$ , mass %), can be obtained during the processing of the results of non-isothermal oxidation under standard conditions of programmed heating in an atmosphere of air using thermogravimetric analysis (TGA) and differential thermal analysis (DTA) curves (Chen, et al., 2009); (Kwon, et al., 2004)).

The medium temperature thermal pre-treatment characteristics of aluminium powder wastes under nitrogen atmosphere (anaerobic condition) and air atmosphere (aerobic condition) were tested by heating the fine powder samples (~5 mg) in an open Pt crucible from room temperature to 1000 °C at the rate of 10 °C/min in a thermogravimetric Q5000 apparatus (TA Instruments, New Castle, DE, USA) interfaced with a TA5000 data station. Then, to achieve 25 °C, the instrument was ventilated until it was completely cooled.

### 3.1.3. Tubular furnace simulation experiments

Four different furnace set points (450, 475, 500 and 525 °C) were selected based on the TGA to identify the ignition delay time, the optimum heating time, and to evaluate the efficiency of medium temperature thermal pre-treatment for reduction of the reactivity of aluminium waste samples. The tubular furnace consists of an air cylinder, a tube furnace, and a temperature controller (Figure 3. 1(b)). When the temperature of the tube furnace reached the set temperature, the air with the flow rate of 300 (l/h) was continuously fed into the quartz tube for 15 min to ensure that air was exhausted. Then, an alumina boat (105×14×9 mm) was loaded with sample (~70 mg); then, it was placed into the centre of the tube furnace.

Ignition delay is the amount of time necessary to destroy the weak oxide film on the surface of Al particles that allows the fresh aluminium core to easily react with oxygen to form a strong oxide film in the presence of temperature. To obtain the ignition delay time of each sample, a video camera was used. In this experiment, ignition delay time ( $t_d$ ) was interpreted as the duration of time between when sample appeared below window and the first

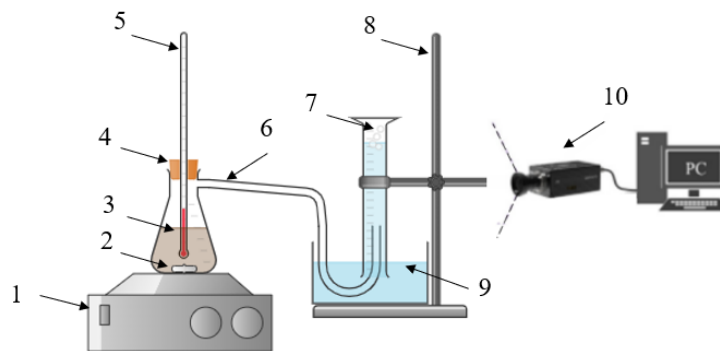
combustion phenomenon occurred. The ignition delay time was captured utilizing a video camera and the ignition delay time ( $t_d$ ) is as follows:

$$t_d = t_i - t_0 \quad \text{Equation 3. 7}$$

where  $t_0$  is the time of the first image of the sample captured inside the tube furnace and  $t_i$  is the time corresponding to the first appearance of ignition phenomenon of sample.

a)

- 1) Magnetic stirrer
- 2) Magnetic stir bar
- 3) Mixture of NaOH solution and sample
- 4) Bung with one hole
- 5) Thermometer
- 6) Elastic tube
- 7) Hydrogen gas
- 8) Iron frame
- 9) Water tank
- 10) Camera



b)

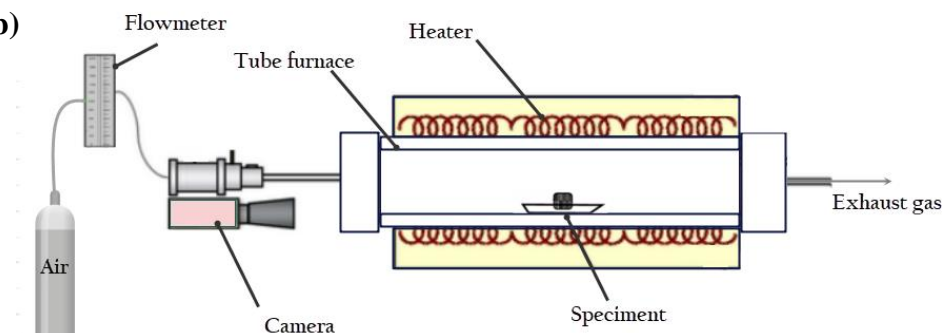


Figure 3.1. Schematic diagram for the experimental systems; (a) Gas volume measurement system; (b) Tubular furnace

## 3.2. Soils contaminated with persistent organic pollutants

### 3.2.1. PCB-contaminated soil

The samples were obtained from the earth canal downstream Caffaro S.p.A. chemical factory, which produced PCBs and PCB mixtures, such as Fenclor and Apirolio, between 1930 and

1984 in Brescia, Italy (Di Guardo, et al., 2017). The temperature of Brescia typically varies from -1 °C to 30 °C and is rarely below -6 °C or above 34 °C and precipitation amounts to 890 mm/year. The earth canal was contaminated by outflowing water and runoff from the factory. Soil samples were collected in winter season when the vegetation has gone dormant, and the canal was dry. The sample was taken from the top 10 cm layer of the irrigation ditch sediments. The sample were homogenised manually to reduce the local variability, wrapped in acetone-washed aluminium containers, and labelled.

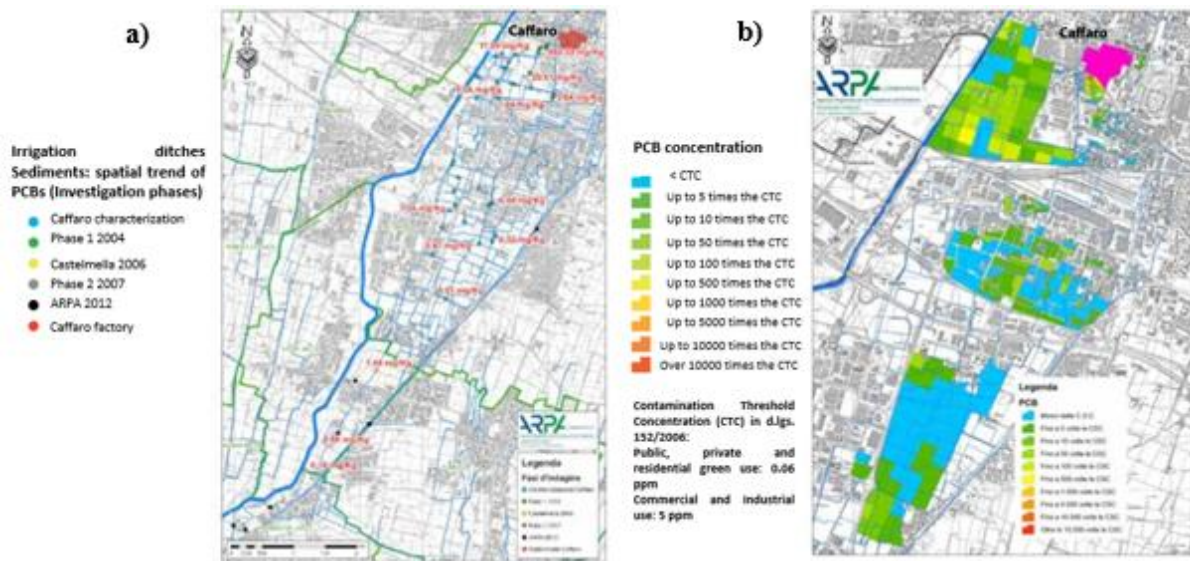


Figure 3. 2. (a) Investigations on irrigation ditch sediments: spatial trend of PCBs; (b) PCB contaminated soils downstream Caffaro S.p.A.

The samples were sequentially pretreated by Soxhlet extraction, solvent exchange and purification before analysing with a gas chromatographer. Gas chromatography results give the sum of the concentrations of PCBs present in the sample. After extraction with n-hexane, each organic extract was submitted to GC analysis three times. Twenty-nine PCBs isomers from Tri- (TCB) to Hepta-chlorinated (HCB) as well as 34 PCDD/Fs isomers from tetra- to octa-chlorinated homologue groups were detected. The total concentrations of PCB/PCDD/PCDF and individual congeners concentrations were quantified by adding a set of mixtures of internal standard solutions applied before extraction, purification and analysis respectively (Figure 3. 3). The general characteristics of the contaminated soil were shown in the Table 3. 1.

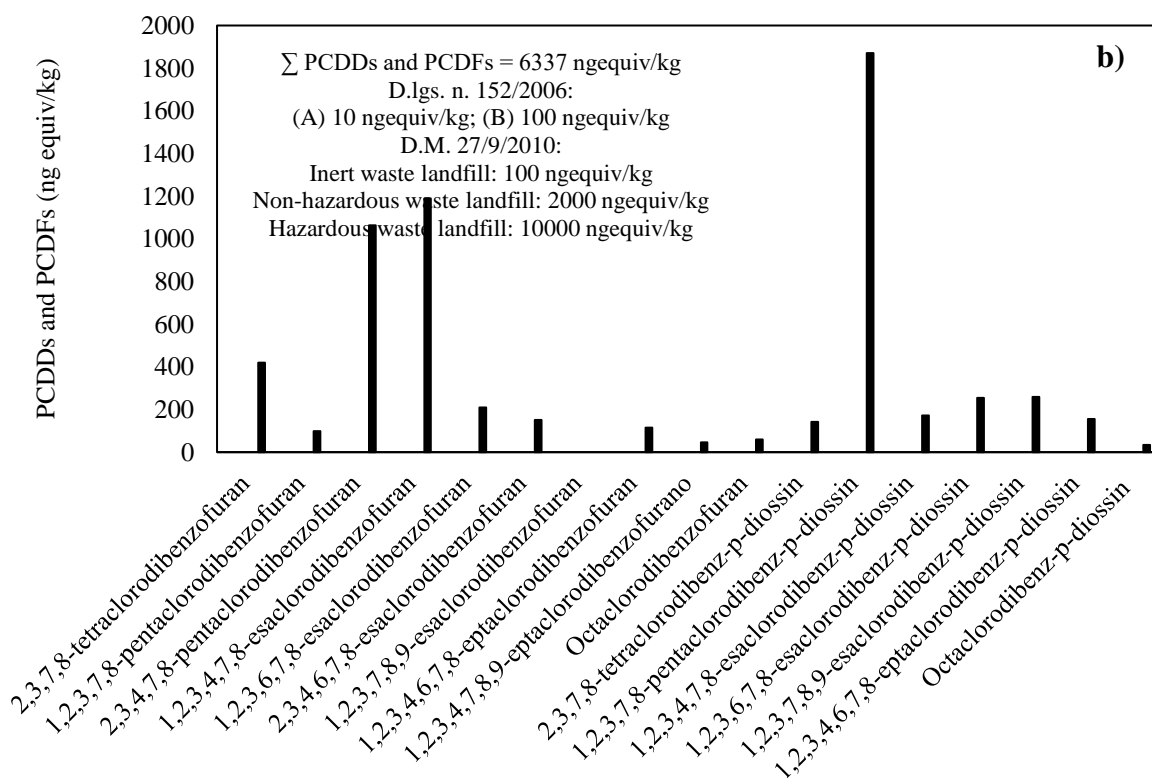
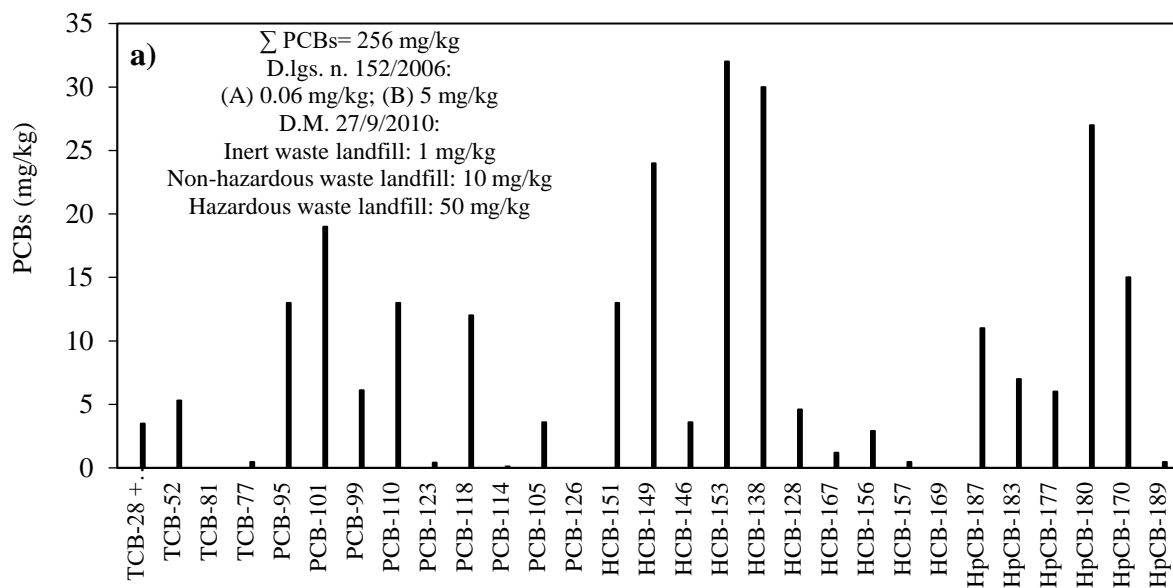


Figure 3.3. Concentration of the PCB congeners; (b) Concentration of PCDD and PCDF congeners



Table 3.1. Physicochemical properties of contaminated soil

| Property                       | Value  |
|--------------------------------|--|
| Soil texture (%)               | Sand (44.63); silt (53.11); clay (2.21)  |
| Total Carbon (TC) (%)          | 7.952  |
| Total Organic Carbon (TOC) (%) | 5.219  |
| C10-C40 (ppm)                  | 180.9  |
| Metals (ppm)                   | Al (9409.22); As (61.64); B (33.02); Cd (4.02); Cr (185.72); Cu (424.69); Fe (27836.98); Mg (15566.68); Mn (966.99); Mo (5.33); Na (489.93); Ni (72.81); Pb (441.45); Sb (14.2); Sn (19.09); Zn (728.87) |

The method used for separating the microplastics from soil samples is briefly comprised of three steps: 1) fully mixing the sample with saturated solution of sodium chloride (NaCl) and sodium iodine (NaI); 2) allowing the sample to rest for flotation and settling; and 3) sieving of the supernatant. As part of the study on the uptake of polychlorinated biphenyls by microplastics in terrestrial systems, the liquid remained in a vacuum filtration unit and the residual soil was assessed for PCB concentrations.

In this study, the thermal treatment characteristics of soils polluted by polychlorinated biphenyls (PCBs) and microplastics under nitrogen atmosphere (anaerobic condition) and air atmosphere (aerobic condition) were tested by heating the sample (~5 mg) in an open Pt crucible from room temperature to 1000 °C at the rate of 10 °C/min in a thermogravimetric Q5000 apparatus (TA Instruments, New Castle, DE, USA) interfaced with a TA5000 data station. Then, to achieve 25 °C, the instrument was ventilated until it was completely cooled.

Contaminated sample was tested simulating ex-situ thermal process conditions using a bench scale apparatus consisted of an air cylinder, a tube furnace, and a temperature controller (Figure 3. 1 (b)). The tubular electric furnace with maximum power of 1.5 kW could reach a maximum temperature of 1100 °C. Once the electric oven reached the desired temperature, air with a flow rate of 300 (l/h) was continuously fed into the quartz tube for 15 min to ensure that air was exhausted. Then, alumina boat (105×14×9 mm) was inserted into the centre of an axially isothermal temperature region of the alumina cylinder tube with a 30-mm diameter and a length of 200 mm.

### 3.2.1.1. Extract and quantify microplastics (MPs) in soil systems

Density separation is a method that can be employed to isolate microplastics (MPs) ranging in size from 1 to 5000  $\mu\text{m}$ . The steps involved in this methodology are as follows:

Assemble the density separator.

- Add 50 mL of  $\text{ZnCl}_2$  solution (concentration = 700 g/L) to the dried sample. It is important to stir the  $\text{ZnCl}_2$  solution for at least 24 hours before adding it to the sample.
- Place the sample in the density separator.
- Rinse the glass bottle with  $\text{ZnCl}_2$  solution to transfer any remaining solids to the density separator.
- Loosely cover the density separator with aluminium foil.
- Allow the solids to settle for 1 hour at room temperature.
- Collect the floating MPs into a flask using forceps and a glass Pasteur pipette.
- Remove the Mohr's pinch clamp and drain any settled solids and  $\text{ZnCl}_2$  solution into a flask.
- Rinse the density separator several times with distilled water to transfer all solids to the flask containing the recovered MPs.
- Stir the flask with MPs and the flask with  $\text{ZnCl}_2$  for 10 to 15 minutes.
- Vacuum filtration is the next step in this process:
- Filter the  $\text{ZnCl}_2$  solution and settled solids (if present) through a 0.45  $\mu\text{m}$  clean membrane filter using a sand funnel connected to a vacuum system. It is important not to rinse with distilled water, as this can cause precipitation of  $\text{ZnCl}_2$ .
- Store the reused solution in a glass bottle at 4°C.
- Filter the plastic samples through a 0.45  $\mu\text{m}$  clean membrane filter using the same filtration process.
- Rinse the filtration setup with distilled water several times to ensure that no MPs were lost.
- Once filtration is complete, carefully remove the membranes and place them in Petri dishes. Place the Petri dishes in a 40°C drying oven for 3 to 5 days.
- Visual inspection is the final step:
- Use a stereomicroscope Optika with 1.5X magnification to select the MPs.
- Count and/or weigh the MPs using an analytical laboratory balance.

- Identification achieved through Fourier-transform infrared spectroscopy (FTIR).

### 3.2.2. Soil contaminated by pesticides

The sample was collected from a contaminated site of an old chemical company that synthesized OC pesticides in North of Italy. The contaminated site was divided into eleven main regions, and a 5 m depth soil core (0–5 m) was collected at each sampling site using professional drilling equipment equipped with a direct push system. Then, samples at the depth of 0 to 1 m, 1 to 2 m, 2 to 3 m, 3 to 4 m, and 4 to 5 m were collected in sequence. The pesticide contents of the collected samples and thresholds values were shown in Figure 3. 4.

The thermal treatment characteristics of organochlorine pesticides under nitrogen atmosphere (anaerobic condition) and air atmosphere (aerobic condition) were tested by heating the samples (~5 mg) in an open Pt crucible from room temperature to 1000 °C at the rate of 10 °C/min in a thermogravimetric Q5000 apparatus (TA Instruments, New Castle, DE, USA) interfaced with a TA5000 data station. Then, to achieve 25°C, the instrument was ventilated until it was completely cooled.

A furnace set point (400 °C) was selected based on the TGA to identify the optimum heating time, and to evaluate the efficiency of thermal treatment of OC pesticides contaminated sample. The tubular furnace consists of an air cylinder, a tube furnace, and a temperature controller (Figure 3. 1 (b)). When the temperature of the tube furnace reached the set temperature, the air with the flow rate of 300 (l/h) was continuously fed into the quartz tube for 15 min to ensure that air was exhausted. Then, an alumina boat (105×14×9 mm) was loaded with sample (~70 mg); then, it was placed into the center of the tube furnace.

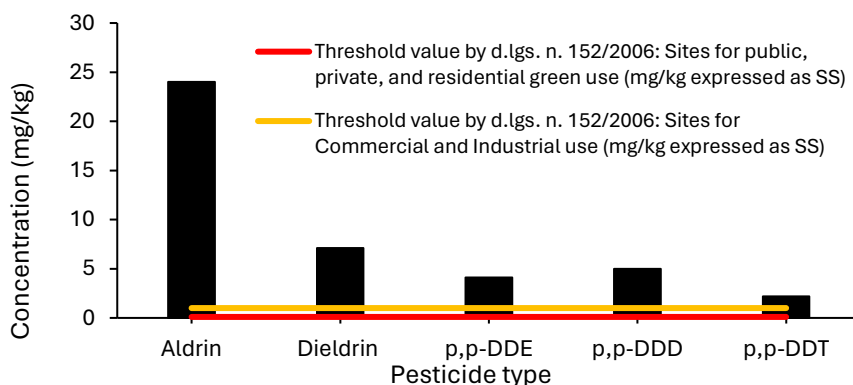


Figure 3.4. The contamination level and threshold for the different pesticides listed in Italian Legislative Decree n. 152/2006

# **Chapter 4: Results and Discussion**

## **4.1. Aluminium alloy waste powders**

### **4.1.1. Basic characteristics of the samples**

The main elements identified in each sample are listed in Table 1. The most abundant element in the analysed samples was Al. Among the elements discovered were Cu, Mg, Pb, and Zn, as well as other elements at low concentrations. The identified elements included Cu, Mg, Pb, Zn, and other elements at low concentrations (Table 4. 1). The S4 and S5 obtained from polishing processes. Therefore, these samples contained a certain amount of the mineral oil and organic matters depending on the age of the polishing tools, and on the pressure and speed adopted to polish the pieces. Although the amounts of these components were relatively low, they constituted a major effect on the particle size distribution and the reactivity behaviour of the samples.

According to the scanning electron microscope images of the samples (Figure 4. 1), it can be concluded that the morphology of the samples is affected to a great extent by the manufacturing process that generates the powders. The powders feature mainly non-spherical. In general, the particle texture appears cluster with smooth surface. In the case of shot blasting samples (Figure 4. 1 (a), (b) and (c)), the repeated fragmentation of particles during blasting causes mechanical breakage of the oxide film and consequently provides the direct contact between oxidiser and fresh surfaces of aluminium. Moreover, some zinc oxide particles have been stuck to aluminium particles during blasting.

The particle size distribution for all tested samples is illustrated in Figure 4. 1 (f). As shown, samples associated with blasting processes contain a high proportion of fine particles. For instance, about 94% particulate S1 compounds by weight were less than 0.1 mm diameter and 66 wt% was less than 0.05 mm. The sample S5 has a fraction over 1 mm about equal to the 30 wt%. However, a total of 22 wt% of the S4 remained over the sieve 1 mm. Essentially, the residues left behind by using cloth, brushes, and sponges to polish the surfaces were remained in this range. The polisher material residues vary in quality and quantity depending on the technique used for polishing a metal surface. The organic matter test revealed 38.78 wt% of the S5 contains organic matters that consists mainly of long threads of organic residues of polishers (Figure 4. 1 (d) and (e)). The organic content of the S4 was about 28.74 wt%.

Table 4.1. Chemical analyses of the selected wastes produced in the aluminium surface treatment industries

| Sample              | S1   | S2   | S3   | S4                                     | S5                                     | A                |        |
|---------------------|--|--|--|--|--|------------------|--------|
| Waste European Code | 12 01 16*                                  | 12 01 16*  | 12 01 16*                                  | 12 01 14*                              | 12 01 14*                              |                  |        |
| Waste origin        | Grinding filter powder; from shot blasting | Grinding filter powder with CaCO <sub>3</sub> ; from shot blasting | Grinding filter powder; from sand blasting | Grinding filter powder; from polishing | Grinding filter powder; from polishing | ZnO alloy powder |        |
| Organic matter      | %wt  | -  | -  | -                                      | 28.74                                  | 38.78            | -      |
| Mineral oil         | %wt  | -  | -  | -                                      | 8.29                                   | 5.14             | -      |
| Al                  | 1519567.4                                  | 514,003.31   | 98,303.09                                  | 11,749.05                              | 38,527.90                              | 78288.94         |        |
| As                  | 37.23                                      | 0.00   | 31.76                                      | 3.84                                   | 2.02                                   | 10.2             |        |
| B                   | 292.62                                     | 236.44   | 94.23                                      | 7.63                                   | 6.92                                   | 32.25            |        |
| Be                  | 0.03                                       | 0.04   | 1.11                                       | 0.03                                   | 0.06                                   | 0                |        |
| Cd                  | 1.10                                       | 0.00   | 59.91                                      | 0.97                                   | 0.28                                   | 3.31             |        |
| Co                  | 0.00                                       | 0.00   | 51.68                                      | 0.00                                   | 0.85                                   | 236.97           |        |
| Cr                  | 42.21                                      | 47.33  | 2747.14                                    | 24.89                                  | 21.59                                  | 512.18           |        |
| Cu                  | 1351.26                                    | 874.58   | 3635.68                                    | 781.03                                 | 1146.02                                | 9647.06          |        |
| Mg                  | 5386.44                                    | 43971.9  | 702.22                                     | 300.34                                 | 409.63                                 | 6058.45          |        |
| Mn                  | mg/kg                                      | 147.04   | 182.94                                     | 5457.92                                | 167.19                                 | 115.29           | 491.07 |
| Mo                  | 32.99                                      | 12.63  | 128.2                                      | 2.20                                   | 2.26                                   | 30.75            |        |
| Na                  | 1076.24                                    | 566.24   | 364.3                                      | 286.89                                 | 487.78                                 | 48406.97         |        |
| Ni                  | 108.47                                     | 72.40  | 1244.07                                    | 9.26                                   | 32.27                                  | 2712.72          |        |
| Pb                  | 530.02                                     | 351.04   | 944.86                                     | 92.04                                  | 53.56                                  | 338.65           |        |
| Sb                  | 146.9                                      | 91.84  | 99.05                                      | 7.7                                    | 5.84                                   | 66.51            |        |
| Se                  | 11.85                                      | 5.26   | 0.00                                       | 0.27                                   | 0.22                                   | 52.06            |        |
| Sn                  | 19.35                                      | 15.80  | 41.30                                      | 1.82                                   | 6.23                                   | 16.6             |        |
| Tl                  | 214.35                                     | 246.1  | 86.97                                      | 6.42                                   | 9.93                                   | 1.59             |        |
| V                   | 0.00                                       | 0.00   | 0.00                                       | 0.00                                   | 0.00                                   | 431.32           |        |
| Zn                  | 345.22                                     | 294.55   | 71895.44                                   | 52958.52                               | 620.08                                 | 138160.47        |        |

Attention: 12 01 14\* machining sludges containing dangerous substances

12 01 16\* waste blasting material containing dangerous substances

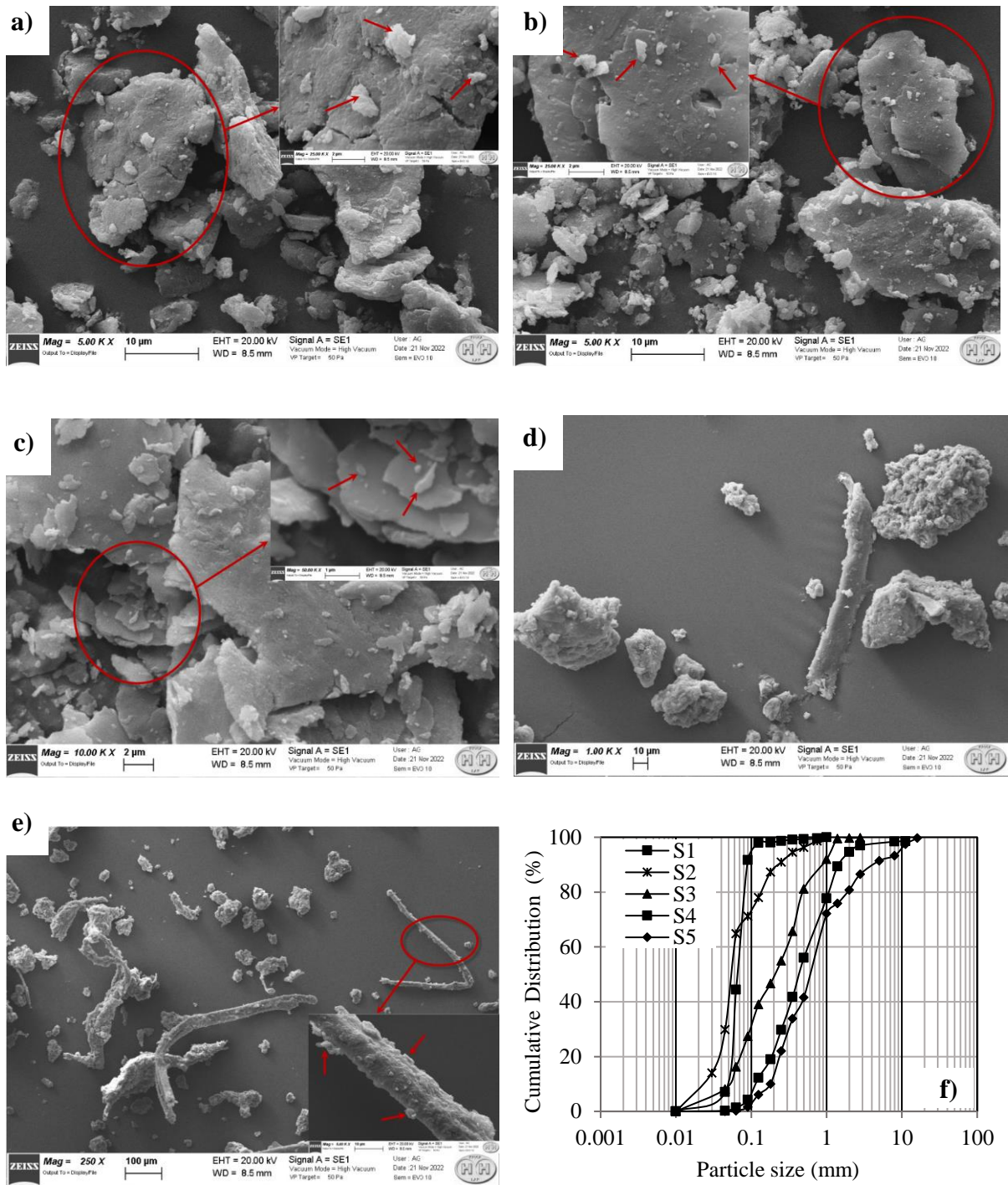


Figure 4. 1. SEM characterization of the tested samples: (a) the S1; (b) the S2; (c) the S3; (d) the S4; (e) the S5; (f) particle size distribution of the tested samples

The remained samples over each sieve were collected and evaluated to determine the effects of particle size on reactivity of the samples. For the S1, results demonstrated that reactivity, which implies the content of metallic aluminium in powders, increases with decreasing

particle size. This result is in agreement with the previous studies conclusions that metal content of such powders typically decreases with increasing particle size ( (Il'in, et al., 2001); (Rufino, et al., 2007)). However, for the polishing samples, the remained samples over sieve 1 mm interestingly release more hydrogen gas respect to the samples with particle size less than 125  $\mu\text{m}$ . Testing for mineral oil revealed that the Samples 4 and 5 contained 8.29 wt% and 5.14 %wt mineral oil, respectively. Mineral oil used in polishing processes basically because of its excellent lubricating properties. Generally, in polishing processes, mineral oil was absorbed by polisher materials. As a result, micro and nano-sized aluminium waste particles were trapped by mineral oil, and they were attached to polisher residues. This might explain the reason of higher reactivity of larger particles compared to those with smaller particles in the S5. Due to the organic content, temperature increase, and release of combustible gas associated with hydrolysis of aluminium, the polisher residues of the S4 and S5 require treatment.

#### **4.1.2. Hydrogen generation capacity of the raw samples**

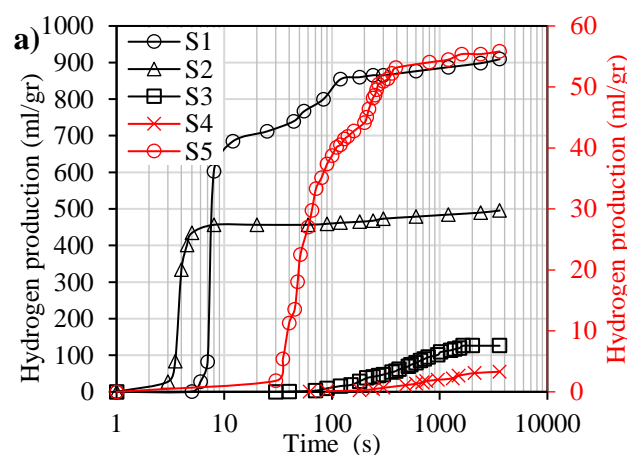
Figure 4. 2 (a) shows a trend of changing hydrogen production (normalized with the weight of tested sample) with increasing reaction time. When the activator solution (NaOH) remains constant in all runs, the hydrogen production start time and the hydrogen production volume of each sample are unique and dependent on both granulometry and chemical properties of the samples. Although the S2 showed the fastest response to the alkaline water solution, 74.4 % of the volume of hydrogen which measured after 24 hours was released within the first hour of the reaction. Because of the greater proportion of the particles smaller than 0.5 mm, the S2 has the fastest start time while its aluminium content is lower than the S1. The S1 released 87.62% of its long-term measured hydrogen in the first hour of the reaction. For the S1 and S2, a large volume of gas was observed in a short period of time after starting the reaction, indicating their potential hazard in the presence of hydroxide promoters. Compared to other blasting samples, the corresponding hydrogen production start time of the S3 took longer than the other blasting samples because of its greater granulometry distribution. Following the first hour of the reaction, the hydrogen production equalled 69.16% of those corresponding to the long-term production.

A lower aluminium content in the polishing samples resulted in significantly small hydrogen production. Therefore, to identify the hydrogen generation changes during the reaction time,



the corresponding values for the S4 and S5 were shown in the second Y-axis. Due to the more aluminium content of the S5 compared to the S4, spontaneous alkaline water-aluminium reaction of the S5 is faster. The results of the S4 and S5 revealed that 22.16% and 99.73%, respectively, of the long-term hydrogen production were achieved within the first hour of the reaction.

The effects of different aluminium waste samples on alkaline water temperature changes are illustrated in Figure 4. 2 (b). A significant temperature rise occurred for the S1. The alkaline water temperature increased from 26 °C to 46.5 °C in 12 (s) for the S1 while increasing to 37°C was observed in 10 seconds for the S2. The alkaline water temperature changes for the S3, S4 and S5 were 5°C, 1.5°C and 11.5°C, respectively. A similar finding corresponding to the rise of temperature in alkaline water-aluminium reactions was reported by (Li, et al., 2011) and (Cai, et al., 2022). A comparison of Figure 4. 2 (b) and (c) indicates that hydrogen generation rate is associated with alkaline water temperature rise. As shown, the temperature of alkaline water increases just before hydrogen is released due to the oxidation reaction. This confirms the (Rosenband & Gany, 2010) conclusion which an increase in alkaline water temperature likely further accelerates hydrogen production rate. Consequently, due to elevated temperatures and explosive gases produced by leachate hydroxyl ions shortly after aluminium samples are dissolved in water, the samples cannot be disposed in landfills without being pre-treated.



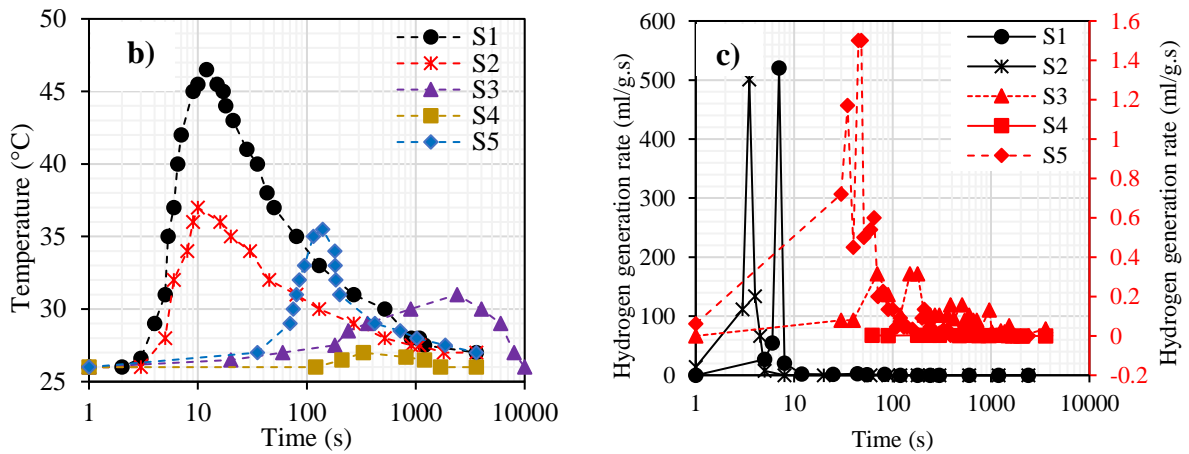
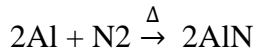


Figure 4. 2. (a) hydrogen production of different samples over an hour; (b) temperature change during the reaction of aluminium and alkaline water; (c) hydrogen generation rate during the reaction of aluminium and alkaline water

#### 4.1.3. Thermal reaction characteristics of the tested samples

Figure 4. 3 shows the TGA and DTG curves of the samples measured under anaerobic and aerobic conditions at a heating rate of 10 °C/min. Different samples exhibited significantly different TGA profiles. For the S1, it is possible to distinguish three main mass change steps. The first mass loss stage is from room temperature to about 400 °C with 2.3% mass loss which can be due to the solvent release. Then, it follows with two continuous mass gain steps. The first mass gain step of about 9.7% ends at 720 °C. In the corresponding DTA curve, an exothermic peak is suddenly affected by the latent heat of aluminium melting at 600 °C. Then, the second intense mass gain step (about 34.9%), which not yet concluded at 1000 °C, took places. This intense mass gain in the second step is because of the melting of Al which causes the volume expansion of Al core and resulting in compress pressure within the tensile stress on the oxide film and the Al core. Therefore, the samples S1 exhibit significant mass gain (around 37%) since the oxidation of Al between 400 °C and 1000 °C. Moreover, the slope of the mass gain steps indicates the oxidation rate of the sample which decreases with increasing the reaction time. Since the thickness of oxide film on the Al surface increases, the slope of mass gain branch or reaction rate decreases.

On the contrary, under nitrogen atmosphere, the S1 shows a slow mass loss from room temperature up to 500 °C, that mass loss step can be due to the solvent release. Although nitrogen is considered as a nearly inert gas, aluminium nitride forms when aluminium is heated above 830 °C in atmosphere of nitrogen and the reaction involve is Equation 4. 1 (Mondolfo, 1976).



Equation 4. 1

The DTA curve (Figure 4. 3 (a)) can be used to investigate the reaction between nitrogen and aluminium. The DTA curve shows an exothermic peak around 820 °C probably related to the aforementioned reaction. As concluded by (Saravanan, et al., 2001) Saravanan et al. (2001), aluminium and nitrogen react even at temperatures as low as 850 °C. Therefore, the consistent mass gain between 500 °C and 1000 °C is mainly due to the transformation of Al to AlN.

To reduce or eliminate the fire and explosion likelihoods, the manufacturer that produced the S2 added calcium carbonate powder as an inert powder into a bag filter powders. By means of thermogravimetric analysis (TGA), influences of CaCO<sub>3</sub> on oxidation process and thermal behaviours of aluminium waste powder are shown in Figure 4. 3(b). Under air atmosphere, the TGA curve includes four weight change steps. With regard to the solvent release, there is a weight loss step during the heating up the sample at 25–575 °C. By increasing the temperature up to 610 °C, there is a continuous weight gain in the TG curve resulting from oxidation process of Al particles. In the zone of 610-730 °C, the TGA/DTA curve is indicative of the overlapping of one peak of exothermic reaction and two peaks of endothermic reactions. The intensity of the endothermic process of the decomposition of CaCO<sub>3</sub> and the process of aluminium melt has overshadowed the exothermic process of oxidation. Because of this, the DTA curves cannot depict these stages clearly. By continuing to increase the temperature up to 1000 °C, a noticeable mass gain is achieved due to the oxidation process, although the gain has not completed. Decomposition of calcium carbonate similarly affects the oxidation behaviour of the S2 under N<sub>2</sub> atmosphere (Figure 4. 3 (b)). However, the total mass gain value obtained for N<sub>2</sub> atmosphere differ considerably from those obtained from air atmosphere.

The corresponding TGA curves of the S3 are shown in Figure 4. 3(c). In air atmosphere, there is no mass gain or any mass loss to the temperature limit of 200 °C. This is indicative of the fact that no significant oxidation or decomposition has taken place within the temperature range of room temperature to 200 °C. As the temperature is increasing, a continuous mass gain is started around 200 °C and the mass gain has not been completed at 1000 °C. The production process of the S3 may give insight into why oxidation is taking place at such low temperature (at 200 °C). During the production of the S3, the manufacturer applies solid lubricants to burnish and compact the coating, thereby optimizing the surface area of the

coating on the substrate. Solid lubricants can react and be oxidised with exposure to temperature. Along with this mass gain, an exothermic peak is not observed in the DTA curves between 200 to 1000 °C. While the temperature increases, the oxidation of the metals takes place, leading to increase in the mass gain reaching a total of about 12.31% at 1000°C.

Figure 4. 3 (d) shows the baseline corrected TGA and DTA traces for the samples S4 under air and nitrogen atmosphere, respectively. In nitrogen atmosphere, after a solvent release step (0.8% up to 125°C), a first mass loss ending at around 275°C leads to a 10% mass loss. After this, releasing the organic matters with low evaporation temperature take place, ending at 320°C (3.4%). Then, it follows with an intense mass loss step at 350 °C (see the DTG peak) due to the desorption of organic matters with high evaporation temperature. By increasing the temperature, two further mass variations of 0.3% and 3% take place between 510 °C and 650 °C and from this temperature value to 1000°C, respectively. The total mass loss of the S4 is about 31%. In addition, the S4 shows mass loss steps under air atmosphere. However, it is less distinguishable. A first multi-step process, from 125°C to 525°C, leads to a strong mass loss of 30.8%. This mass loss step mainly occurs because of the desorption of organic matters. Finally, a small mass increase of 0.4% is detected between 650 and 1000 °C, indicating that Al particles react with oxygen in the chamber.

For the sample S5, the solvent release ends at about 100°C under nitrogen (Figure 4. 3(e)). A desorption step accounting for 6.2 % mass gain takes place, ending at 205°C. Subsequently, due to the presence of organic matters with the high evaporation temperature, a strong mass loss (34.8%) is recorded up to 600°C, including 4 steps which the most important one was ended at 410 °C. The mass remains constant starting from 800°C. However, the total mass loss is about 42.34%. Under air, the sample S5 shows a negligible solvent release (Figure 4. 3(e)). By increasing the temperature, a 4-step decomposition process accounting of 36.4% mass loss is recorded from 100°C to 500°C. From 530°C to 620°C a 1.2 wt% mass gain is recorded, and then a 2.2 % mass loss ends at 700°C. A further increase in temperature leads to a mass gain of about 2.5% at 1000°C.

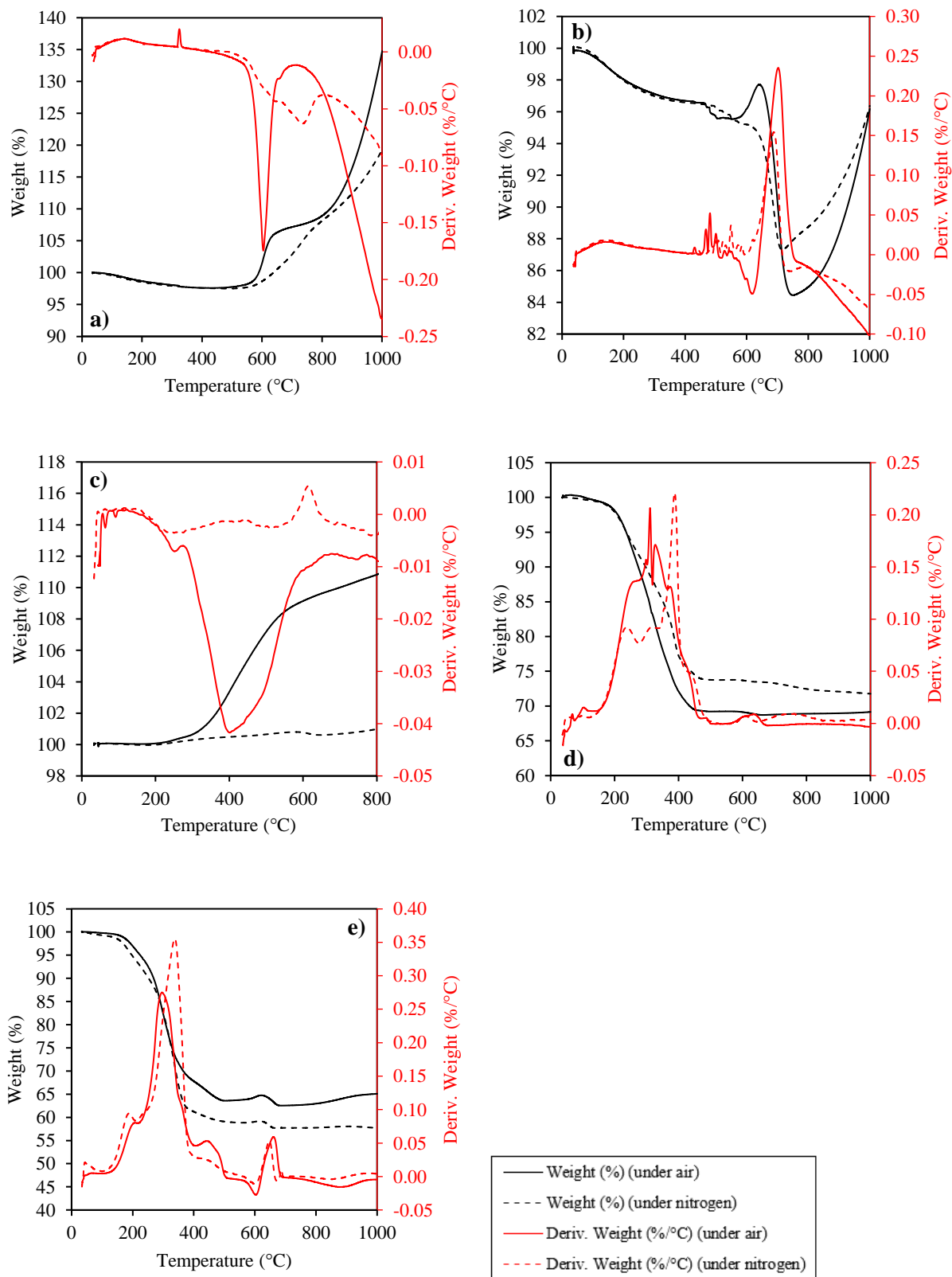


Figure 4. 3. TGA/DTA curves of (a) the S1; (b) the S2; (c) the S3; (d) the S4; (e) the S5

#### **4.1.4. Pre-treatment simulation experiment of the samples in a tubular furnace**

The blasting samples and polishing samples showed different combustion behaviour inside the furnace (Figure 4. 4). When the blasting samples (S1 and S2) are loaded into the tube furnace, they absorbed heat and slowly turned red. Depending on the furnace set point, chemical composition of the samples, and more importantly the thickness of oxide shell which has been formed due to the aging of Al particles, the S1 and S2 are ignited after a specific delay times. Firstly, the samples are partially ignited, then the combustion area spreads out. The brightness of combustion area of the S1 is obviously higher than that of the S2, indicating that the release heat of the S1 is larger. As the S1 and S2 ignited, the tube furnace temperature increased, verifying the release of heat. Both samples exhibit the highest ignition delay at 450 °C and it decreases with increasing the furnace set point. In comparison with the S1, the S2 has a relatively low Al content, but it showed a strong ignition at the tested temperatures. This is principally because of its high percentage of small particles with large self-heating rate, which becomes dominant for the ignition of Al particles ( (Trunov, et al., 2005a) and (Trunov, et al., 2005b)). In addition, a considerable percentage of magnesium (Mg) as an alloying component leads to decrease the Al ignition delay time and temperature (Yagodnikov, et al., 2006).

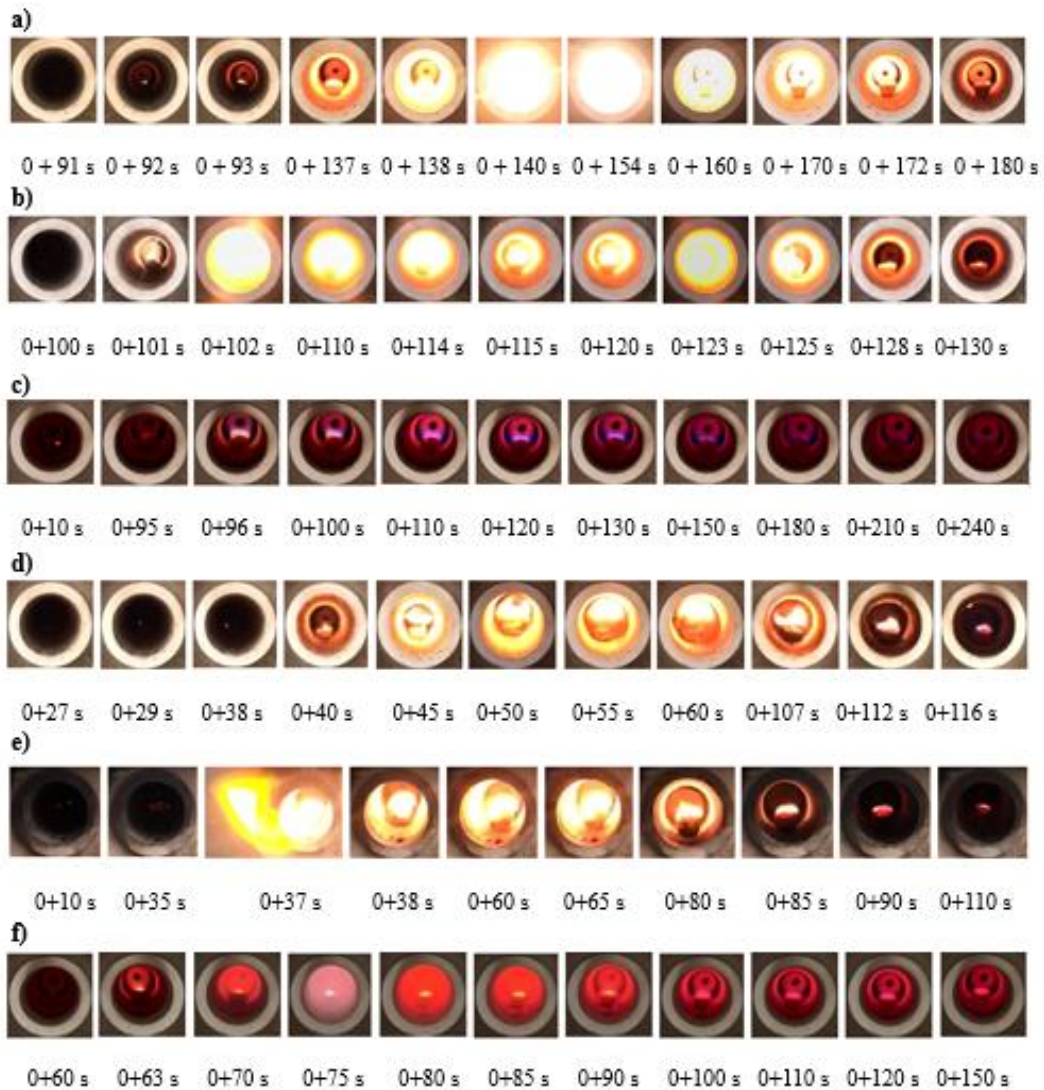


Figure 4.4. The ignition and combustion phenomena of the samples; a) the S1 at 500 °C; b) the S2 at 500 °C; c) the S3 with additive 1:4 (w:w) at 525 °C; d) the S4 at 500 °C; e) the S5 without additive at 500 °C; f) the S5 with additive 1:2 at 525 °C.

The reduction efficiency of hydrogen production of Al powder represents its effectively oxidized amount, which is a very important parameter to characterize the reactive Al content. For estimating the effect of heating time on thermal treatment efficiency to reduce the reactivity of different samples, unreacted Al content was calculated by measuring the volume of gas. According to Figure 4. 5 and Table 4. 2, the samples that are taken out of the furnace before ignition occurs are much more reactive than those left inside the furnace for longer periods of time. This is because the ignition causes the weak alumina shell on the Al particle surface to be broken, and the exposed active Al rapidly reacts with oxygen. Therefore, ignition contributes as an important heat feedback mechanism for influencing the oxidation rate.

The XRD patterns of the combustion products of the tested samples, after being heated in the tube furnace, are shown in Figure 4. 6, the diffraction peaks of metal oxide be detected. In the SEM images shown in Figure 4. 7, the combustion products of the S1 and S2 are submicron needles, and the combustion products of the S3, S4 and S4 are spheres. Thus, the microstructure of the combustion products of all the tested samples changed radically in comparison with the initial powders. Obviously, the appearance of combustion products in the form of needles of submicron diameters results from participation of the gaseous phase in the formation of the final products (Il'in, et al., 1999).

The S3 without an additive cannot be ignited at any of the tested furnace set points, so its ignition delay time is not presented in Table 4. 2. Some methods have been introduced to improve the ignition of Al particles. One approach is to increase the proportion of nano-sized Al compared to micron-sized Al since nanosized Al particles have lower ignition temperature and faster burning rate ( Parr, et al., 2003); (Ohkura, et al., 2011)). In addition, for the enhancement of the ignition process of Al powders, Al can be blended with some materials. Many efforts have been made to understand the effects of different additives (e.g. chromium chloride (CrCl<sub>3</sub>) (Rozenband, et al., 1990), sodium fluoroaluminate (Na<sub>3</sub>AlF<sub>6</sub>) (Shi, et al., 2021), sodium fluoride (NaF) (Zhu, et al., 2019), potassium fluoride (KF) (Shi, et al., 2019), nickel (Ni) (Rosenband & Gany, 2007), magnesium (Mg) (Shoshin, et al., 2002), silicon (Si) (Parimi et al., 2017), silica (SiO<sub>2</sub>) (Zhu, et al., 2022), zinc addition (Tsao, et al., 2002)) on pure aluminium/aluminium alloys' thermal characteristics. Since resources shortage and environmental concerns are increasing, moving toward a resource-efficient and circular economy is essential. Waste prevention target which defined by circular economy strategy can be achieved through eco-design, reuse, repair, refurbishment, re-manufacturing, and extended producer responsibility (EPR) schemes (Busu, 2019). Several researchers have studied the aluminothermic reaction in Al/ZnO system leading to the formation of in-situ Al<sub>2</sub>O<sub>3</sub> at relatively lower temperatures ( (Maleki, et al., 2010); (Durai, et al., 2008a); (Durai, et al., 2008b); (Hedayati, et al., 2011); (Durai, et al., 2007a)). According to Ellingham diagram for oxides, zinc oxide reacts with aluminium as following ( (Karimzadeh, et al., 2008); (Durai, et al., 2007b ); (Tavoosi, et al., 2008)):



According to the Equation 4. 2, this reaction is exothermic. While this reaction is thermodynamically possible at room temperature, the reaction normally occurs at very high



temperatures due to kinetics difficulties. A proper combination of suitable alloy addition and thermal process can modify the reaction of the system. For the S3 with addition of 1:1, 1:2, and 1:4 (w:w) ZnO alloy powder, at 525 °C, the ignition delay times are 75, 70, and 61 s, respectively. The results showed that the ignition delay times of the S3 significantly decreased with addition of ZnO alloy powder. (Maleki, et al., 2018) confirmed that a short time high temperature contact between aluminium and ZnO leads to the formation of epitaxially grown layers of ZnAl<sub>2</sub>O<sub>4</sub> and Al<sub>2</sub>O<sub>3</sub>. The XRD patterns of the oxidation products of the mixed S3 with ZnO alloy powder (with 1:4 w:w), at 525°C for 5 min, is in good agreement with the results of (Maleki, et al., 2018). Therefore, the addition of ZnO alloy powder can decrease the ignition delay time and, consequently, improve the efficiency of thermal treatment of the S3. This can be certified by the results of reactivity test (Figure 4. 5), that is, the reaction reactivity of the S3 with addition of ZnO alloy powder is remarkably higher than that of the S3 without additive.

According to the XRD pattern of the S3, at least nine reactions may have taken place between 200 and 1000 °C, which justifies the presence of the nine new oxide compounds identified in the XRD pattern: CuMn<sub>2</sub>O<sub>4</sub>, Sb<sub>2</sub>O<sub>4</sub>, ZnAl<sub>2</sub>O<sub>4</sub>, CuAl<sub>2</sub>O<sub>4</sub>, Al<sub>2</sub>O<sub>3</sub>, MgCr<sub>2</sub>O<sub>4</sub>, ZnAl<sub>2</sub>O<sub>4</sub>, ZnO and MoO<sub>2</sub>. Regarding the reaction between solid lubricant like Sb<sub>2</sub>S<sub>3</sub>, Cu and Zn, (Lee, et al., 2013) and (Cho, et al., 2006) reported that Sb<sub>2</sub>S<sub>3</sub> oxidation takes place in the temperature range of 300-430 °C, where Sb<sub>2</sub>S<sub>3</sub> is converted to Sb<sub>2</sub>O<sub>5</sub> and Sb<sub>2</sub>O<sub>3</sub> and then to Sb<sub>2</sub>O<sub>4</sub> at 570 °C. The study by (Martinez & Echeberria, 2016) was confirmed that the reaction between the metal powders and the lubricant starts at temperatures between 350 and 400 °C, except for the Cu–Sb<sub>2</sub>S<sub>3</sub> system, where it starts at a lower temperature (200 °C).

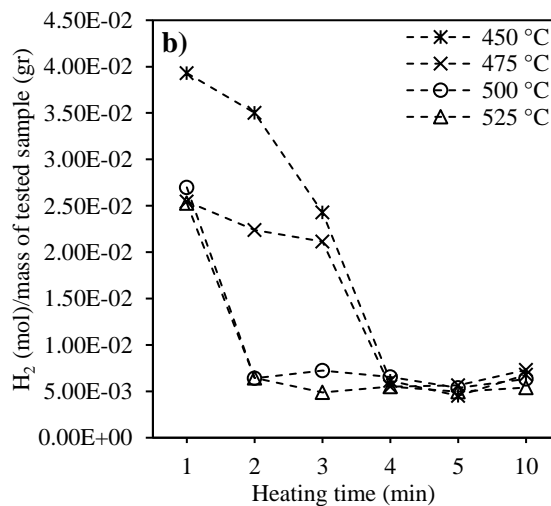
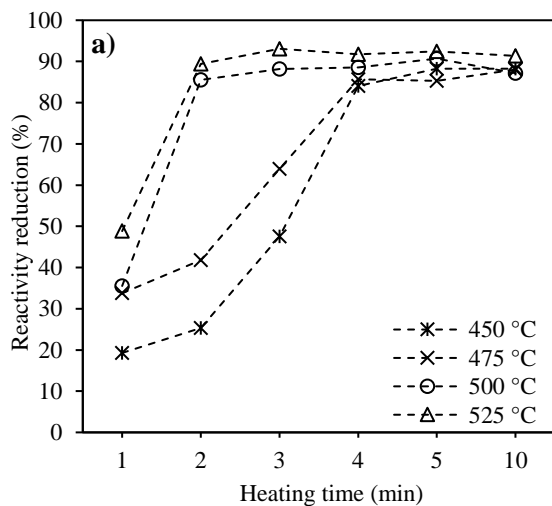
For the S4, observations obtained by ignition test in the tube furnace complete and confirm results obtained by TGA analysis. Both methods prove that oxide film formation is not thermally stable and if the temperature below 475°C, only desorption of organic matters and mineral oil occurs. At 450 °C, the combustion of organic matters proceeds and the presence of CO<sub>2</sub> in off-gas is probable. Although the intermittent flame was observed in this temperature, the S4 could not be ignited, so its ignition delay times are not presented in Table 4. 2 Ignition delay time (expressed in seconds) corresponding to the tested samples at different furnace set temperatures. When the S4 exposed to temperature above 475 °C, the ignition delay times are 54, 43, and 25 s, respectively. As a result of ignition, the degradation of organic parts is complete, and only the inorganic parts remain, which have been tested for their reactivity. The ignition delay time is considerably affected by the heating temperature,

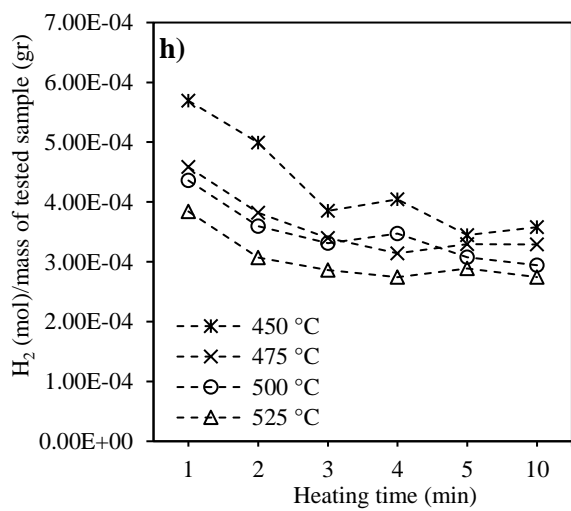
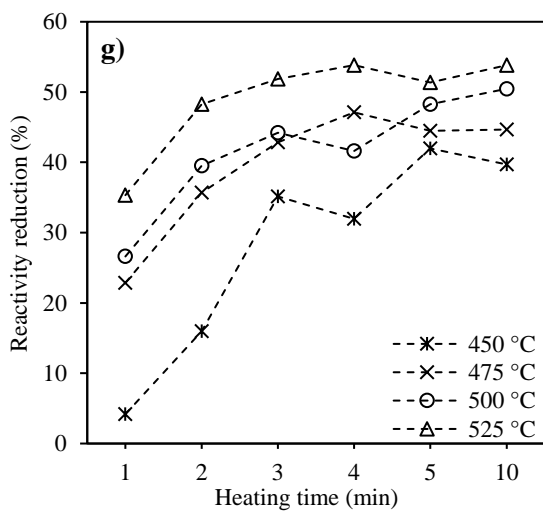
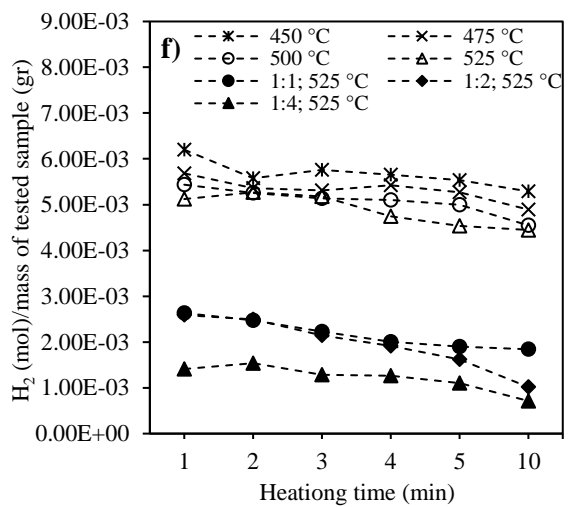
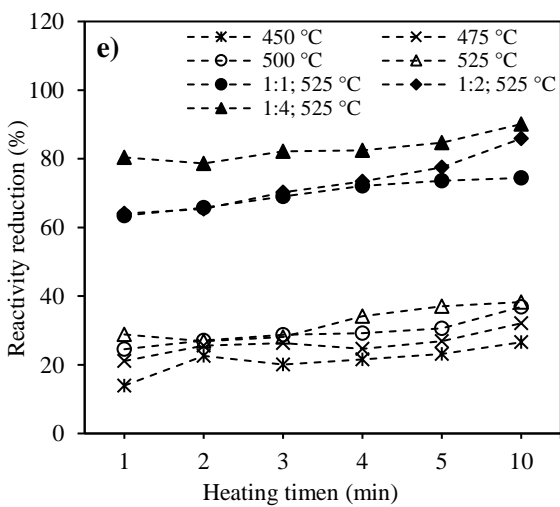
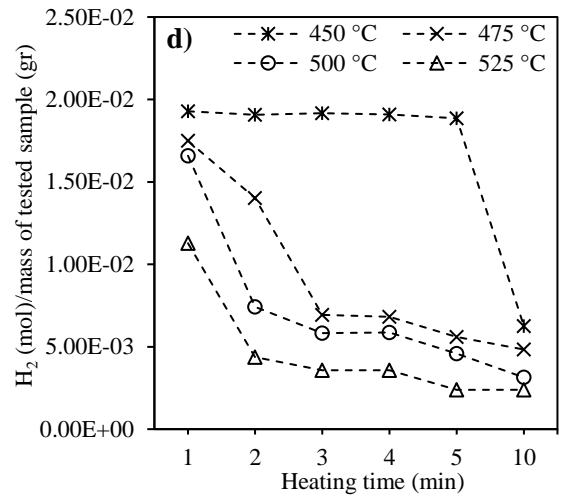
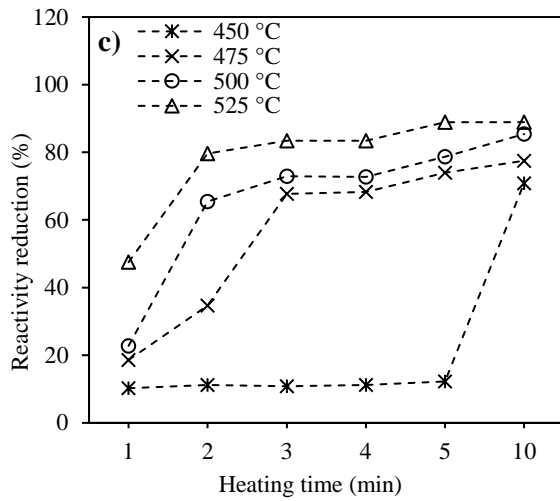
especially, when it increased from 500 to 525°C. The corresponding reactivity values of the combustion products confirmed that for proper decreasing of reactivity, the S4 need to remain in a furnace for at least 4 min at 525 °C. It should be noted that the reactivity of the S4 in a highly alkaline solution was illustrated in Figure 4. 5 (d). However, reactivity of the S4 with deionised water during a month observation was zero.

In the S5, organic compounds were decomposed after exposure to higher temperature, without occurring ignition. The reactivity test on the remaining mass after exposure to high temperature showed that the thermal treatment of the S5 without additive is not sufficient to reduce the reactivity of this sample. Therefore, the S5 was blended with ZnO alloy powder with specific proportions of 1:1 and 1:2 (w:w). The ignition tests demonstrated that the adding ZnO alloy powder improves the ignition and decreases the ignition delay time of the S5.

Table 4. 2. Ignition delay time (expressed in seconds) corresponding to the tested samples at different furnace set temperatures

| Furnace set point (°C) | Sample |     |    |                |                |                |    |                |                |     |
|------------------------|--------|-----|----|----------------|----------------|----------------|----|----------------|----------------|-----|
|                        | S1     |     | S2 |                | S3             |                |    | S4             | S5             |     |
|                        |        |     |    | 1:1<br>(S3: A) | 1:2<br>(S3: A) | 1:4<br>(S3: A) |    | 1:1<br>(S5: A) | 1:2<br>(S5: A) |     |
| 450                    | 222    | 375 | -  | 98             | 92             | 85             | -  | -              | 125            | 121 |
| 475                    | 178    | 217 | -  | 90             | 85             | 78             | 54 | -              | 119            | 114 |
| 500                    | 137    | 101 | -  | 84             | 76             | 74             | 43 | -              | 107            | 101 |
| 525                    | 132    | 64  | -  | 75             | 70             | 61             | 25 | -              | 101            | 96  |





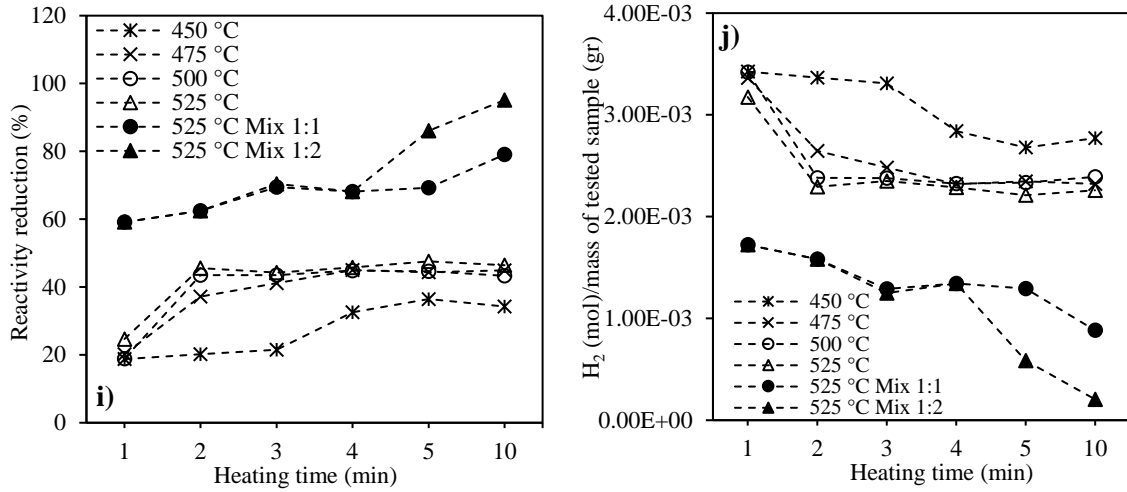


Figure 4. 5. The reactivity reduction and hydrogen production of pre-treated products vs. heating time at different set temperatures; (a and b) the S1; (c and d) the S2; (e and f) the S3; (g and h) the S4; (i and j) the S5

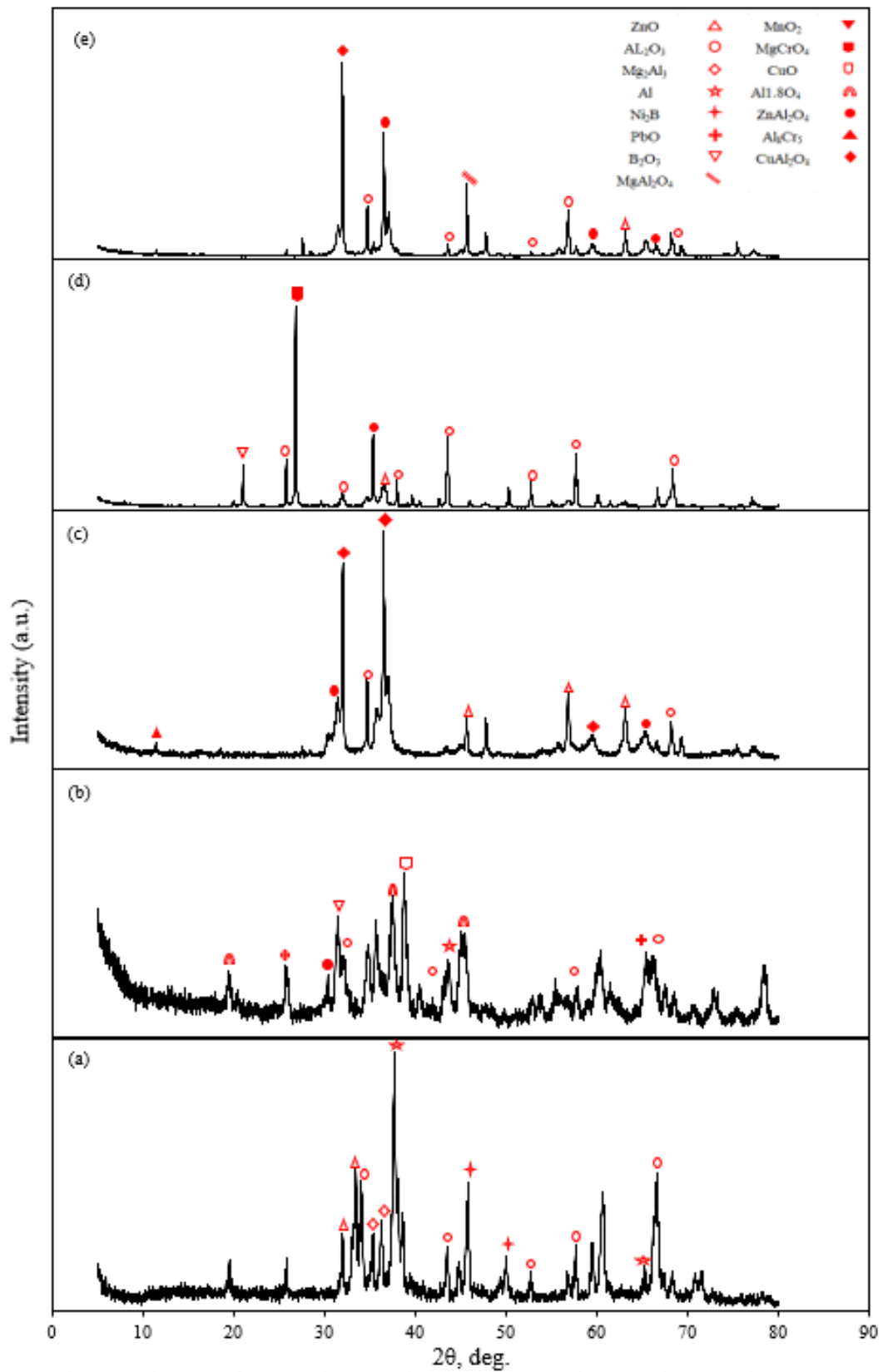


Figure 4. 6. Typical XRD result for the investigated powders; (a) the S1; (b) the S2; (c) the S3; (d) the S4; (e) the S5

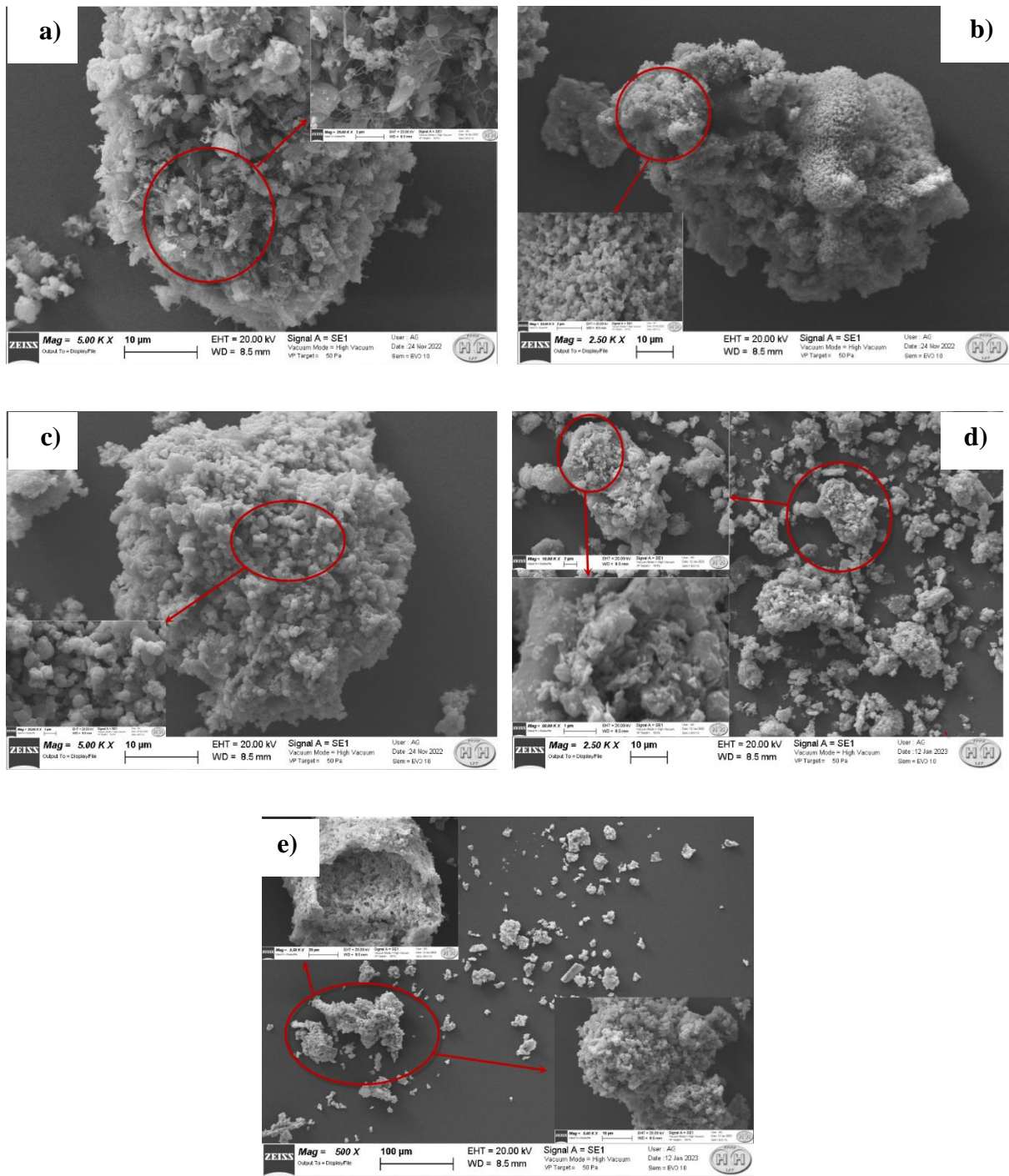


Figure 4. 7. The SEM images of the pre-treated samples in the furnace; (a) the S1 treated at 475°C for 4 min; (b) the S2 treated at 475°C for 4 min; (c) the S3 with additive (1:4) treated at 525 °C for 5 min; (d) the S4 treated at 525°C for 5 min; (e) the S5 with additive (1:2) treated at 525 °C for 10 min

#### **4.1.5. Suggestions for handling and storage of the samples**

The concept of inherent safety in the process industries utilizes for the properties of a material or process to eliminate or reduce their hazard (Amyotte, et al., 2009). One of the main principles of the inherent safety is to moderate the hazardous materials in their less severe forms. (Amyotte & Eckhoff, 2010) suggested that inertization of powders or the modification of their composition by the admixture of solid inertants, reducing dust cloud formation by increasing particle size resulting in a decrease in powder reactivity, and preventing hybrid mixtures (which involve the mixture of flammable dust, gas or solvent) can all be helpful in reactive powders modification. According to these suggestions, in this study, a thermal oxidation process was carried out on the aluminium alloy waste powders to modify the composition, morphology and hydrogen gas production capacity of the samples. Although all the raw samples react with DO water, any of the pretreated samples did not react with DO water even after a month. Nevertheless, consideration must be given to hazard prevention and mitigation when transporting, storing, and landfilling aluminium reactive powders. Great care must be taken to prevent the contact of strong acids (e.g. HCl, H<sub>2</sub>SO<sub>4</sub>, HNO<sub>3</sub>), oxidizing agents (e.g. perchlorates, peroxides, permanganates, chlorates, nitrates, chlorine, bromine and fluorine), acid chlorides, strong bases (e.g. NaOH, KOH), chlorinated hydrocarbons, and alcohols.

For raw aluminium powder wastes, attention to the general safety in the working spaces is not enough. It is strongly recommended to avoid any condition that will suspend or float powder particles in the air, creating a dust cloud. It is better if powder is transferred from one container to another using a non-sparking, conductive metal scoop with the most minimal amount of agitation. Moreover, great care must be taken to prevent the contact of water with the non-treated samples. Also, as a result of static electricity discharge, an electric spark can be generated, causing powder particles surrounding the spark to reach temperatures above their ignition temperature, causing a fire or explosion. Therefore, anything that produces a spark, such as an electric switch, a broken light bulb, a commutator on an electric motor, or a loose electric power connection (even a metal-to-metal impact), can cause an explosion of pre-treated aluminium waste powders. An explosion can be caused even by continuous metal to metal rubbing (as in a dry sleeve bearing).

## 4.2. PCB-contaminated soil

### 4.2.1. TG results

In the initial stage, the first peak on the DTG curve, below 200°C, represents the reduction in water content due to a thermal dehydration process within the samples. During the subsequent phase, 200 to 350°C, decomposition of the organic components occurs. Specifically, between 200 and 300°C (noted by the second peak on the DTG), the thermal breakdown involves simple organic matter and semi-volatile compounds. The heightened DTA peak observed in this phase under aerobic condition, compared to the peak under anaerobic condition, demonstrates the better volatilization of simple organic compounds in the presence of oxygen.

In the third phase, at higher temperatures (350–700°C, observed as the third peak on the DTG), the degradation involves aromatic structures, organic polymers, and other compounds synthesized, such as Polychlorinated biphenyls (PCBs), associated with the thermal process. The peaks on the DTG curve in this region are more pronounced when the thermogravimetric analysis is performed under anaerobic conditions. This pattern hints at a gradual shift from highly chlorinated PCBs to those with lower degrees of chlorination (e.g. from decachlorobiphenyls to monochlorobiphenyls), suggesting a transition towards lower molecular complexity and aromaticity during the thermal process.

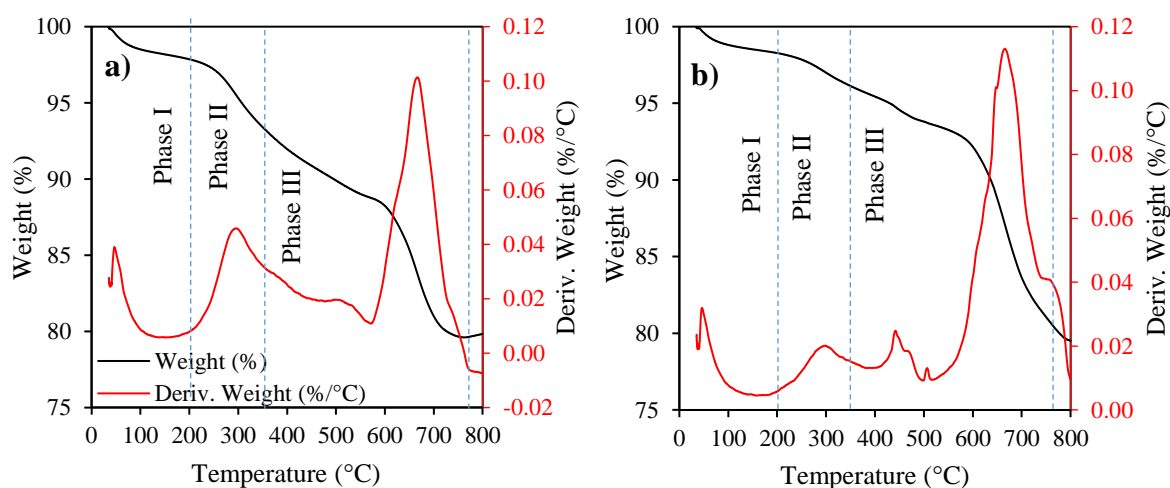


Figure 4. 8. TGA/DTA curves under (a) air; (b) nitrogen

Molecules adsorbed onto surfaces are expected to undergo volatilization in a random manner. In cases of uncomplicated surface adsorption without the presence of heterogeneous trapping sites, the desorption behavior adheres to first-order kinetics.



The kinetic equation can be expressed as follows ( (Ounas, et al., 2011); (Weishi, et al., 2021):

$$\frac{dx}{dt} = k(T)f(x) \quad \text{Equation 4. 3}$$

where, t denotes time,  $\alpha$  represents the degree of conversion, T represents temperature in kelvin (K), k(T) is called as reaction rate constant which is a temperature-dependent term and f( $\alpha$ ) is the function of conversion (Gupta & Mondal, 2019)(Gupta and Mondal, 2019). Fractional conversion of the organic fraction ( $\alpha$ ) can be calculated by the following expression:

$$x = \frac{w_i - w_t}{w_i - w_f} \quad \text{Equation 4. 4}$$

where,  $w_i$  is the initial mass of the sample;  $w_t$  is the mass of the sample at any given time t and  $w_f$  is the final mass of the sample.

The relationship between the rate constant of a reaction and temperature can be demonstrated using the Arrhenius equation, outlined as follows:

$$k(T) = A \exp\left(-\frac{E_a}{RT}\right) \quad \text{Equation 4. 5}$$

In this context, A represents the pre-exponential factor or frequency factor (measured in min<sup>-1</sup>),  $E_a$  stands for activation energy (measured in J mol<sup>-1</sup>), T signifies the reaction's temperature (K), and R denotes the universal gas constant (R = 8.3143 J mol<sup>-1</sup> K<sup>-1</sup>).

Combining Eqs. (4.3) and (4.5), the rate of conversion can be written as follows:

$$\frac{dx}{dt} = A \exp\left(-\frac{E_a}{RT}\right) f(x) \quad \text{Equation 4. 6}$$

In our investigation, we employed a dynamic TG technique with non-isothermal conditions to study the kinetics. As a result, the heating rate ( $\beta$  K/min) can be expressed as follows:

$$\beta = \frac{dT}{dt} \quad \text{Equation 4. 7}$$

by applying chain rule, it can also be written as follows:

$$\beta = \frac{dT}{dx} \times \frac{dx}{dt} \quad \text{Equation 4. 8}$$

$$\frac{dx}{dT} = \frac{1}{\beta} \frac{dx}{dt} \quad \text{Equation 4. 9}$$

From Eqs. (4.6) and (4.9):

$$\frac{dx}{dT} = \left(\frac{A}{\beta}\right) \exp\left(-\frac{E_a}{RT}\right) f(x) \quad \text{Equation 4. 10}$$

$$\frac{dx}{f(x)} = \left(\frac{A}{\beta}\right) \exp\left(-\frac{E_a}{RT}\right) dT \quad \text{Equation 4. 11}$$

Integrating Eq. (4.11) we get the following:

$$G(x) = \int_0^x \frac{dx}{f(x)} = \frac{A}{\beta} \int_0^T \exp\left(-\frac{E_a}{RT}\right) dT \quad \text{Equation 4. 12}$$

In this context, G(x) represents an integral function relating to the degree of conversion, while f(x) is a mathematical expression that characterizes the kinetics of decomposition. The Coats-Redfern method is extensively employed in the kinetic assessment of solid wastes, including biomass and medical waste, and is well-suited for non-isothermal first-order reactions, aligning with the thermal treatment of PCB-contaminated soil ( (Mian, et al., 2019) (Yan, et al., 2009) (Song, et al., 2019)). The TG data for PCB-contaminated soil during low to medium-temperature pretreatment under anaerobic and aerobic conditions were scrutinized using the Coats-Redfern integration method (Feng, et al., 2012). In the realm of thermal analysis kinetics, the first-order Arrhenius Law is commonly applied in the kinetic analysis of solid waste pyrolysis, but it can be applied for oxidation process as well (Rath & Staudinger, 2001), where f(x)=(1-x) and G(x)=-ln(1-x). Therefore, the Coats- Redfern equation is the following:

$$\text{LN}\left(\frac{-\text{LN}(1-x)}{T^2}\right) = \text{LN}\left(\frac{AR}{\beta E_a}\left(1 - \frac{2RT}{E_a}\right)\right) - \frac{E_a}{RT} \quad \text{Equation 4. 13}$$

Foremost value of action energy and within the general range of reaction temperature,  $\frac{RT}{E_a} \ll$

1. So,  $\frac{2RT}{E_a}$  can be assumed as a constant and simplify the Eq. 4.13:

$$\text{LN}\left(\frac{-\text{LN}(1-x)}{T^2}\right) = -\frac{E_a}{R} \frac{1}{T} + \text{LN}\left(\frac{AR}{\beta E_a}\right) \quad \text{Equation 4. 14}$$

The plot of  $\ln\left(\frac{-\ln(1-x)}{T^2}\right)$  as a function of 1/T is a straight line with a slope of -Ea/R and an intercept of  $\ln\left(\frac{AR}{\beta E_a}\right)$ , which allows for the determination of the kinetic parameters of thermal treatment of PCB-contaminated soil (Ea and A).

Analyzing the TG results with a heating rate of 10°C per minute revealed a clear indication that the initial phase adhered to a linear pattern, verifying that the volatilization process under both atmospheric conditions followed a first-order reaction (Figure 4. 9). This observation aligns with findings reported (Uzgiris, 1995).

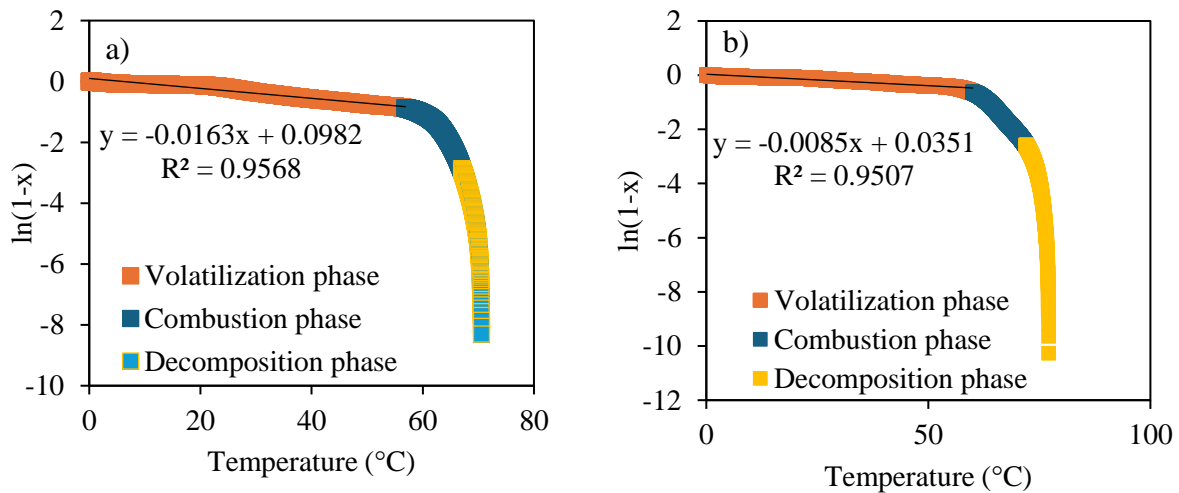


Figure 4. 9. Verification of First-Order Reaction Assumption: Controlling Curve Analysis; a) aerobic condition; b) anaerobic condition

The slope of this line (Figure 4.10) allowed for the determination of the rate constant ( $k(T)$ ) for the volatilization phase, and the half-life ( $t_{1/2}$ ) was calculated using Eq. (4. 15).

$$t_{1/2} = \frac{0.693}{k(T)} \quad \text{Equation 4. 15}$$

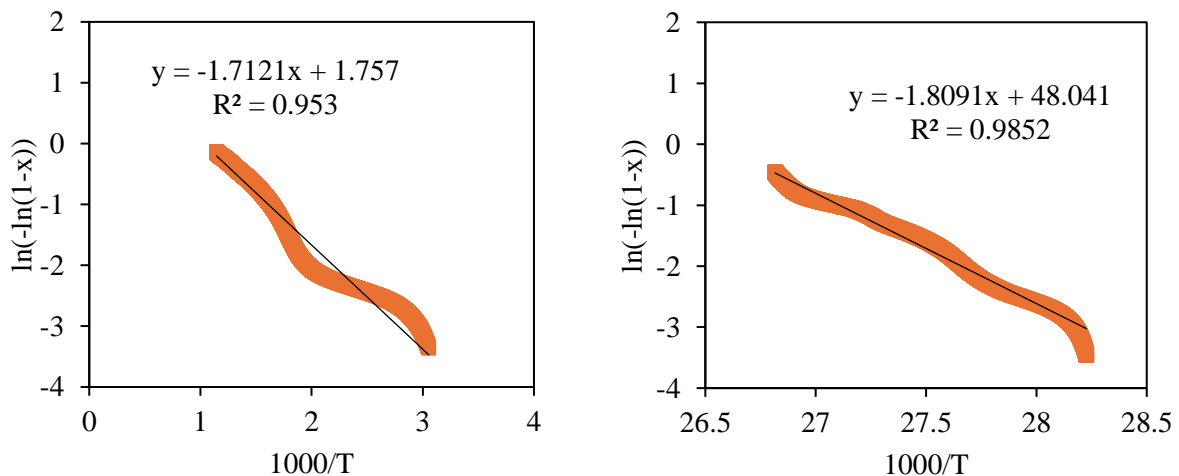


Figure 4. 10. Calculation of reaction rate constant  $k(T)$

By plotting graphs correlating  $\ln(-\ln(1-x))$  against  $1000/T$  for the volatilization phase, and additional parameters were computed based on the subsequent equations.

$$E_a = Slope \times R \quad \text{Equation 4. 16}$$

and pre-exponential factor or frequency factor (A) can be calculated using the Equation 4.17:

$$A = \left(\frac{\beta E_a}{RT^2}\right) \exp(\text{Intercep of Eq. 4. 14}) \quad \text{Equation 4. 17}$$

$$\Delta s = R * \text{LN} \left(\frac{Ah}{MT}\right) \quad \text{Equation 4. 18}$$

where,  $\Delta s$  denotes Entropy change,  $h$  represents Plank's constant with a defined value of  $6.63 \times 10^{-34}$  and  $M$  is Boltzman's constant having a value of  $1.38 \times 10^{-23}$ . Then, Enthalpy change ( $\Delta H$ ) and Gibbs free energy ( $\Delta G$ ) were calculated based on the following equations.

$$\Delta H = E_a - RT \quad \text{Equation 4. 19}$$

$$\Delta G = \Delta H - T\Delta s \quad \text{Equation 4. 20}$$

Table 4. 3 summarizes the kinetic parameters determined for PCB-contaminated soil under anaerobic and aerobic conditions. The values suggest that, for similar temperature conditions, more energy is required for aerobic reaction than for aerobic reaction. Table 4. 3 shows the calculated values of all the thermodynamic parameters and the pre-exponential factor.

Table 4. 3. Calculation of pre-exponential factor and thermodynamic parameters using four iso-conversional models

| Condition | Temperature range °C | k(T) min <sup>-1</sup> | t <sub>1/2</sub> min | E <sub>a</sub> J/mol×10 <sup>3</sup> | $\frac{\Delta H}{K^{-1} \times 10^3}$ Jmol <sup>-1</sup> | $\frac{\Delta s}{1 \times 10^3}$ Jmol <sup>-1</sup> K <sup>-1</sup> | $\frac{\Delta G}{1 \times 10^4}$ Jmol <sup>-1</sup> |
|-----------|----------------------|------------------------|----------------------|--------------------------------------|--|---|---|
| Anaerobic | 100-630              | 0.0085                 | 81.5                 | 15041.4                              | 7533.6   | -303.7  | 281777.2  |
| Aerobic   | 100-560              | 0.0163                 | 42.5                 | 15157.8                              | 7899.4   | -302.8  | 272240.2  |

#### 4.2.2. Experimental Simulation of PCB-Contaminated Soil Treatment Processes

Figure 4. 11 illustrates the removal efficiency of PCBs in thermally treated soil under different heating time and temperatures. The overall quantity of residual PCBs decreased with increasing thermal treatment temperature. Following 30 min at 500 °C, the total PCBs in the soil decreased from 256 mg/kg to 30.2 mg/kg of untreated soil, resulting in a total PCB removal efficiency of 88.2%. For 20 min residence time, additional removal efficiency values include 31.7% at a furnace temperature of 300 °C, 72.7% at 400 °C, and 74.9% at 500 °C (Fig. 3). Therefore, thermal desorption effectively eliminates PCBs from the soil with an optimal combination of treatment time (20 min) and temperature. The removal efficiency of PCBs exhibits a rapid increase between 300 and 400 °C, followed by a slower increase as the temperature surpasses 400 °C. This pattern suggests two distinct phases in the thermal removal of semi-volatile organics from the soil. Initially, there is rapid contaminant evaporation from the soil particle surface, followed by a subsequent phase where the evaporation rate is progressively constrained by internal diffusion within the particle pores (Keyes B, 1994). The PCB removal efficiency in this study is lower than that reported in (Risoul, et al., 2002), where a higher removal efficiency, nearly 99.9%, was achieved after thermal treatment at 450 °C for only 30 minutes. Two potential reasons for this disparity include: (a) the soil used in this study was genuinely PCB-contaminated soil, while the soil used by Risoul et al. (2002) was artificially contaminated, and (b) differences in experimental devices and operating conditions.

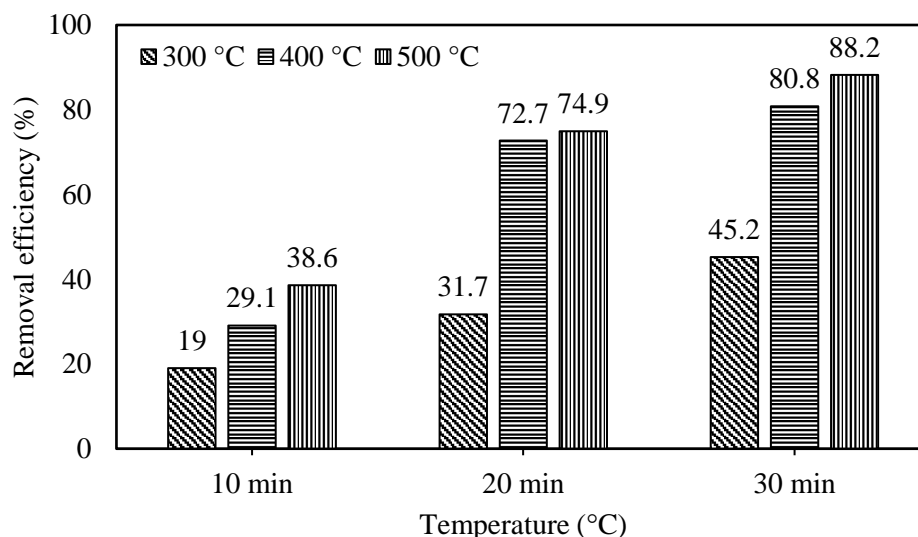


Figure 4. 11. oval efficiencies of PCBs for raw and thermally treated soil

In the untreated soil, hexachlorobiphenyl (HCB) prevails among the PCB homologues, constituting 43.6% of the total PCB weight. Pentachlorobiphenyl, heptachlorobiphenyl, and tetrachlorobiphenyl make up 26.2%, 25.9%, and 3.6% of the PCB content, respectively. Figure 4. 12 illustrates the composition of PCB isomer groups in both untreated and thermally treated soil at 500°C for 20 minutes. Generally, as the temperature increases, the concentration of low-chlorinated PCB homologues rises, while that of highly chlorinated PCB homologues decreases. After 20 minutes of heating at 500°C, the concentration of the HCB group in treated samples decreased to 9.2% compared to the untreated soil.

In the thermal desorption of complex hydrocarbon mixtures, the desorption rate depends significantly on soil type and temperature. The lighter components tend to desorb selectively first without substantial reaction ( (Lighty, 1988); (Lighty, et al., 1989)). (Gryglewicz & Piechocki, 2011) and (Murena & Schioppa, 2000) studied chlorination pathways of PCBs through catalytic hydrodechlorination under a hydrogen atmosphere. They found that Cl atoms in the meta-position are preferentially attacked, and ortho-substitution is slower than meta-substitution and para-substitution.

Similar to total PCBs, the removal efficiency (RE) of dl-PCBs experienced a rapid increase in the temperature range of 300 to 400 °C, but the increase slowed down when the temperature exceeded 400 °C. The combined concentration of 12 dioxin-like PCB (dl-PCBs) congeners was 21.6 mg/kg in the raw sample. Notably, three of these congeners (2,3',4,4',5-PentaCB (#118), 2,3,3',4,4'-PentaCB (#105), and 2,3,3',4,4',5-HexaCB (#156)) made a substantial contribution to the dl-PCBs, amounting to 87.5% of the total concentration. Following thermal desorption at 500 °C for 20 min, the concentration of these congeners reduced to 0.68 mg/kg.

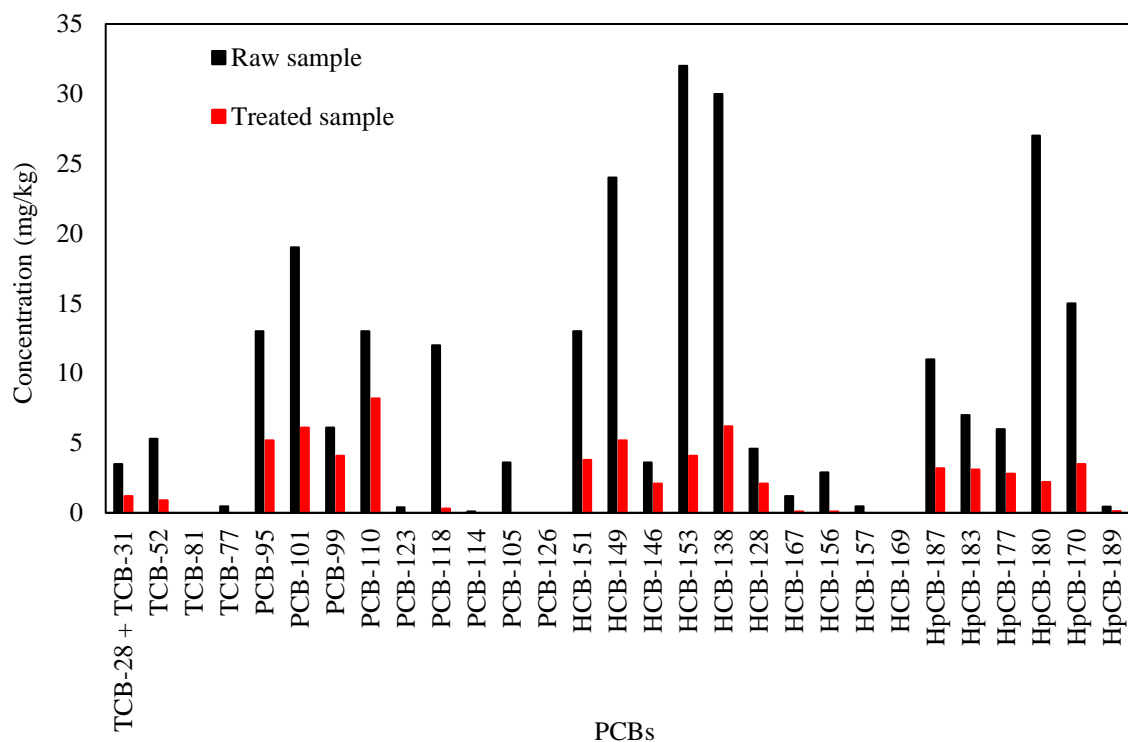


Figure 4. 12. Composition of PCB isomer groups in both untreated and thermally treated soil at 500°C for 20 min

Figure 4. 13 illustrates the concentration of different PCDD/Fs congeners in the raw sample and the treated sample at 500°C for 20 min. In the untreated soil, the concentrations of PCDDs and PCDFs were 2887 ng/g and 3352 ng/g, respectively. Following thermal treatment, both PCDDs and PCDFs in the soil exhibited a decrease to 358.4 and 663.8, respectively. In comparison with PCDDs, PCDFs in the soil were not efficiently removed under oxidative conditions due to the formation of PCDFs from PCBs, aligning with the findings of (Sato, et al., 2010). The presence of oxygen impedes PCDF removal as it contributes to PCDF generation. Conversely, it is reported that under anaerobic conditions, thermal desorption proves to be an effective method for PCDF destruction (Qi, et al., 2014).

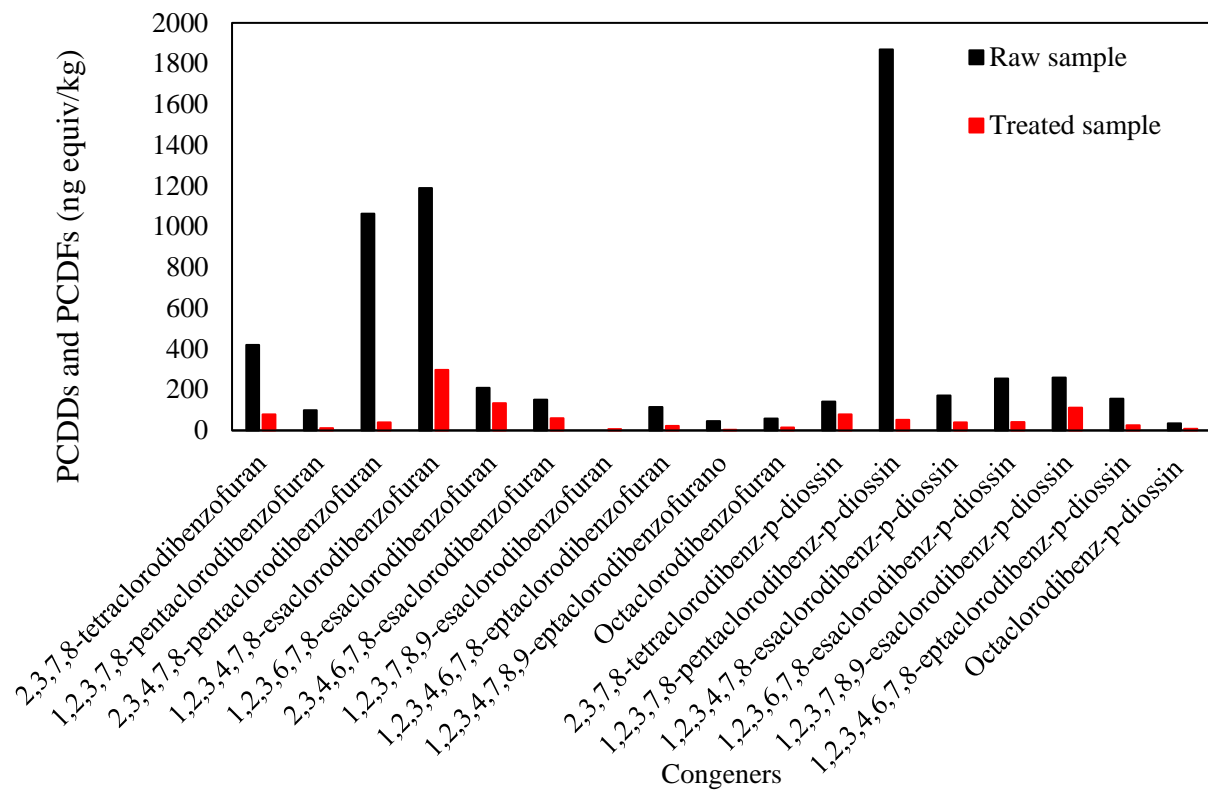


Figure 4. 13. Concentration of different PCDD/Fs congeners in the raw sample and the treated sample at 500°C for 20 min



### 4.3. Pesticides-contaminated soil

#### 4.3.1. TG results

Dieldrin, existing as a stereoisomer, bears a structural dissimilarity because it possesses an oxygen atom that is not found in Aldrin and DDT (Figure 4. 14). Its thermal behaviour highlights a transition phase manifesting at a temperature of 119°C, devoid of any fusion process (Figure 4. 15 (a)). In contrast, Aldrin displays a phase transition at a temperature of 93°C, along with a fusion of its second form commencing at 104°C. The absence of the oxygen atom appears to significantly disrupt Aldrin's stability, affecting both its thermodynamic and kinetic aspects. Therefore, the compound rapidly undergoes decomposition with increasing temperatures due to this structural divergence. This impact is evident in the onset temperatures of decomposition, activation energies as outlined in Table 4. 4. The kinetic parameters were calculated using a non-isothermal TG technique (Fig. 4. 15 (b)), with the detailed calculation steps provided in the subsequent section.

The measurements assessing thermal stability—such as the values of activation energy for the same process and half-life—consistently follow the sequence of Dieldrin preceding Aldrin. This pattern suggests that Dieldrin demonstrates greater stability compared to Aldrin based on these evaluated parameters.

Another category of insecticides sharing akin structures includes DDT, DDE, and DDD. Upon examining structures that vary solely due to a substituent or a double bond, certain conclusions can be drawn. Thermodynamic and kinetic information indicates that the chlorine atom provides more stability to the shared structure than the methoxy group. Additionally, it's observed that the structure of DDE, despite having a double bond, exhibits greater stability compared to DDT and DDD (Figure 4. 14).

Table 4. 4. Kinetic parameters of thermal degradation of Aldrin, Dieldrin and DDT

| Compounds | Activation energy ( $E_a$ kJ.mo $1^{-1}$ ) | In A | $t_{1/2}$ (min) |
|-----------|--|------|-----------------|
| Aldrin    | 57.2                                       | 12.5 | 14              |
| Dieldrin  | 65.9                                       | 13.1 | 40.5            |

DDT

67.9

13.3

25

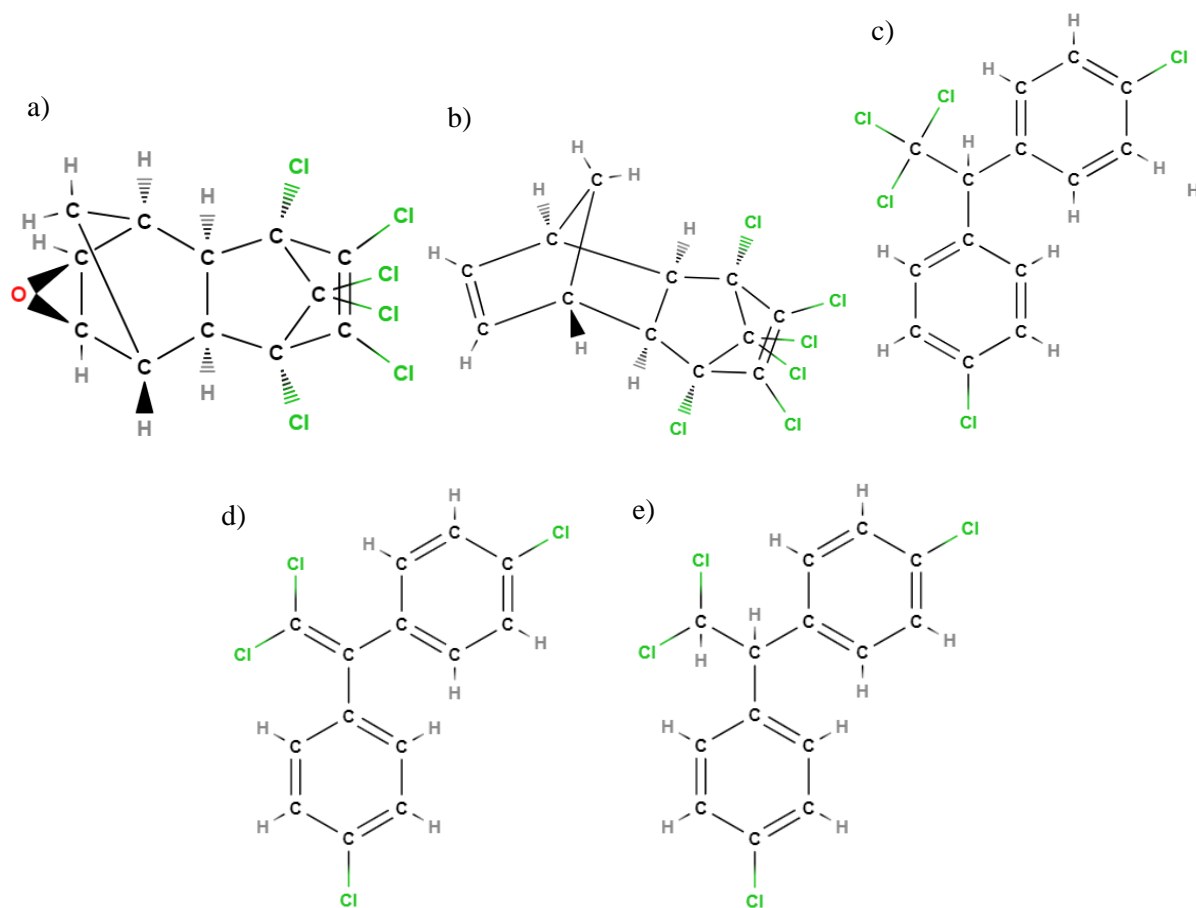


Figure 4. 14. Molecular geometry of a) Dieldrin; b) Aldrin; c) DDT; d) DDE; e) DDD

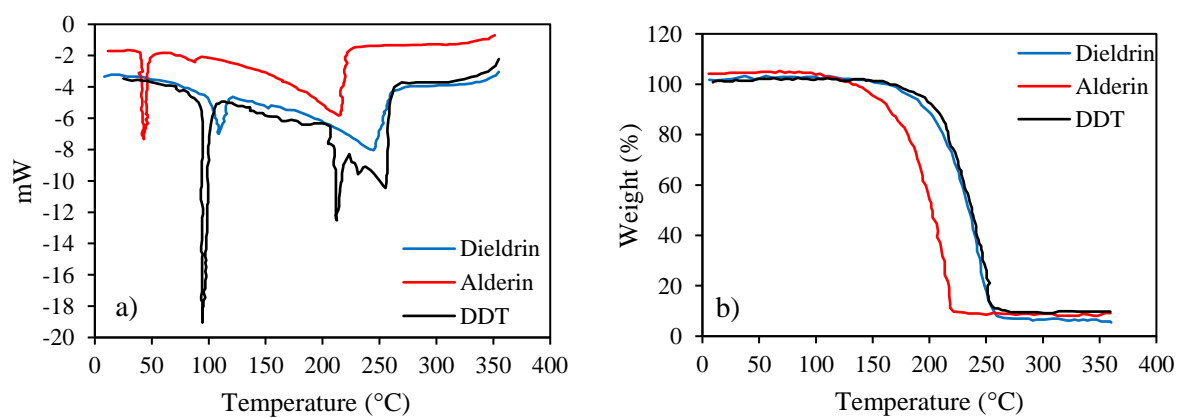


Figure 4. 15. a) thermogravimetry and b) differential scanning calorimetry analysis of aldrin, dieldrin and DDT (liquid state)

Figure 4. 16 shows the TG/DTG curves of pesticide in the soil samples measured under aerobic and anaerobic conditions at a heating rate of 10 °C/min. The same sample showed similar TG/DTG curve pattern in different atmospheres, indicating that atmospheres do little affect the temperature at the end of the thermal treatment of pesticide-contaminated soil. The results of thermal desorption of pesticides-contaminated soils under oxidative atmospheres yielded noteworthy findings (Figure 4. 16). The study indicated that the process of oxidative decomposition of pesticides initiates at temperatures lower than their boiling points. As the temperature rises, the conversion of pesticides reaches 100% at around 680°C. This implies a thorough breakdown and elimination of the pesticide contaminants from the soil matrix. Furthermore, the efficacy of the thermal desorption process was evident in an oxidative environment, where the contaminants exhibited a significant reduction under the influence of oxygen. The oxidative atmosphere played a crucial role in enhancing the decomposition efficiency of the pesticides during thermal desorption.

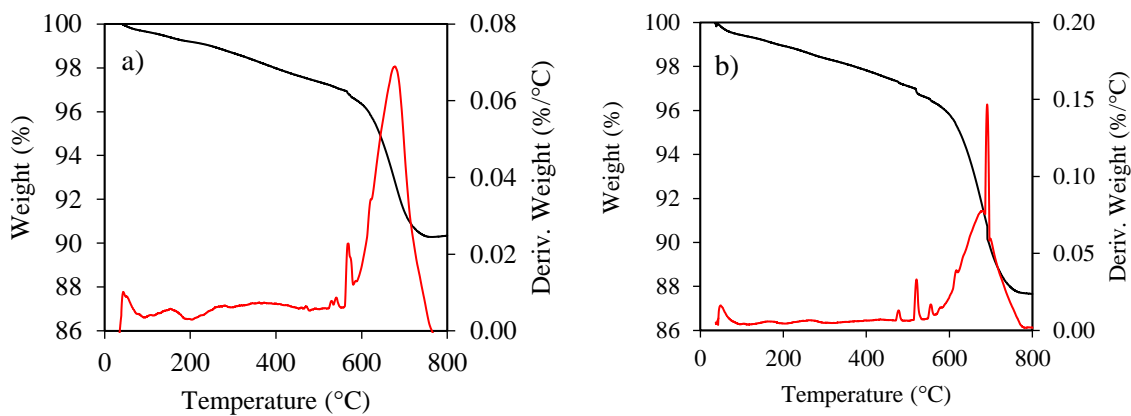


Figure 4. 16. TGA/DTA curves of the tested sample (a) under air atmosphere; (b) under nitrogen atmosphere

#### 4.3.2. Analysis of pesticide-contaminated soil reaction kinetics

The reaction kinetics of pesticide WS in low to medium-temperature pretreatment under aerobic and anaerobic conditions belong to the category of non-isothermal reaction kinetics. The kinetic equation can be expressed as follows ( (Ounas, et al., 2011); (Weishi, et al., 2021)):

$$\frac{dx}{dt} = k(T)f(x) \quad \text{EQUATION 4. 3}$$

where,  $t$  denotes time,  $\alpha$  represents the degree of conversion,  $T$  represents temperature in kelvin (K),  $k(T)$  is called as reaction rate constant which is a temperature-dependent term and

$f(\alpha)$  is the function of conversion (Gupta & Mondal, 2019) (Gupta and Mondal, 2019). Fractional conversion of the organic fraction ( $\alpha$ ) can be calculated by the following expression:

$$x = \frac{w_i - w_t}{w_i - w_f} \quad \text{EQUATION 4.}$$

4

where,  $w_i$  is the initial mass of the sample;  $w_t$  is the mass of the sample at any given time  $t$  and  $w_f$  is the final mass of the sample. The relationship between the rate constant of a reaction and temperature can be demonstrated using the Arrhenius equation, outlined as follows:

$$k(T) = A \exp\left(-\frac{E_a}{RT}\right) \quad \text{EQUATION 4.}$$

5

In this context,  $A$  represents the pre-exponential factor or frequency factor (measured in  $\text{min}^{-1}$ ),  $E_a$  stands for activation energy (measured in  $\text{J mol}^{-1}$ ),  $T$  signifies the reaction's temperature (K), and  $R$  denotes the universal gas constant ( $R = 8.3143 \text{ J mol}^{-1} \text{ K}^{-1}$ ).

Combining Eqs. (4. 3) and (4. 5), the rate of conversion can be written as follows:

$$\frac{dx}{dt} = A \exp\left(-\frac{E_a}{RT}\right) f(x) \quad \text{EQUATION 4.}$$

6

In our investigation of the decomposition reaction, we employed a dynamic TG technique with non-isothermal conditions to study the kinetics. As a result, the heating rate ( $\beta \text{ K/min}$ ) can be expressed as follows:

$$\beta = dT/dt \quad \text{EQUATION 4. 7}$$

by applying chain rule, it can also be written as follows:

$$\frac{dx}{dT} = \frac{1}{\beta} \frac{dx}{dt} \quad \text{EQUATION 4. 9}$$

From Eqs. (4. 6) and (4. 9):

$$\frac{dx}{dT} = \left(\frac{A}{\beta}\right) \exp\left(-\frac{E_a}{RT}\right) f(x) \quad \text{EQUATION 4.}$$

10

$$\frac{dx}{f(x)} = \left(\frac{A}{\beta}\right) \exp\left(-\frac{E_a}{RT}\right) dT \quad \text{EQUATION 4.}$$

11

Integrating Eq. (4. 12) we get the following:

$$G(x) = \int_0^x \frac{dx}{f(x)} = \frac{A}{\beta} \int_0^T \exp\left(-\frac{E_a}{RT}\right) dT \quad \text{EQUATION 4.}$$

12

In this context, G(x) represents an integral function relating to the degree of conversion, while f(x) is a mathematical expression that characterizes the kinetics of decomposition. The Coats-Redfern method is extensively employed in the kinetic assessment of solid wastes, including biomass and medical waste, and is well-suited for non-isothermal first-order reactions, aligning with the thermal treatment of pesticide ( (Mian, et al., 2019) (Yan, et al., 2009) (Song, et al., 2019)). The TG data for pesticide-contaminated soil during low to medium-temperature pretreatment under anaerobic and aerobic conditions were scrutinized using the Coats-Redfern integration method (Feng, et al., 2012). In the realm of thermal analysis kinetics, the first-order Arrhenius Law is commonly applied in the kinetic analysis of solid waste pyrolysis, but it can be applied for oxidation process as well (Rath & Staudinger, 2001), where f(x)=(1-x) and G(x)=-ln(1-x). Therefore, the Coats- Redfern equation is the following:

$$\ln\left(\frac{-\ln(1-x)}{T^2}\right) = \ln\left(\frac{AR}{\beta E_a}\left(1 - \frac{2RT}{E_a}\right)\right) - \frac{E_a}{RT} \quad \text{Equation}$$

4. 13

Foremost value of action energy and within the general range of reaction temperature,  $\frac{RT}{E_a} \ll$

1. So,  $\frac{2RT}{E_a}$  can be assumed as a constant and simplify the Eq. 11:

$$\ln\left(\frac{-\ln(1-x)}{T^2}\right) = -\frac{E_a}{R} \frac{1}{T} + \ln\left(\frac{AR}{\beta E_a}\right) \quad \text{Equation 4.}$$

14

The plot of  $\ln\left(\frac{-\ln(1-x)}{T^2}\right)$  as a function of 1/T is a straight line with a slope of -Ea/R and an intercept of  $\ln\left(\frac{AR}{\beta E_a}\right)$ , which allows for the determination of the kinetic parameters of thermal treatment of pesticide-contaminated soil (Ea and A).

Let's delve into a discussion regarding the impact of heating rate on the volatilization curve. The significance of the heating rate becomes evident, as observed in Figure 4. 17. For temperatures greater than 100°C, two lines are almost parallel. Under an nitrogen atmosphere, an equivalent weight loss occurred, with a heat rate of 25°C per minute being 1.14% greater than when the sample was heated at 10°C per minute. A similar pattern was observed for the test under aerobic condition, although the difference between the curves corresponding to the heat rates of 25°C per minute and 10°C per minute was less prominent, equalling 0.94%.

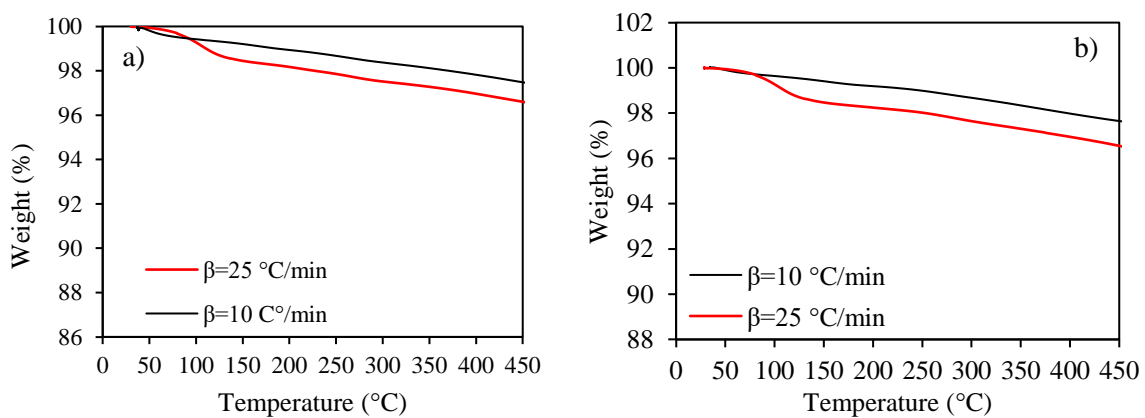


Figure 4. 17. Effect of heating rate on thermal behaviour of PCB-contaminated soil

Analyzing the TG results with a heating rate of 10°C per minute revealed a clear indication that the initial phase adhered to a linear pattern, verifying that the volatilization process under both atmospheric conditions followed a first-order reaction (Fig. 4. 18).

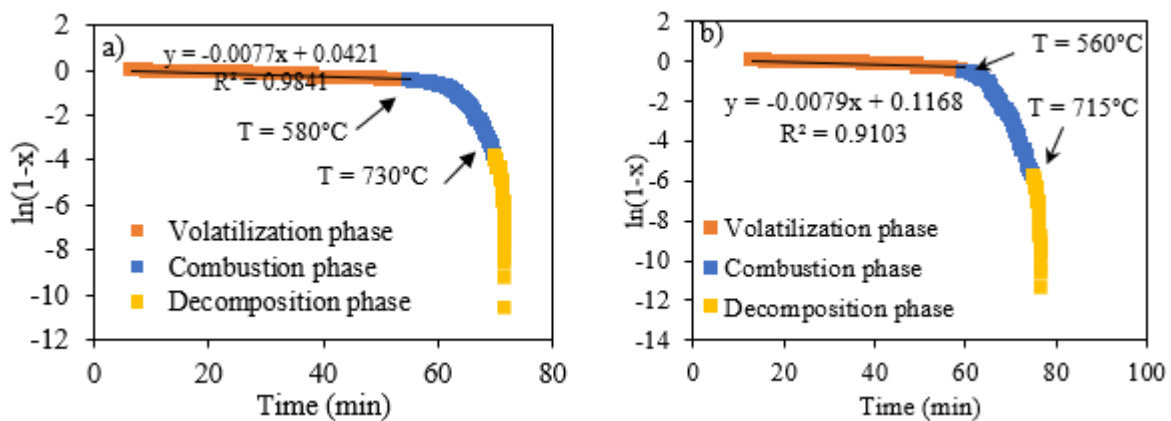


Figure 4. 18. Verification of first-order reaction assumption: controlling curve analysis; a) aerobic condition; b) anaerobic condition.

The slope of this line allowed for the determination of the rate constant (k) for the volatilization

$$t_{1/2} = \frac{0.693}{k(T)} \quad \text{Equation 4. 15}$$

By plotting graphs correlating  $\ln\left[\frac{f_0}{1-x}\right](-\ln(1-x))$  against  $1000/T$  for the volatilization phase, and additional parameters were computed based on the subsequent equations.

$$E_a = \text{Slope} \times R \quad \text{Equation 4. 16}$$

and pre-exponential factor or frequency factor (A) can be calculated using the Eq. 4. 17:

$$A = \left(\frac{\beta E_a}{RT^2}\right) \exp(\text{Intercep of Eq. 4. 14}) \quad \text{Equation 4. 17}$$

$$\Delta s = R * \ln\left(\frac{Ah}{MT}\right) \quad \text{Equation 4. 18}$$

where,  $\Delta s$  denotes Entropy change,  $h$  represents Plank's constant with a defined value of  $6.63 \times 10^{-34}$  and  $M$  is Boltzman's constant having a value of  $1.38 \times 10^{-23}$ . Then, Enthalpy change ( $\Delta H$ ) and Gibbs free energy ( $\Delta G$ ) were calculated based on the following equations.

$$\Delta H = E_a - RT \quad \text{Equation 4. 19}$$

$$\Delta G = \Delta H - T\Delta s \quad \text{Equation 4. 20}$$

Table 5 summarizes the kinetic parameters determined for pesticide-contaminated soil under anaerobic and aerobic conditions. The values suggest that, for similar temperature conditions, more energy is required for anaerobic reaction than for aerobic reaction.

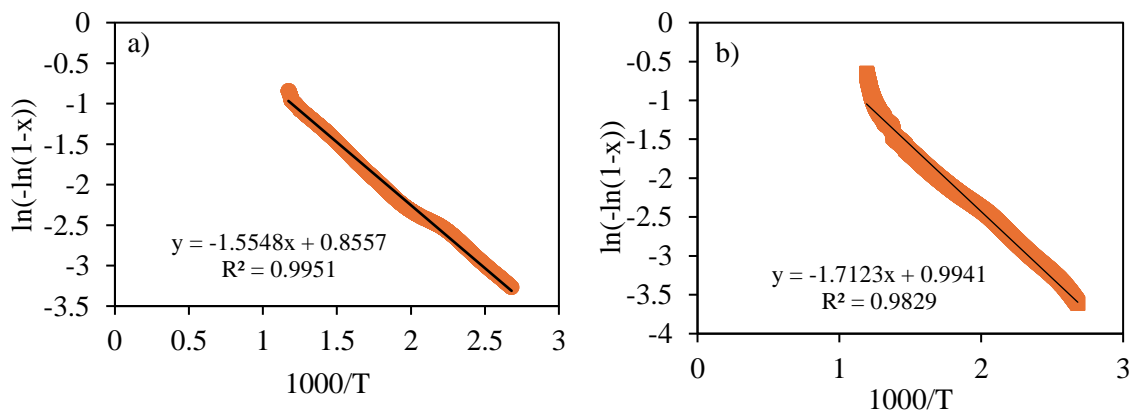


Figure 4. 19. Calculation of reaction rate constant  $k(T)$

Table 4. 5. Calculation of pre-exponential factor and thermodynamic parameters using four iso-conversional models

| Condition | Temperature range °C | k(T) min <sup>-1</sup> | t <sub>1/2</sub> min | E <sub>a</sub> J/mol×10 <sup>3</sup> | $\frac{\Delta H}{K^{-1} \times 10^3}$ Jmol <sup>-1</sup> | $\frac{\Delta s}{1 \times 10^3}$ Jmol <sup>-1</sup> K <sup>-1</sup> | $\frac{\Delta G}{1 \times 10^4}$ Jmol <sup>-1</sup> |
|-----------|----------------------|------------------------|----------------------|--------------------------------------|--|---|---|
| Aerobic   | 100-580              | 0.0077                 | 90                   | 12.9271                              | 5.8349   | -0.30354  | 26.4755   |
| Anaerobic | 100-560              | 0.0079                 | 87.7                 | 14.2365                              | 7.3107   | -0.30214  | 25.8999   |

#### 4.3.4. Treatment simulation experiment of pesticide-contaminated soil

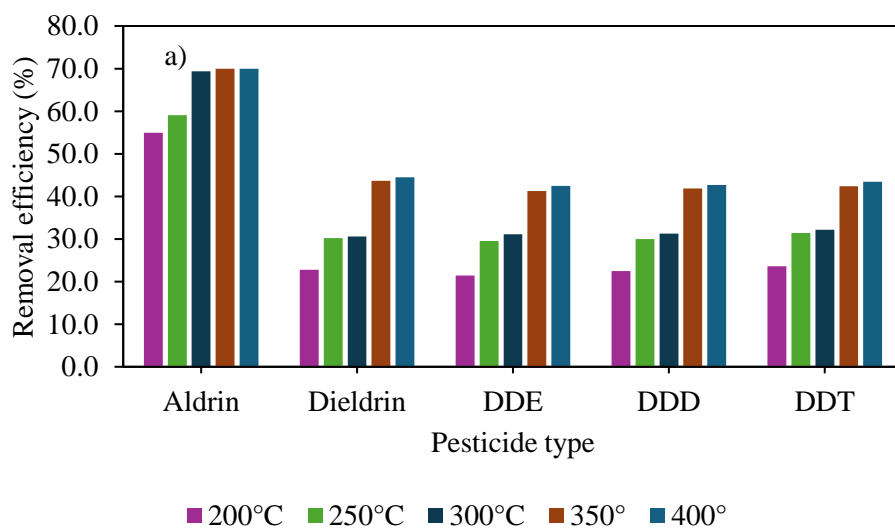
Research findings indicate that chlorinated phenols exhibit the highest potential for PCDD production, while chlorinated benzenes have the capability to generate PCDF ( (Altwicker & Milligan, 1993); (Ghorishi & Altwicker, 1996)). Both chlorinated phenols and chlorinated benzenes, serving as precursors for PCDD/F, are anticipated to be identified in the oxidation process of organochlorine pesticides at temperatures exceeding 450°C. However, the initiation of PCDD/F formation was reported at 550°C during the oxidation of organochlorine pesticides, resulting in the generation of various PCDD/F congeners ( (Dharmarathne, et al., 2019); (Zhao, et al., 2017)).

The tubular furnace set point and residence time of the sample inside the furnace were selected based on the TG results, with careful consideration to choose operational parameters in a manner that prevents PCDD/F formation during thermal treatment. The experiments were conducted in an air environment, and the airflow was calculated to be 300 l/h based on the inner diameter and effective length of the tubular furnace. The optimal retention time was determined by conducting three sets of parallel experiments, and the data were smoothed using a moving average to eliminate random fluctuations and obtain relatively smooth charts (Wakefield, 2014).

The efficiency curves for removal of pesticides from soils showed that keeping the sample for a duration longer than 10 minutes did not result in significant changes. At a 5-minute retention time, the experimental data indicated inadequate efficiency, except for Aldrin, which exhibited a removal efficiency exceeding 50%, while the other controlled pesticides



had removal efficiencies below 50%. Consequently, the optimal retention time for organochlorine pesticides was established at 10 minutes. The optimal parameters identified for all the examined samples are provided in Table 6.



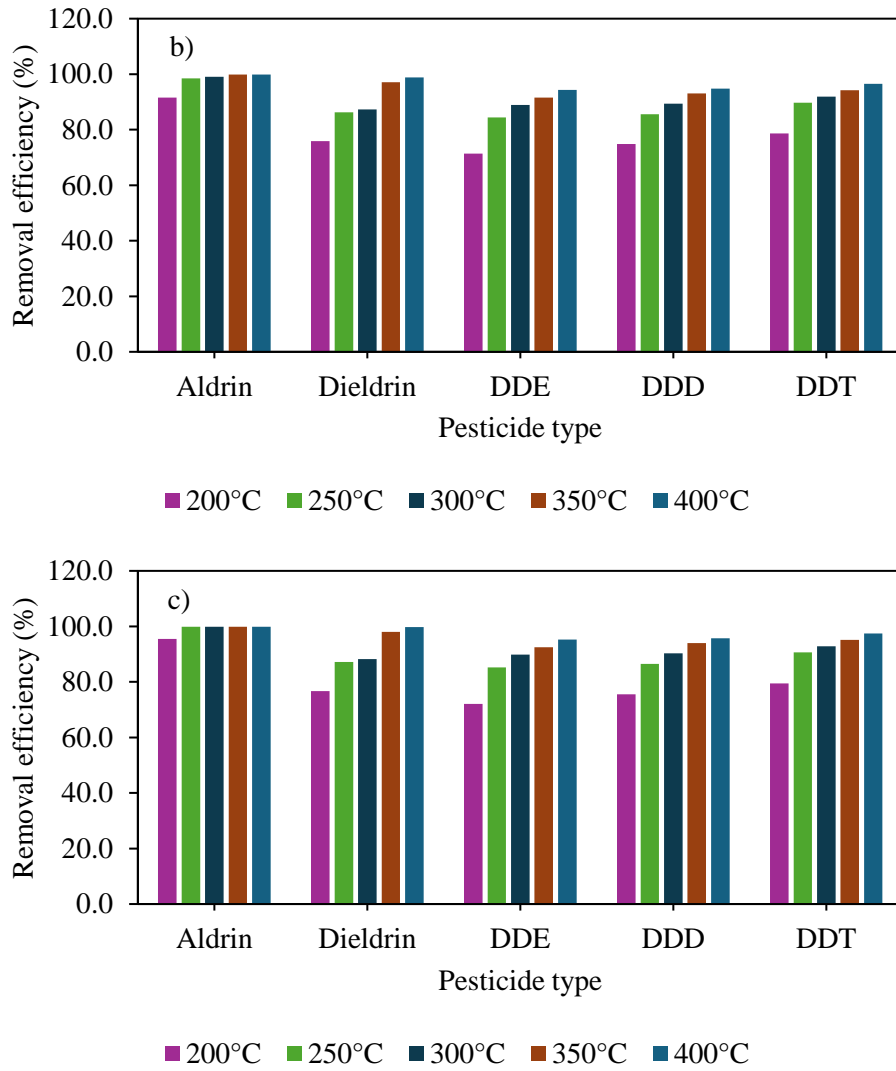


Figure 4. 20 . Removal Efficiency of Different Pesticides from Soil Samples at Various Temperatures and Residence Times (a) 5 min, (b) 10 min, (c) 15 min.

Table 4. 6. Removal efficiency of various pesticides via thermal treatment under varied operational parameters

| Setpoint of furnace (°C) | Pesticide | Retention time (min) |      |      |
|--------------------------|-----------|----------------------|------|------|
|                          |           | 5.0                  | 10.0 | 15.0 |
| 200°C                    | Aldrin    | 55.0                 | 91.6 | 95.5 |
|                          | Dieldrin  | 22.8                 | 75.9 | 76.7 |
|                          | DDE       | 21.4                 | 71.4 | 72.1 |
|                          | DDD       | 22.4                 | 74.8 | 75.5 |
|                          | DDT       | 23.6                 | 78.7 | 79.5 |
| 250°C                    | Aldrin    | 59.1                 | 98.5 | 99.9 |
|                          | Dieldrin  | 30.2                 | 86.3 | 87.2 |
|                          | DDE       | 29.5                 | 84.4 | 85.2 |

|       |          |      |      |      |
|-------|----------|------|------|------|
| 300°C | DDD      | 30.0 | 85.6 | 86.5 |
|       | DDT      | 31.4 | 89.7 | 90.6 |
|       | Aldrin   | 69.4 | 99.1 | 99.9 |
|       | Dieldrin | 30.6 | 87.3 | 88.2 |
|       | DDE      | 31.1 | 88.9 | 89.8 |
|       | DDD      | 31.3 | 89.4 | 90.3 |
| 350°C | DDT      | 32.2 | 91.9 | 92.8 |
|       | Aldrin   | 69.9 | 99.9 | 99.9 |
|       | Dieldrin | 43.7 | 97.1 | 98.1 |
|       | DDE      | 41.2 | 91.6 | 92.5 |
|       | DDD      | 41.9 | 93.1 | 94.0 |
|       | DDT      | 42.4 | 94.2 | 95.1 |
| 400°C | Aldrin   | 69.9 | 99.9 | 99.9 |
|       | Dieldrin | 44.5 | 98.8 | 99.8 |
|       | DDE      | 42.4 | 94.3 | 95.2 |
|       | DDD      | 42.7 | 94.8 | 95.7 |
|       | DDT      | 43.4 | 96.5 | 97.5 |

Although no estimations of electron density have been made within this work to assess the most probable fragmentations, Mass Spectrometry analysis represented the most dominant spectra can be tentatively attributed to specific groups of decomposition products (Fig 4. 21). The specific gases generated during the thermal decomposition of pesticides can vary based on the chemical composition of the pesticide itself. However, for temperatures below 400°C, the thermal decomposition of pesticides led to the release of gases such as carbon dioxide (CO<sub>2</sub>), carbon monoxide (CO), water vapor (H<sub>2</sub>O), and various organic compounds. The exact composition and quantity of these gases depend on the structure and properties of the pesticide undergoing thermal treatment, and the results are shown in the Table. Additionally, the presence of chlorine or other halogens in some pesticides can result in the formation of chlorinated organic compounds, including chlorinated gases such as hydrogen chloride (HCl) and other chlorinated hydrocarbons. However, it's worth noting that, due to the specific furnace temperature conditions employed in this study (low thermal desorption), chlorinated organic compounds were not identified in the results.

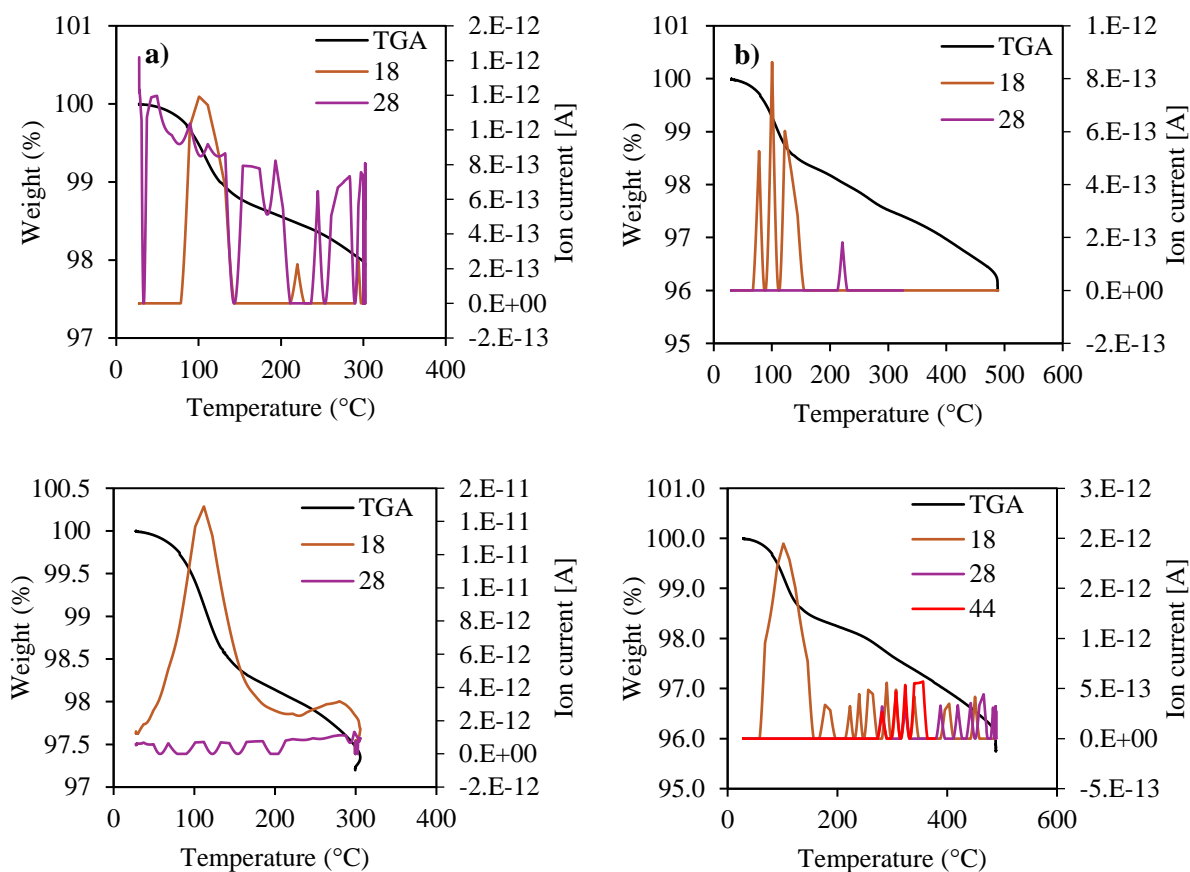
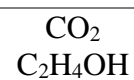
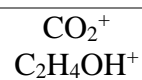


Figure 4. 21. Mass Spectrometry analysis of pesticide-contaminated soil; a) anaerobic conditions at 300 °C for 10 min; b) anaerobic conditions at 350 °C for 10 min; c) aerobic conditions at 300 °C for 10 min; d) aerobic conditions at 350 °C for 10 min

Table 4. 7. Key fragment ions identified by TG-MS during the thermal desorption of soils contaminated by hazardous pesticides

| Mass Number (m/e) | Key fragments              | Probable Parent Molecule(s) |
|-------------------|----------------------------|-----------------------------|
| 18                | $\text{H}_2\text{O}^+$     | $\text{H}_2\text{O}$        |
| 28                | $\text{C}_2\text{H}_4^+$   | $\text{C}_x\text{H}_y$      |
|                   | $\text{CO}^+$              | $\text{CO}$                 |
|                   | $\text{CO}^+$              | $\text{CO}_2$               |
|                   |                            |                             |
| 36                | $\text{H}_{35}\text{Cl}^+$ | $\text{HCl}$                |
| 44                | $\text{C}_3\text{H}_8^+$   | $\text{C}_3\text{H}_8$      |



## Conclusions

The study encompasses a multifaceted exploration: firstly, delving into the characterization of aluminium waste powders from surface treatment industries, elucidating their elemental composition, morphology, and reactivity, with the goal of optimizing the operational parameters of thermal treatment to decrease sample reactivity. Secondly, extending the investigation to the thermal treatment of PCB-contaminated soil, the focus remains on optimizing operational parameters. Lastly, the study explores the thermal behaviour and

stability of organochlorine pesticides, specifically Aldrin, Dieldrin, and DDT, in pesticide-contaminated soil under diverse conditions.

**D)** The study provides valuable insights into the composition, morphology, and reactivity of aluminium waste powders generated in surface treatment industries. The main findings can be summarized as follows:

1. **Elemental Composition:** Aluminium (Al) was identified as the most abundant element in the analysed samples. The origin of the waste samples, whether from grinding, shot blasting, sand blasting, or polishing, influenced the composition.
2. **Morphological Impact of Manufacturing Processes:** Scanning electron microscope (SEM) images revealed that the manufacturing process significantly influenced the morphology of the samples. Non-spherical particles with a cluster and smooth surface texture were predominant. Shot blasting samples showed repeated fragmentation, causing mechanical breakage of the oxide film, allowing direct contact between oxidizer and fresh aluminium surfaces.
3. **Particle Size Distribution:** Blasting processes resulted in samples with a high proportion of fine particles. Polishing processes, on the other hand, left residues in a larger size range. The presence of organic matters, including long threads of polishers' residues, affected particle size distribution, impacting reactivity behaviour.
4. **Hydrogen Generation Capacity:** The study explored the hydrogen production of the samples when reacting with alkaline water. The hydrogen production varied among samples, with different ignition delay times and temperature changes. The results suggest the need for careful handling of these samples due to the potential for elevated temperatures and the release of explosive gases during reactions.
5. **Thermal Reaction Characteristics:** Thermal gravimetric analysis (TGA) revealed distinct mass change steps for each sample. Oxidation of aluminium and the presence of other compounds contributed to the observed mass changes. The study highlighted the importance of understanding the oxidation behaviour of the samples under different atmospheres.
6. **Pre-treatment Simulation:** Pre-treatment simulation experiments in a tubular furnace showed variations in combustion behaviour among different samples. Ignition delay times were influenced by factors such as heating temperature and sample

composition. The addition of ZnO alloy powder was found to decrease ignition delay times.

7. **Suggestions for Handling and Storage:** The study emphasized the importance of inherent safety principles, recommending measures such as inertization of powders and modification of composition to reduce reactivity. Careful handling and storage practices were suggested to avoid contact with hazardous substances.

In short, the detailed characterization of aluminium waste powders and the investigation into their reactivity provide valuable information for safe handling, storage, and disposal practices. The study underscores the need for considering inherent safety measures in the processing and management of such reactive materials.

**II)** The thermal treatment of PCB-contaminated soil was systematically investigated, and the obtained results provide valuable insights into the complex decomposition processes involved. The conclusions drawn from the experimental findings are as follows:

### **1. Thermal Decomposition Phases:**

- The thermal decomposition process can be divided into distinct phases based on temperature ranges.
- The initial phase (below 200°C) involves the reduction of water content due to thermal dehydration.
- Between 200 and 300°C, simple organic matter and semi-volatile compounds undergo thermal breakdown.
- At higher temperatures (350–700°C), degradation involves aromatic structures, organic polymers, and synthesized compounds, such as Polychlorinated biphenyls (PCBs).

### **2. Influence of Oxygen:**

- The presence of oxygen enhances the volatilization of simple organic compounds during the second phase (200–300°C).

### **3. Kinetic Analysis:**

- The kinetics of thermal decomposition were analysed using the Coats-Redfern integration method.
- The application of the first-order Arrhenius Law allowed the determination of kinetic parameters.
- The kinetic analysis confirmed that the volatilization process follows a first-order reaction under both aerobic and anaerobic conditions.

#### **4. Temperature-Dependent Removal Efficiency:**

- The removal efficiency of PCBs increases with higher thermal treatment temperatures.
- Optimal conditions for PCB removal were identified as 20 minutes at 500°C, resulting in an 88.2% removal efficiency.

#### **5. PCB Homologue Composition:**

- The composition of PCB homologues in untreated soil indicates the prevalence of hexachlorobiphenyl (HCB).
- Heating at 500°C for 20 minutes led to an increase in low-chlorinated PCB homologues and a decrease in highly chlorinated PCBs.

#### **6. Removal of dl-PCBs:**

- The removal efficiency of dioxin-like PCBs (dl-PCBs) experienced a rapid increase between 300 and 400 °C.
- The concentration of key dl-PCB congeners reduced significantly after thermal desorption.

#### **7. PCDD/F Removal:**

- Thermal treatment effectively decreased the concentrations of PCDDs and PCDFs in the soil.
- PCDFs were less efficiently removed under oxidative conditions, aligning with findings in the literature.

#### **8. Temperature-Dependent Changes in PCDD/Fs:**



- The concentration of different PCDD/F congeners decreased with rising treatment temperatures.
- Under anaerobic conditions, thermal desorption proved effective for PCDF destruction.

### **9. Thermodynamic Parameters:**

- Thermodynamic parameters, including activation energy, entropy change, enthalpy change, and Gibbs free energy, were calculated.
- The values suggest that more energy is required for aerobic reactions compared to anaerobic reactions.

In summary, the experimental simulation of PCB-contaminated soil treatment processes, coupled with thorough kinetic and thermodynamic analyses, provides a comprehensive understanding of the thermal decomposition dynamics and removal efficiencies. The results contribute valuable information for designing effective and environmentally sound remediation strategies for PCB-contaminated sites.

**III)** The study provides valuable insights into the thermal behaviour and stability of organochlorine pesticides, specifically focusing on Aldrin, Dieldrin, and DDT, as well as their degradation in pesticide-contaminated soil under different conditions.

#### **1. Structural Dissimilarity and Thermal Behaviour:**

- Dieldrin, with its unique structural features, exhibits dissimilarity from Aldrin and DDT, primarily due to the presence of an oxygen atom. This structural divergence significantly impacts Aldrin's stability, leading to a more rapid decomposition with increasing temperatures.
- The thermal analysis, including thermogravimetry and kinetic parameters, consistently indicates that Dieldrin surpasses Aldrin in stability. This is evident in the higher activation energy and longer half-life of Dieldrin compared to Aldrin and DDT.

#### **2. Comparison with Similar Structures (DDT, DDE, DDD):**

- Analysing insecticides with similar structures (DDT, DDE, and DDD) reveals that the chlorine atom imparts more stability than the methoxy group. Additionally, DDE, despite having a double bond, demonstrates greater stability compared to DDT and DDD.

### **3. Thermal Desorption of Pesticide-Contaminated Soil:**

- The study explores the thermal desorption of pesticide-contaminated soil under aerobic and anaerobic conditions. It indicates that an oxidative atmosphere enhances the decomposition efficiency of pesticides during thermal desorption.
- The kinetic analysis, employing the Coats-Redfern method, provides a deeper understanding of the non-isothermal reaction kinetics, with the first-order Arrhenius Law applied for oxidation processes.

### **4. Treatment Simulation Experiment:**

- The research identifies optimal operational parameters for the thermal treatment of pesticide-contaminated soil, considering temperature and residence time. The efficiency curves show that a 10-minute retention time is optimal for removing pesticides.

### **5. Mass Spectrometry Analysis:**

- Mass spectrometry analysis of the thermal desorption products identifies key fragment ions, shedding light on the decomposition products. Gases such as CO<sub>2</sub>, CO, H<sub>2</sub>O, and organic compounds are released during the thermal decomposition of pesticides.

### **6. Implications for Environmental Remediation:**

- The findings suggest that the thermal treatment method is effective in reducing pesticide contaminants in soil, with varying efficiency for different pesticides at different temperatures and retention times.

Finally, this comprehensive study contributes valuable data on the thermal behaviour, stability, and degradation kinetics of organochlorine pesticides, offering insights that can inform environmental remediation strategies for pesticide-contaminated soil.

## **Recommendations for Further Research**

- Investigate the potential applications of recovered aluminium from waste powders in the development of new materials or products.
- Utilize computational modelling and simulation studies to predict and understand the explosive potential under different conditions. This can aid in identifying critical parameters and developing strategies for risk mitigation.
- Explore the feasibility of combining thermal treatment with other remediation techniques for enhanced PCB removal.
- Research and develop effective emission control technologies to minimize the release of harmful gases into the atmosphere during PCB-contaminated soil thermal treatment.
- Investigate how varying thermal treatment conditions (temperature, residence time, etc.) influence the composition and quantity of gaseous emissions, aiming to find optimal conditions that minimize environmental impact.
- Explore the efficacy of thermal treatment for a broader range of pesticide contaminants and soil types.
- Investigate the potential by-products and environmental implications of thermal degradation of different pesticides.
- Assess the scalability and cost-effectiveness of thermal treatment methods for large-scale pesticide-contaminated sites.
- After all, it is recommended to investigate the optimization of operational parameters during the scale-up process. Understand how factors such as temperature, pressure, and residence time may need adjustment when transitioning from the laboratory to a larger, real-scale system.

## **Bibliography**

- Abu-Hamdeh, N. & Reeder, R., 2000. Soil thermal conductivity: effects of density, moisture, salt concentration, and organic matter.. *Soil Sci Soc Am J* , Volume 64, pp. 1285-1290.
- Acea, M. & Carballas, T., 1999. Microbial fluctuations after soil heating and organic amendment.. *Bioresour Technol*, Volume 67, pp. 65-71..
- Adipah, S., 2019. Introduction of petroleum hydrocarbons contaminants and its human effects.. *Journal of Environmental Science and Public Health*, 3(1), pp. 1-9.

- Adipah, S., 2019. Introduction of petroleum hydrocarbons contaminants and its human effects.. *Journal of Environmental Science and Public Health*, 3(1), pp. 1-9.
- Altwicker, E. & Milligan, M., 1993. Formation of dioxins: competing rates between chemically similar precursors and de novo reactions.. *Chemosphere*, Volume 27, pp. 301-307.
- Alviani, V. et al., 2019. Mechanisms and possible applications of the Al-H<sub>2</sub>O reaction under extreme pH and low hydrothermal temperatures.. *Int J Hydrogen Energy*, Volume 44, pp. 29903-21. .
- Ambaye, T. et al., 2022. Remediation of soil polluted with petroleum hydrocarbons and its reuse for agriculture: recent progress, challenges, and perspectives.. *Chemosphere* , Volume 293, p. 133572.
- Amer, A. M., 2002. Extracting aluminium from dross tailings.. *J. Mater.*, 54(11), p. 72–75. .
- Amyotte, P. R. & Eckhoff, R. K., 2010. Dust explosion causation, prevention and mitigation: An overview. *J. Chem. Health Saf.*, 17(1), p. 15–28.
- Amyotte, P. R. & Eckhoff, R. K., 2010. Dust explosion causation, prevention and mitigation: An overview.. *J. Chem. Health Saf.*, 17(1), p. 15–28.
- Amyotte, P. R., Pegg, M. J. & Khan, F. I., 2009. Application of inherent safety principles to dust explosion prevention and mitigation.. *Process Saf. Environ. Protect.*, 87(1), pp. 35-39.
- Anning, A. & Akoto, R., 2018. Assisted phytoremediation of heavy metal contaminated soil from a mined site with *Typha latifolia* and *Chrysopogon zizanioides*.. *Ecotoxicol Environ Saf* , Volume 148, p. 97–104. .
- Ardolino, F., Boccia, C. & Arena, U., 2020. Environmental performances of a modern waste-to-energy unit in the light of the 2019 BREF document. *Waste Management*, Volume 104, p. 94–103.
- Arm, M. & Lindeberg, J., 2006. Gas generation in incinerator ash.. I: Wascon, pp. 629-637..
- Australian Gov. Dept. of the Environment and Water, 2007. Proposal to regulate salt slag under the hazardous waste (Regulation of Exports and Imports) regulations.
- Baars, A. et al., 2001. Re-evaluation of human-toxicological maximum permissible risks levels. Bilthoven (NL): , s.l.: s.n.
- Badia, D. & Marti, C., 2003. Plant ash and heat intensity effects on chemical and physical properties of two contrasting soils.. *Arid Land Res Manag*, Volume 17, pp. 23-41.
- Barton, R. G., Clark, W. D. & Seeker, W. R., 1990. Fate of metals in waste combustion systems.. *Combustion science and technology*, 74(1-6), pp. 327-342..
- Board, C. S., 2005. Investigation Report, Aluminum Dust Explosion, Huntington: s.n.
- Bocio, A., Nadal, M. & Domingo, J., 2005. Human exposure to metals through the diet in Tarragona, Spain: temporal trend.. *Biol. Trace Elem. Res.* , Volume 104, p. 193–201.
- Bone, J. et al., 2010. Soil quality assessment under emerging regulatory requirements. *Environ Int*, Volume 36, p. 609–622.

- Bonnard, M. et al., 2010. The influence of thermal desorption on genotoxicity of multipolluted soil.. *Ecotoxicol Environ Saf*, Volume 73, p. 955–960.
- Borchardt, G., 1989. Dixon JB, Weed SB (eds) *Minerals in soil environments*. s.l.:Madison, WI,.
- Braconnier, A., Chauveau, C., Halter, F. & Gallier, S., 2020. Experimental investigation of the aluminum combustion in different O<sub>2</sub> oxidizing mixtures: Effect of the diluent gases. *Exp. Therm. Fluid Sci.*, Volume 117, p. 110110.
- BREF, S., 2006. *Integrated Pollution Prevention and Control Reference Document on Best Available Techniques for the Surface Treatment of Metals and Plastics*.. European Commission, p. 546.
- Brunner, P. & Rechberger, H., 2015. Waste to energy – key element for sustainable waste management. *Waste Management* , Volume 37, p. 3–12.
- Budnik, L. T., Wegner, R., Rogall, U. & Baur, X., 2014. Accidental exposure to polychlorinated biphenyls (PCB) in waste cargo after heavy seas. *Global waste transport as a source of PCB exposure. International archives of occupational and environmental health*, Volume 87, pp. 125-135.
- Bulmau, C., Marculescu, C., Lu, S. & Qi, Z., 2014. Analysis of thermal processing applied to contaminated soil for organic pollutants removal.. *J Geochem Explor* , Volume 147, pp. 298-305.
- Busu, M., 2019. Adopting Circular economy at the European Union level and its impact on economic growth.. *Soc. Sci.* , 8(5), p. 159.
- Cai, J. et al., 2022. Investigating the explosion hazard of hydrogen produced by activated aluminium in a modified Hartmann tube. *International journal of hydrogen energy* , Volume 47, pp. 15933-15941.
- Cai, J. et al., 2022. Investigating the explosion hazard of hydrogen produced by activated aluminium in a modified Hartmann tube.. *International journal of hydrogen energy*, Volume 47, pp. 15933-15941. .
- Cai, Z., Bager, D. H. & Christensen, T. H., 2004. Leaching from solid waste incineration ashes used in cement-treated base layers for pavements. *Waste Management*, 24(6), pp. 603-612.
- Calder, G. V. & Stark, T. D., 2010. Aluminium reactions and problems in municipal solid waste landfills. *Pract. Period. Hazard. Toxic Radioact.. Waste Manage.*, 14(4), p. 258–265. .
- Campbell, T., Kalia, R. K., Nakano, A. & Vashishta, P., 1999. Dynamics of oxidation of aluminium nanoclusters using variable charge molecular-dynamics simulations on parallel computers.. *The American Physical Society*, 82(24), pp. 4866- 4869. .
- Catolico, N., Ge, S. & McCartney, J., 2016. Numerical modeling of a soil-borehole thermal energy storage system.. *Vadose Zone J*, 15(1).
- Cavallero, D., Debernardi, M., Marmo, L. & Piccinini, N., 2004. Two aluminium powder explosion that occurred in superficial finishing plants. *Berlin*, s.n., p. 14–18.

- Cébron, A. et al., 2009. Influence of vegetation on the in situ bacterial community and polycyclic aromatic hydrocarbon (PAH) degraders in aged PAH-contaminated or thermal-desorption-treated soil *Appl. Environ Microbiol* , Volume 75, p. 6322–6330.
- Certinini, G., 2005. Effects of fire on properties of forest soils: a review. *Oecologia* , Volume 143, pp. 1-10.
- Chang, N. B., Wang, H. P., Huang, W. L. & Lin, K. S., 1999. The assessment of reuse potential for municipal solid waste and refuse-derived fuel incineration ashes.. *Resources, Conservation and Recycling*, 23(3-4), pp. 255-270.
- Cheng, H. & Hu, Y., 2010. Municipal solid waste (MSW) as a renewable source of energy: Current and future practices in China. *Bioresource technology*, 101(11), pp. 3816-3824.
- Chen, L. et al., 2009. Effect of heating rates on TG-DTA results of aluminium nanopowders prepared by laser heating evaporation,. *J. Therm. Anal. Calorim.*, 141–145. (96).
- Chen, L. et al., 2009. Effect of heating rates on TG-DTA results of aluminium nanopowders prepared by laser heating evaporation.. *J Therm Anal Calorim*, Volume 96, p. 141–145.
- Cho, M., Ju, J., Kim, S. & Jang, H., 2006. Tribological properties of solid lubricants (Graphite, Sb<sub>2</sub>S<sub>3</sub>, MoS<sub>2</sub>) for automotive brake friction materials. *Wear*, Volume 260, p. 855.
- Chuai, X. et al., 2022. Fate and emission behavior of heavy metals during hazardous chemical waste incineration.. *Journal of Hazardous Materials*, Volume 431, p. 128656..
- Crettaz, P. et al., 2002. Assessing human health response in life cycle assessment using ED10s and DALYs, part 1: Cancer effects.. *Risk Anal* , Volume 22, p. 931–945.
- Cundy, A. et al., 2013. Developing principles of sustainability and stakeholder engagement for ‘gentle’ remediation approaches: The European context.. *J. Environ. Manag.*, Volume 129, p. 283–291.
- D.lgs. n. 152, 2006. Norme in materia ambientale.
- D.lgs. n. 179, 2002. Disposizioni in materia ambientale.
- D.lgs. n. 22, 1997. Attuazione delle direttive 91/156/CE sugli imballaggi e rifiuti di imballaggio.
- D.lgs. n. 426, 1998. Nuovi interventi in campo ambientale.
- D.M. n. 471, 1999. Regolamento recante criteri, procedure e modalità per la messa in sicurezza, la bonifica e il ripristino ambientale dei siti inquinati, ai sensi dell'articolo 17 del decreto legislativo 5 febbraio 1997, n. 22, e successive modificazioni e integrazioni..
- Dardouri, S. & Sghaier, J., 2018. Adsorption characteristics of layered soil as delay barrier of some organic contaminants: experimental and numerical modeling.. *Environ Model Softw* , Volume 110, p. 95–106.
- Decreto 24 febbraio, 2003. Decreto Ministeriale di approvazione del certificato di bilancio di previsione 2003 di Province, Comuni, Comunità Montane e Unioni di comuni..

- Decreto Legislativo 5 febbraio, 1997. Attuazione delle direttive 91/156/CEE sui rifiuti, 91/689/CEE sui rifiuti pericolosi e 94/62/CE sugli imballaggi e sui rifiuti di imballaggio.
- Deluca, L., Shimada, T., Sinditskii, V. & Calabro, M., 2017. *Chemical Rocket Propulsion—A Comprehensive Survey of Energetic Materials*. Springer International Publishing: Cham.
- Dharmarathne, N. K., Mackie, J. C., Kennedy, E. M. & Stockenhuber, M., 2019. Thermal oxidation of dieldrin and concomitant formation of toxic products including polychlorinated dibenzo-p-dioxin and dibenzofuran (PCDD/F).. *Chemosphere*, Volume 225, pp. 209-216.
- Di Guardo, A. et al., 2017. Differentiating current and past PCB and PCDD/F sources: The role of a large contaminated soil site in an industrialized city area. *Environmental Pollution* , Volume 223, pp. 367-375. .
- Di Maria F, B. G. B. G. e. a., 2018a. On time measurement of the efficiency of a waste-to-energy plant and evaluation of the associated uncertainty. *Applied Thermal Engineering*, Volume 129, p. 338–344.
- Ding, D., Song, X., Wei, C. & LaChance, J., 2019. A review on the sustainability of thermal treatment for contaminated soils.. *Environ Pollut* , Volume 253, p. 449–463.
- Dixon, J., 1989. Kaolin and serpentine group minerals. In: Dixon JB, Weed SB (eds) *Minerals in soil environments*. s.l.:Madison, WI.
- Domingo, J., 1994. Metal-induced developmental toxicity in mammals: a review.. *J. Toxicol. Environ. Health* , Volume 42, p. 123–141.
- Durai, G., Das, K. & Das, S., 2008b. Corrosion behavior of Al–Zn/Al<sub>2</sub>O<sub>3</sub> and Al–Zn–X/Al<sub>2</sub>O<sub>3</sub> (X = Cu, Mn) composites synthesized by mechanical–thermal treatment. *J. Alloy. Compd.*, Volume 462, p. 410–415.
- Durai, T., Das, K. & Das, S., 2007a. Wear behavior of nano structured Al(Zn)/Al<sub>2</sub>O<sub>3</sub> and Al(Zn)–4Cu/Al<sub>2</sub>O<sub>3</sub> composite materials synthesized by mechanical and thermal process. *Mater. Sci. Eng.* , Volume 471, p. 88–94.
- Durai, T., Das, K. & Das, S., 2007b . Synthesis and characterization of Al matrix composites reinforced by in situ alumina particulates. *Mater. Sci. Eng. A*, Volume 445–446, p. 100–105.
- Durai, T., Das, K. & Das, S., 2008a. Al(Zn)–4Cu/Al<sub>2</sub>O<sub>3</sub> in-situ metal matrix composite synthesized by displacement reactions. *J. Alloy. Compd.*, Volume 457, p. 435–439.
- EC, 1975. Council Directive 75/442/EEC of 15 July 1975 on waste.
- EC, 1991. Council Directive 91/689/EEC of 12 December 1991 on hazardous.
- EC, 1993. Council Regulation (EEC) No. 259/93 on the supervision and control of shipments of waste within, into and out of the European Community..
- EC, 2003. *Handbook on the Implementation of EC Environmental Legislation*, Regional Environmental Center.,.
- EC, 2008. Waste Framework Directive 2008/98/EC on waste and repealing certain directives. *Official Journal of European Union*, Volume 312, p. 3–30..

EC, 2014a. Commission Decision 2014/955/EU of 18 December 2014 amending Decision 2000/532/EC on the list of waste pursuant to Directive 2008/98/EC of the European Parliament and of the Council..

EC, 2014b. Commission Regulation (EU) No 1357/2014 of 18 December 2014 replacing Annex III to Directive 2008/98/EC of the European Parliament and of the Council on waste and repealing certain Directives. Official Journal of the European Union. 19.12.2014. L365/89.

EC, C. D. 2. o. 3. M. 2. r. D. 9., 2000. establishing a list of wastes pursuant to Article 1(a) of Council Directive 75/442/EEC on waste and Council Decision 94/904/EC establishing a list of hazardous waste pursuant to Article 1(4) of Council Directive 91/689/EEC on hazardous waste..

EC—European Commission , 2019. The European Green Deal—COM (2019) 640 Final; European Commission: Brussels, Belgium, p. 1–24.

EC—European Commission, 2021. Pathway to a Healthy Planet for All EU Action Plan: “Towards Zero Pollution for Air, Water and Soil. —COM 400 Final; European Commission: Brussels, Belgium,, p. 1–22..

Ellis, D. & Hadley, P., 2009. Sustainable remediation white paper – integrating sustainable principles, practices, and metrics into remediation projects.. Remediat J , Volume 19, p. 5–14.

Emsley, J., 1991. The elements., 2nd ed. ed. s.l.:UK: Oxford University Press..

EPA, 5.-R.-0.-0., 2008. Green remediation: incorporating sustainable environmental practices into remediation of contaminated sites, Washington, DC, USA.: s.n.

EPA, 5.-F.-0.-0., 2009. Green remediation: best management practices for site investigation, Washington, DC, USA.: s.n.

EPA, 5.-F.-1.-0., 2012. A citizen’s guide to thermal desorption., Washington, DC, USA.: s.n.

EPA, U., 2020. Hazardous Waste..

Erdem, S., Dawson, A. R. & Thom, N. H., 2011. Microstructure-linked strength properties and impact response of conventional and recycled concrete reinforced with steel and synthetic macro fibres. Construction and Building Materials, 25(10), pp. 4025-4036.

Esposit, P. et al., 2020. Influence of texture and microstructure on the reactivity of aluminium powders.. Materialia, Volume 14, p. 100880..

European Chemical Agency, 2023. European Chemical Agency. [Online]

Available at: <https://echa.europa.eu/it/list-of-substances-subject-to-pops-regulation>

European Commission, 2019 Edition.. Energy, Transport and Environment Statistics.

European Commission, 2018a. Directive (EU) 2018/850 of the European Parliament and of the Council of 30 May 2018 Amending Directive 1999/31/EC on waste.. Official Journal of European Union, Volume 150, p. 100–108..



European Commission, 2018b. Directive (EU) 2018/851 of the European Parliament and of the Council of 30 May 2018 amending Directive 2008/98/EC on waste.. Official Journal of European Union, Volume 150, p. 109–140.

European Commission, 2018c. Directive (EU) 2018/852 of the European Parliament and of the Council of 30 May 2018 amending Directive 94/62/ EC on packaging and packaging waste.. Official Journal of European Union , Volume 150, p. 141–154..

Eurostat, 2020. Waste Statistics.

Fanning, D., Keramidas, V. & El-Desoky, M., 1989. Micas. In: Dixon JB, Weed SB (eds) Minerals in soil environments. s.l.:Madison, WI.

FAO and UNEP, 2021. Global Assessment of Soil Pollution: Report., Rome: s.n.

FAO, 2015a. FAO. Revised World Soil Charter..

FAO, 2015b. State of the World's Soil Resources: main report..

Fayiga, A. & Saha, U., 2016. Soil pollution at outdoor shooting ranges: health effects, bioavailability and best management practices.. Environ Pollut , Volume 216, p. 135–145.

Feng, Y. et al., 2012. Volatilization behavior of fluorine in fluoroborate residue during pyrolysis.. Environ. Sci. Technol. , 46(1), p. 307–311.

Ferdos, F. & Rosen, L., 2013. Quantitative environmental footprints and sustainability evaluation of contaminated land remediation alternatives for two case studies.. Remed. J. , 24(1), pp. 77-98.

Ferrante, M. et al., 2010. Poly.

FISE, 2019. Assoambiente PER UNA STRATEGIA NAZIONALE DEI RIFIUTI. [A national strategy for waste].

Gabarrón, M., Faz, A., Martínez-Martínez, S. & Acosta, J., 2018. Change in metals and arsenic distribution in soil and their bioavailability beside old tailing ponds.. J Environ Manag, Volume 212, p. 292–300.

Galang, M., Markewitz, D. & Morris, L., 2010. Soil phosphorus transformations under forest burning and laboratory heat treatments.. Geoderma, Volume 155, pp. 401-408.

Gan, X. et al., 2017. Optimization of ex-situ washing removal of polycyclic aromatic hydrocarbons from a contaminated soil using nano-sulfonated graphene.. Pedosphere, 27(3), p. 527–536.

Gao, Y., Yang, H., Zhan, X. & Zhou, L., 2013. Scavenging of BHCs and DDTs from soil by thermal desorption and solvent washing.. Environ Sci Pollut Res, Volume 20, pp. 1482-1492.

Ghorishi, S. & Altwicker, E., 1996. Rapid formation of polychlorinated dioxins/furans during the heterogeneous combustion of 1,2-dichlorobenzene and 2,4-dichlorophenol.. Chemosphere, Volume 32, pp. 133-144.

Gil, A., 2005. Management of the salt cake from secondary aluminium fusion processes.. Ind. Eng. Chem. Res. , 44(23), p. 8852–8857..

- Glass, D., Johnson, D., Blank, R. & Miller, W., 2008. Factors affecting mineral nitrogen transformations by soil heating: a laboratory-simulated fire study.. *Soil Sci*, Volume 173, pp. 387-400.
- Gohlke, O. & Martin, J., 2007. Drivers for innovation in waste-to-energy technology. *Waste Manage. Res*, Volume 25, p. 214–219.
- González, N. et al., 2019. Dietary intake of arsenic, cadmium, mercury and lead by the population of Catalonia, Spain: analysis of the temporal trend.. *Food Chem. Toxicol.* , Volume 132, p. 110721.
- González-Pérez, J., González-Vila, F., Almendros, G. & Knicker, H., 2004. The effect of fire on soil organic matter—a review.. *Environ Int*, 30(6), p. 855–870.
- Gryglewicz, S. & Piechocki, W., 2011. Hydrodechlorination of dichlorobenzenes and their derivatives over Ni-Mo/C catalyst: kinetic analysis and effect of molecular structure of reactant.. *Chemosphere* , 83(3), p. 334–339.
- GSR-1, 2011. Green and sustainable remediation: state of the science and practice, Washington, DC, USA: ITRC—Interstate Technology & Regulatory Council.
- Gupta, G. K. & Mondal, M., 2019. Kinetics and thermodynamic analysis of maize cob pyrolysis for its bioenergy potential using thermogravimetric analyzer. *Journal of Thermal Analysis and Calorimetry*, Volume 137, pp. 1431-1441..
- Hartwig, A. & Jahnke, G., 2012. Toxic metals and metalloids in foods. In *Chemical contaminants and residues in food*. Woodhead Publishing, pp. 233-249.
- Hedayati, A., Golestan, Z., Ranjbar, K. & Borhani, G., 2011. Effect of ball milling on formation of ZnAl<sub>2</sub>O<sub>4</sub> by reduction reaction of ZnO and Al powder mixture. *Powder Metall. Met. Ceram.*, Volume 50, p. 268–274.
- He, Y. et al., 2014. Thermal desorption of mercury from contaminated soil with the addition of FeCl<sub>3</sub> as enhancement.. *Res Environ Sci*, 27(9), pp. 1074-1079.
- Holland, K., 2011. A framework for sustainable remediation. *Environ Sci Technol* , Volume 45, p. 7116–7117.
- Hou, D. et al., 2018. Climate change mitigation potential of contaminated land redevelopment: a city-level assessment method.. *J Clean Prod* , Volume 171, p. 1396–1406.
- Hou, N. et al., 2022. Fundamental functions of physical and chemical principles in the polishing of titanium alloys: mechanisms and problems.. *The International Journal of Advanced Manufacturing Technology*, Volume 118, p. 2079–2097.
- Huang, C. M., Yang, W. F., Ma, H. W. & Song, Y. R., 2006. The potential of recycling and reusing municipal solid waste incinerator ash in Taiwan. *Waste Management* , 26(9), pp. 979-987.
- Huang, Y., Hseu, Z. & His, H., 2011. Influences of thermal decontamination on mercury removal, soil properties, and repartitioning of coexisting heavy metals.. *Chemosphere*, Volume 84, pp. 1244-1249.

Hu, Y. et al., 2021. The fate of heavy metals and salts during the wet treatment of municipal solid waste incineration bottom ash. *Waste Management*, Volume 121, pp. 33-41.

IARC, I. A. f. R., 1997. Cancer working group on the evaluation of carcinogenic risks to humans: polychlorinated dibenzo-p-dioxins and polychlorinated dibenzofurans. *IARC Monogr. Eval. Carcinog. Risks Hum.*

Idowu, I. et al., 2019. An analyses of the status of landfill classification systems in developing countries: Sub Saharan Africa landfill experiences. *Waste Manag*, Volume 87, p. 761–771.

Il'in, A. P., Gromov, A. A. & Yablunovskii, G. V., 2001. Reactivity of Aluminium Powders. *Combustion, Explosion, and Shock Waves*, 37(4), pp. 418-422.

Il'in, A. P. et al., 1999. Combustion of mixtures of ultrafine powders of aluminium and boron in air.. *Combust Explos Shock Waves*, Volume 35, p. 656–659.

Italian Institute for Environmental Protection and, 2018. *Rapporto rifiuti urbani – edizione 2018 [Municipal Waste Report – Edition 2018]*. ISPRA.

Jackson, R. et al., 2017. Warning signs for stabilizing global CO<sub>2</sub> emissions.. *Environ Res Lett*, Volume 12, p. 110202.

Jan, A. et al., 2015. Heavy metals and human health: mechanistic insight into toxicity and counter defense system of antioxidants. *Int. J. Mol. Sci.*, Volume 16, p. 29592–29630.

Jeurgens, L., Sloof, W., Tichelaar, F. & Mittemeijer, E., 2000. Thermodynamic stability of amorphous oxide films on metals: Application to aluminum oxide films on aluminum substrates. *Phys. Rev. B* , Volume 62, p. 4707–4719.

Jeurgens, L., Sloof, W., Tichelaar, F. & Mittemeijer, E., 2002. Growth kinetics and mechanisms of aluminum-oxide films formed by thermal oxidation of aluminum. *J. Appl. Phys.*, Volume 92, p. 1649–1656.

Jeurgens, L., Sloof, W., Tichelaar, F. & Mittemeijer, E., 2002. Structure and morphology of aluminium-oxide films formed by thermal oxidation of aluminium. *Thin Solid Film*, Volume 418, p. 89–101.

Jiang, D. Z. G. et al., 2018. Remediation of contaminated soils by enhanced nanoscale zero valent iron.. *Environ Res* , Volume 163, p. 217–227.

Jiang, Y. et al., 2009.. Occurrence, distribution and possible sources of organochlorine pesticides in agricultural soil of Shanghai, China. *J. Hazard Mater* , Volume 170, pp. 989-997.

Jin, X. et al., 2020. Effect of Heating Rate on Ignition Characteristics of Newly Prepared and Aged Aluminum Nanoparticles. *Propellants Explos. Pyrotech.*, Volume 45, p. 1428–1435.

Joshi, N., Mathur, N., Mane, T. & Sundaram, D., 2018. Size effect on melting temperatures of alumina nanocrystals: Molecular dynamics simulations and thermodynamic modeling. *Comput. Mater. Sci.* , Volume 145, p. 140–153.

JRC, 2008. Scientific and technical report; end of waste criteria, s.l.: s.n.

JRC, 2009. Final Report; End of Waste Criteria, s.l.: s.n.

- JRC, 2010. Scientific and technical report; End-of-waste Criteria for Aluminium and Aluminium Alloy Scrap, s.l.: s.n.
- Karimzadeh, F., Enayati, M. & Tavoosi, M., 2008. Synthesis and characterization of Zn/Al<sub>2</sub>O<sub>3</sub> nanocomposite by mechanical alloying,. *Mater. Sci. Eng.* , Volume 486, p. 45–48.
- Karlsson, P., Baeza, A., Palmqvist, A. & Holmberg, K., 2008. Surfactant inhibition of aluminium pigments for waterborne printing inks. *Corros. Sci.*, Volume 50, p. 2282–2287. .
- Keown, D., 2016. Aluminium metal combustible dust explosion from improper design, construction and use of dust collection system sends two employees by life flight to burn centers.. *J. Occup. Environ. Hyg.*, 13(9), p. D135–D137.
- Ketterings, Q., Bigham, J. & Laperche, V., 2000. Changes in soil mineralogy and texture caused by slash-and-burn fires in Sumatra, Indonesia.. *Soil Sci Soc Am J*, Volume 64, pp. 1108-1117.
- Keyes B, S. G. (., 1994. Fundamental study of the thermal desorption of toluene from montmorillonite clay particles.. *Environ Sci Technol*, 28(5), p. 840–849.
- Kiersch, K., Kruse, J., Regier, T. & Leinweber, P., 2012. Temperature resolved alteration of soil organic matter composition during laboratory heating as revealed by C and N XANES spectroscopy and Py-FIMS.. *Thermochim Acta*, Volume 537, pp. 36-43.
- Kleinhans, U., Wieland, C., Frandsen, F. J. & Spliethoff, H., 2018. Ash formation and deposition in coal and biomass fired combustion systems: Progress and challenges in the field of ash particle sticking and rebound behavior. *Progress in energy and combustion science*, Volume 68, pp. 65-168.
- Kristanti, R. et al., 2022. A review on thermal desorption treatment for soil contamination.. *Tropical Aquat Soil Pollut* , 2(1), p. 45–58.
- Kumar, A. et al., 2015. Direct air capture of CO<sub>2</sub> by physisorbent materials. *Angew. Chem. Int. Ed.* , Volume 54, p. 14372–14377. .
- Kwon, Y. et al., 2004. Estimation of the reactivity of aluminium superfine powders for energetic applications. *Combust. Sci. Technol*, Volume 176, p. 277–288..
- Lam, C. H., Ip, A. W., Barford, J. P. & McKay, G., 2010. Use of incineration MSW ash: a review.. *Sustainability*, 2(7), pp. 1943-1968.
- Lansdown, A., 2014. *The Carcinogenicity of Metals: Human Risk through Occupational and Environmental Exposure*. RSC Publishing, Issue Issues in Toxicology.
- Leckner, B., 2015. Waste Management. Process aspects in combustion and gasification Waste-toEnergy (WtE) units, Volume 37, p. 13–25.
- Lee, J. et al., 1998. Remediation of petroleum contaminated soils by fluidized thermal desorption.. *Waste Manag*, 18(6-8), pp. 503-507.
- Lee, W., Rhee, T., Kim, H. & Jang, H., 2013. Effects of Antimony Trisulfide (Sb<sub>2</sub>S<sub>3</sub>) on sliding friction of automotive brake friction materials. *Met. Mater. Int.*, Volume 19, p. 1101.

- Lembo, F. et al., 2001. Aluminium airborne particles explosions: risk assessment and management at Northern Italian factories. Torino, Italy,, s.n.
- Liang, D., Xiao, R., Liu, J. & Wang, Y., 2019. Ignition and heterogeneous combustion of aluminum boride and boron–aluminum blend. *Aerosp. Sci. Technol.*, Volume 84, p. 1081–1091.
- Liang, L., Guo, X., Liao, X. & Chang, Z., 2020. Improve the interfacial adhesion, corrosion resistance and combustion properties of aluminum powder by modification of nickel and dopamine. *Appl. Surf. Sci.* , Volume 508, p. 144790.
- Liang, T. et al., 2023. Life cycle assessment-based decision-making for thermal remediation of contaminated soil in a regional perspective.. *J Clean Prod*, Volume 392, p. 136260.
- Li, C., LoK, C. & Su, W. L. T., 2015. A study on soil and groundwater pollution remediation of the surrounding real estate prices and tax revenue impact.. *Sustainability*, 7(11), pp. 14618-14630.
- Lighty, J., 1988. Fundamentals of thermal treatment for the cleanup of contaminated solid wastes.. Ph.D Dissertation, University of Utah.
- Lighty, J. et al., 1989. Fundamental experiments on thermal desorption of contaminants from soils. *Environ Prog*, 8(1), p. 57–61.
- Lim, M., Von Lau, E. & Poh, P., 2016. A comprehensive guide of remediation technologies for oil contaminated soil e present works and future directions. *Mar. Pollut. Bull.* , Volume 109, pp. 14-45.
- Li, Q. et al., 2016. Explosion severity of micro-sized aluminum dust and its flame propagation properties in 20 L spherical vessel.. *Powde Technol*, Volume 301, p. 1299–1308.
- Li, R. et al., 2011. Influence factor of hydrogen generation from aluminium-water reaction.. *IEEE* , pp. 852-5.
- Liu, J. et al., 2014. Thermal desorption of PCBs from contaminated soil using nano zerovalent iron.. *Environ Sci Pollut Res*, Volume 21, p. 12739–12746. .
- Liu, J. et al., 2015b. Effect of oxygen content on the thermal desorption of polychlorinated biphenyl-contaminated soil.. *Environ Sci Pollut Res* , Volume 22, p. 12289–12297.
- Liu, J. et al., 2015a. Thermal desorption of PCB-contaminated soil with sodium hydroxide.. *Environ Sci Pollut Res* , Volume 22, p. 19538–19545.
- Liu, J. et al., 2019. Thermal desorption of PCBs contaminated soil with calcium hydroxide in a rotary kiln. *Chemosphere*, Volume 220, pp. 1041-1046.
- Liu, X. et al., 2022. Solar-driven soil remediation along with the generation of water vapor and electricity.. *Nanomaterials*, Volume 12, p. 1800..
- Lobmann, M. et al., 2016. The occurrence of pathogen suppressive soils in Sweden in relation to soil biota, soil properties, and farming practices.. *Appl Soil Ecol*, Volume 107, pp. 57-65.

- Lucheva, B., Tsonev, T. & Petkov, R., 2005. Non-waste aluminium dross recycling.. *J. Univ. Chem. Technol. Metall.*, 40(4), p. 335–338..
- Lü, H. et al., 2018. Soil contamination and sources of phthalates and its health risk in China: a review.. *Environ Res*, Volume 164, p. 417–429..
- Maalouf, A., Mavropoulos, A. & El-Fadel, M., 2020. Global municipal solid waste infrastructure: Delivery and forecast of uncontrolled disposal.. *Waste Management & Research*, Volume 38, p. 1028–1036..
- Ma, F. et al., 2015. Citric acid facilitated thermal treatment: an innovative method for the remediation of mercury contaminated soil. *J Hazard Mater*, Volume 300, pp. 546-552.
- Ma, F. et al., 2014. Mercury removal from contaminated soil by thermal treatment with FeCl<sub>3</sub> at reduced temperature.. *Chemosphere*, Volume 117, pp. 388-393.
- Maggi, F., Gariani, G., Galfetti, L. & DeLuca, L., 2012. Theoretical analysis of hydrides in solid and hybrid rocket propulsion.. *Int. J. Hydrog. Energy*, Volume 37, p. 1760–1769.
- Maleki, A., Hosseini, N. & Niroumand, B., 2018. A review on aluminothermic reaction of Al/ZnO system.. *Ceramics International*, 44(1), pp. 10-23.
- Maleki, A., Panjepour, M., Niroumand, B. & Meratian, M., 2010. Mechanism of zinc oxide aluminium aluminothermic reaction. *J. Mater. Sci.*, Volume 45, p. 5574–5580.
- Marani, D., Braguglia, C., Mininni, G. & Maccioni, F., 2003. Behaviour of Cd, Cr, Mn, Ni, Pb, and Zn in sewage sludge incineration by fluidised bed furnace.. *Waste Manag* , Volume 23, pp. 117-124..
- Marmo, L., Cavallero, D. & Debernardi, M., 2004. Aluminium dust explosion risk analysis in metal workings.. *J. Loss Prev. Process Ind.*, Volume 17, p. 449–465. .
- Marmo, L., Piccinini, N. & Danzi, E., 2015. Small magnitude explosion of aluminium powder in an abatement plant: a telling case.. *Process Safety. Environ. Prot.* , Volume 98, p. 221–230. .
- Marmo, L. R. D. D. E. 2., 2017. Explosibility of metallic waste dusts.. *Process Safety and Environmental Protection*, Volume 107, p. 69–80. .
- Martinez, A. M. & Echeberria, J., 2016. Towards a better understanding of the reaction between metal powders and the solid lubricant Sb<sub>2</sub>S<sub>3</sub> in a low-metallic brake pad at high temperature.. *Wear*, Volume 348-349, p. 27–42.
- Mataix-Solera, J. et al., 2009. Forest fire effects on soil microbiology. In: Cerdà A, Robichaud P (eds) *Fire effects on soils and restoration strategies*.. p. 133–175.
- Ma, W. et al., 2018. Contamination source apportionment and health risk assessment of heavy metals in soil around municipal solid waste incinerator: a case study in North China.. *Sci. Total Environ.* , p. 631–63.
- McAlexander, B., Krembs, F. & Mendoza, M., 2014. Treatability testing for weathered hydrocarbons in soils: bioremediation, soil washing, chemical oxidation, and thermal desorption.. *Soil Sediment Contam*, Volume 24, pp. 882-897.

- Menon, A., Chang, J. & Kim, J., 2016. Mechanisms of divalent metal toxicity in affective disorders.. *Toxicology*, Volume 339, p. 58–72.
- Merino, J. & Bucala, V., 2007. Effect of temperature on the release of hexadecane from soil by thermal treatment.. *J Hazard Mater*, 143(1), pp. 455-461.
- Mian, I. et al., 2019. Kinetic study of biomass pellet pyrolysis by using distributed activation energy model and coats redfern methods and their comparison. *Bioresour. Technol.*, Volume 294, p. 122099.
- Miao, N., Zhong, S. & Yu, Q., 2016. Ignition characteristics of metal dusts generated during machining operations in the presence of calcium carbonate.. *J. Loss Prev. Process Ind.* , Volume 40, p. 174–179. .
- Miškuřová, A., Štifner, T., Havlik, T. & Jančok, J., 2006. Recovery of valuable substances from aluminium dross.. *Acta Metall. Slovaca*, Volume 12, p. 303–312..
- Mondolfo, L., 1976. *Aluminium Alloys: Structure and Properties*. Butterworths and Co., Ltd., London, p. 806.
- Montuori, P. et al., 2014. Spatial distribution and partitioning of polychlorinated biphenyl and organochlorine pesticide in water and sediment from Sarno River and Estuary, Southern Italy.. *Environ. Sci. Pollut. R.*, Volume 21, pp. 5023-5035.
- Murena, F. & Schioppa, E., 2000. Kinetic analysis of catalytic hydrodechlorination process of polychlorinated biphenyls (PCBs). *Appl Catal B* , 27(4), p. 257–267.
- Nakamura, T., Senior, C., Burns, E. & Bell, M., 2000. Solar-powered soil vapor extraction for removal of dense nonaqueous phase organics from soil.. *J Environ Sci Health Part A*, Volume 35, pp. 795-816..
- Naso, B. et al., 2003. Persistent organochlorine pollutants in liver of birds of different trophic levels from coastal areas of Campania, Italy. *Arch. Environ. Con Tox*, Volume 45, pp. 407-414.
- Navarro, A. et al., 2009. Application of solar thermal desorption to remediation of mercury-contaminated soils. *Sol Energy*, Volume 83, pp. 1405-1414..
- Navarro, A., Canadas, I. & Rodríguez, J., 2014. Thermal treatment of mercury mine wastes using a rotary solar kiln.. *Minerals* , Volume 37, p. 51.
- Navarro, A., Cardellach, E., Canadas, I. & Rodríguez, J., 2013. Solar thermal vitrification of mining contaminated soils.. *Int J Miner Process*, Volume 119, pp. 65-74..
- Nellemann, C. et al., 2009. The environmental food crisis – the environment’s role in averting future food crises. In: *A UNEP rapid response assessment.. United Nations Environment Programme, GRID-Arendal*.
- Nguyen, T., Pham, Q., Nguyen, T. & al., e., 2023. Distribution characteristics and ecological risks of heavy metals in bottom ash, fly ash, and particulate matter released from municipal solid waste incinerators in northern Vietnam. *Environ Geochem Health*, Volume 45, pp. 2579-2590.

- Nie, H., Schoenitz, M. & Dreizin, E., 2012. Calorimetric investigation of the aluminium–water reaction. *Int. J. Hydrogen Energy*, Volume 37, p. 11035–11045. .
- Nithiya, A., Saffarzadeh, A. & Shimaoka, T., 2018. Waste Manag.. Hydrogen gas generation from metal aluminium-water interaction in municipal solid waste incineration (MSWI) bottom ash., Volume 73, pp. 342-350.
- Nordmark, D., Kumpiene, J., Andreas, L. & Lagerkvist, A., 2011. Mobility and fractionation of arsenic, chromium and copper in thermally treated soil.. *Waste Manag Res*, Volume 29, pp. 2-12.
- Ohkura, Y., Rao, P. & Zheng, X., 2011. Flash ignition of al nanoparticles: mechanism and applications. *Combust Flame*, Volume 158, pp. 2544-8.
- Okoh, M. P., 2015. Exposure to Organo-Chlorinated Compound, PolyChlorinated Biphenyl (PCB), environmental and public health Implications: A Nigeria Case study.. *Int. J. Chem. Stud*, Volume 2, pp. 14-21.
- Oppelt, E., 1987. Incineration of hazardous waste: a critical review.. *JAPCA*, 37(5), p. 558–586.
- Ornebjerg, H. et al., 2006. Management of Bottom Ash from WTEPlants. International Solid Waste Association.
- Ostad-Ali-Askari, K., 2022. Management of risks substances and sustainable development.. *Applied Water Science*, 12(4), p. 65.
- Ounas, A. et al., 2011. Pyrolysis of olive residue and sugar cane bagasse: non-isothermal thermogravimetric kinetic analysis.. *Bioresour. Technol.*, 102(24), p. 11234–11238..
- Pape, A., Switzer, C., McCosh, N. & Knapp, C., 2015. Impacts of thermal and smouldering remediation on plant growth and soil ecology.. *Geoderma*, Volume 243-244, pp. 1-9.
- Parimi, V. S., Huang, S. D. & Zheng, X. L., 2017. Enhancing ignition and combustion of micron-sized aluminium by adding porous silicon.. *Proc Combust Inst*, Volume 36, pp. 2317-24 .
- Parr, T. et al., 2003. Evaluation of advanced fuels for underwater propulsion. s.l., 39th JANNAF combustion subcommittee meeting. NASA Technical Reports Serve..
- Pathak, C. & Dodkar, P., 2020. Effect of shot blasting and shot peening parameters on residual stresses induced in connecting rod.. *Trans. Indian Inst. Met.*, 73(3), p. 571–576..
- Peng, Z. et al., 2020. Characterization of PCDD/Fs and heavy metal distribution from municipal solid waste incinerator fly ash sintering process.. *Waste Manag*, Volume 103, p. 260–267.
- Petrovic, J. & Thomas, G., 2008. Reaction of aluminum with water to produce hydrogen.. US Department of Energy, Volume 1, pp. 1-26..
- Pozo, K. et al., 2016. Assessing persistent organic pollutants (POPs) in the Sicily Island atmosphere, Mediterranean, using PUF disk passive air samplers. *Environ. Sci. Pollut. R.*, Volume 23, pp. 20796-20804.



- Qi, Z. et al., 2014. Effect of temperature and particle size on the thermal desorption of PCBs from contaminated soil.. *Environ Sci Pollut Res*, Volume 21, p. 4697–4704.
- Qi, Z. et al., 2014. Effect of temperature and particle size on the thermal desorption of PCBs from contaminated soil.. *Environmental science and pollution research*, Volume 21, pp. 4697-4704.
- Qu, C. et al., 2016. The status of organochlorine pesticide contamination in the soils of the Campanian Plain, southern Italy, and correlations with soil properties and cancer risk. *Environ. Pollut.*, Volume 216, pp. 500-511.
- Ramón, F. & Lull, C., 2019. Legal measures to prevent and manage soil contamination and to increase food safety for consumer health: The case of Spain.. *Environmental Pollution*, Volume 250, pp. 883-891.
- Rath, J. & Staudinger, G., 2001. Cracking reactions of tar from pyrolysis of spruce wood.. *Fuel*, 80(10), p. 1379–1389.
- Reinmann, J., Weber, R. & Haag, R., 2010. Long-term monitoring of PCDD/PCDF and other unintentionally produced POPs—concepts and case studies from Europe.. *Science China Chemistry*, Volume 1017-1024., p. 53.
- Ren, J., Song, X. & Ding, D., 2020. Sustainable remediation of diesel-contaminated soil by low temperature thermal treatment: improved energy efficiency and soil reusability.. *Chemosphere*, Volume 241, p. 124952.
- Resource Efficient and Cleaner Production, 2014. United Nations Environment Programme, Division of Technology, Industry, and Economics.
- Risoul, V., Renauld, V., Trouvé, G. & P., G., 2002. A laboratory pilot study of thermal decontamination of soils polluted by PCBs. Comparison with thermogravimetric analysis.. *Waste Manag*, 22(1), p. 61–72.
- Rodríguez-Eugenio, N., McLaughlin, M. & Pennock, D., 2018. Soil Pollution: a hidden reality. *FAO*, p. 142.
- Roh, Y. et al., 2000. Thermal treated soil for mercury removal: soil and phytotoxicity tests.. *J Environ Qual* , Volume 29, pp. 415-424.
- Rosenband, V. & Gany, A., 2007. Agglomeration and Ignition of aluminium Particles Coated by Nickel. *Advancement in Energetic Materials and Chemical Propulsion*., J. Rivera and K. K. Kuo, pp. 141-149..
- Rosenband, V. & Gany, A., 2010. Application of activated aluminium powder for generation of hydrogen from water.. *Int J Hydrogen Energy*, Volume 35, pp. 10898-904. .
- Rovira, J., Nadal, M., Schuhmacher, M. & Domingo, J., 2018. Concentrations of trace elements and PCDD/Fs around a municipal solid waste incinerator in Girona (Catalonia, Spain). *Sci. Total. Environ.*, Volume 630, pp. 34-45.
- Rozenband, V., Afanas'eva, L., Lebedeva, V. & Chernenko, E., 1990. Activation of ignition of aluminium and its mixtures with oxides by chromium chloride.. *Combust Explos Shock Waves*, Volume 26, pp. 13-5.

- Ruano, O., Wadsworth, J. & Sherby, O., 2003. Deformation of fine-grained alumina by grain boundary sliding accommodated by slip. *Acta Mater.*, Volume 51, p. 3617–3634.
- Rufino, B. et al., 2007. Influence of particles size on thermal properties of aluminium powder. *Acta Materialia*, Volume 55, p. 2815–2827.
- Sakaguchi, I. et al., 2014. Assessment of soil remediation technologies by comparing health risk reduction and potential impacts using unified index, disability-adjusted life years.. *Clean Technol Environ Policy*, 17(6), pp. 1663-1670.
- Saravanan, R. et al., 2001. Effects of nitrogen on the surface tension of pure aluminium at high temperatures.. *Scripta Materialia*, 44(6), pp. 965-97.
- Sato, T. et al., 2010. Behavior of PCDDs/PCDFs in remediation of PCBs-contaminated sediments by thermal desorption.. *Chemosphere* , 80(2), p. 184–189.
- Scarlat, N., Fahl, F. & Dallemand, J., 2019. Valorization Status and opportunities for energy recovery from municipal solid waste in Europe. *Waste and Biomass*, Volume 10, p. 2425–2444.
- Schulten, H. & P., L., 1999. Thermal stability and composition of mineral-bound organic matter in density fractions of soil.. *Eur J Soil Sci*, Volume 50, p. 545–547..
- Sheldon, R., 2014. Green and sustainable manufacture of chemicals from biomass: State of the art.. *Green Chem*, Volume 16, p. 950.
- Shimamura, K. et al., 2014. Hydrogen-on-demand using metallic alloy nanoparticles in water. *Nano Lett*, Volume 14, p. 4090–4096. .
- Shinzato, M. C. & Hypolito, R., 2005. Solid waste from aluminium recycling process: Characterization and reuse of its economically valuable constituents.. *Waste Manage. J.*, 25(1), p. 37–46. .
- Shi, W. et al., 2019. Potassium fluoride improving the ignition and combustion performance of micron-sized aluminium particles in high temperature water vapor. *Environ. Eff.*, Volume 1556-7036,, pp. 1556-72.
- Shi, W., Sun, Y., Zhu, B. & Liu, J., 2021. Sodium fluoroaluminate promoting the combustion of micron-sized aluminium powder with different particle sizes in carbon dioxide. *Energy* , Volume 226, p. 120393..
- Shi, W., Sun, Y., Zhu, B. & Liu, J., 2021. Sodium fluoroaluminate promoting the combustion of micron-sized aluminium powder with different particle sizes in carbon dioxide.. *Energy*, Volume 226, p. 120393.
- Shmelev, V., Nikolaev, V., Lee, J. H. & Yim, C., 2016. Hydrogen production by reaction of aluminium with water.. *Int J Hydrogen Energy*, Volume 41, pp. 16664-73. .
- Shoshin, Y. L., Mudryy, R. S. & Dreizin, E. L., 2002. Preparation and characterization of energetic Al-Mg mechanical alloy powders.. *Combustion and Flame*, 128(3), pp. 259-269.
- Sierra, M. et al., 2016. Sustainable remediation of mercury contaminated soils by thermal desorption.. *Environmental Science and Pollution Research*, Volume 23, pp. 4898-4907.

- Simon, J., 2020. Best management practices for sustainable remediation.. In: Hou D (ed) Sustainable Remediation of Contaminated Soil and Groundwater. Butterworth-Heinemann, p. 75–91.
- Sodhi, G. S. & Kaur, J., 2001. Powder method for detecting latent fingerprints: a review.. *Forensic science international*, 120(3), pp. 172-176..
- Song, F. et al., 2019. Spectroscopic analyse combined with Gaussian and coats-redfern models to investigate the characteristics and pyrolysis kinetics of sugarcane residue-derived biochars. *J. Clean. Prod.*, Volume 237, pp. 117855.1-117855.11.
- Spadaro, J. & Rabl, A., 2004. Pathway analysis for population-total health impacts of toxic metal emissions.. *Risk Anal* , Volume 24, p. 1121–1141.
- Stark, T. et al., 2012. Aluminium waste reaction Indicators in a municipal solid waste landfill.. *J Geotech Geoenviron.* , 138(3), pp. 252-261. .
- Stark, T. et al., 2012. Aluminium waste reaction Indicators in a municipal solid waste landfill.. *J Geotech Geoenviron.* , 138(3), p. 252 261..
- Stegemeier, G. & Vinegar, H., 2001. Thermal conduction heating for insitu thermal desorption of soils. In: Oh CH (ed) Hazardous and radioactive waste treatment technologies handbook. s.l.:CRC Press, Boca Raton.
- Stockholm Convention, 2001. Stockholm Convention on persistent.
- Sun, Y. et al., 2022. Redevelopment of urban brownfield sites in China: Motivation, history, policies and improved management.. *Eco-Environment & Health*, 1(2), pp. 63-72.
- Sverak, T., Baker, C. & Kozdas, O., 2013. Efficiency of grinding stabilizers in cement clinker processing,. *Miner. Eng.* , Volume 43–44:, p. 52–57. .
- Tabasová, A., Kropáč, J., Kermes, V. & al., e., 2012. Waste-to-energy technologies: Impact on environment. *Energy*, Volume 44, p. 146–155.
- Tang, P., Florea, M. V. A., Spiesz, P. R. & Brouwers, H. J. H., 2014. The application of treated bottom ash in mortar as cement replacement. s.l., EurAsia Waste Management Symposium.
- Tang, Y. et al., 2017. Combustion of aluminum nanoparticle agglomerates: From mild oxidation to microexplosion. *Proc. Combust. Inst.*, Volume 36, p. 2325–2332.
- Tao, S. et al., 2008. Organochlorine pesticides contaminated surface soil As reemission source in the Haihe Plain. China. *Environ. Sci. Technol.*, Volume 42, pp. 8395-8400.
- Tatano, F., Felici, F. & Mangani, F., 2013. Lab-scale treatability tests for the thermal desorption of hydrocarbon-contaminated soils.. *Soil Sediment Contam*, Volume 22, pp. 433-456.
- Tavoosi, M., Karimzadeh, F. & Enayati, M., 2008. Fabrication of Al–Zn/ $\alpha$ -Al<sub>2</sub>O<sub>3</sub> nanocomposite by mechanical alloying. *Mater. Lett.* , Volume 62, p. 282–285.

- Terefe, T., Mariscal-Sancho, I., Peregrina, F. & Espejo, R., 2008. Influence of heating on various properties of six Mediterranean soils. A laboratory study.. *Geoderma* , Volume 143, pp. 273-280.
- Thekdi, A. & Nimbalkar, S., 2015. Industrial waste heat recovery potential applications. In: Available technologies and crosscutting R&D opportunities. Oak Ridge National Lab (ORNL), Oak Ridge..
- Trunov, M., Schoenitz, M. & Dreizin, E., 2005a. Ignition of aluminium powders under different experimental conditions.. *Propell Explos Pyrot.*, Volume 30, p. 36–43. .
- Trunov, M., Schoenitz, M. & Dreizin, E., 2006. Effect of polymorphic phase transformations in alumina layer on ignition of aluminium particles. *Combust. Theory Model.*, Volume 10, p. 603–623.
- Trunov, M., Schoenitz, M., Zhu, X. & Dreizin, E., 2005b. Effect of polymorphic phase transformations in Al<sub>2</sub>O<sub>3</sub> film on oxidation kinetics of aluminium powders.. *Combust Flame*, Volume 140, p. 310–18..
- Tsakiridis, P., Oustadakis, P. & Agatzini-Leonardou, S., 2013. Aluminium recovery during black dross hydrothermal treatment.. *J. Environ. Chem. Eng.* , Volume 1, p. 23–32. .
- Tsao, L. et al., 2002. Effects of zinc additions on the microstructure and melting temperatures of Al-Si-Cu filler metals.. *Materials Characterization*, Volume 48, pp. 341-346.
- U.S. EPA, 2002. Hazardous Waste Management System; Definition of Solid Waste; Toxicity Characteristic. Final Rule. *Fed Regist.*, Volume 67 FR 11251, p. 11251–11254.
- UNEP, 2006. About the difficulties of classifying waste.
- United Nations Environment Programme , 2019. Waste-to-Energy: Considerations for Informed Decision-Making. United Nations Environment Programme, p. 58.
- UN—United Nations;, 2015. Transforming our world: The 2030 agenda for sustainable development.. In A/RES/70/1 Resolution Adopted by the General Assembly on 25 September; UN General Assembly, p. 1–41.
- Uzgiris, E. E. E. W. A. P. H. R. & I. I. T. (., 1995. Complex thermal desorption of PCBs from soil.. *Chemosphere*, 30(2), pp. 377-387..
- Vaccari, M., Collivignarelli, M. & Canato, M., 2012. Reuse of hydrocarbon-contaminated sludge from soil washing process: issues and perspectives.. *Chem Eng Trans* , Volume 28, p. 169–174.
- Van den Berg, M., Birnbaum, L., Bosveld, A. & al, e., 1998. Toxic equivalency factors (TEFs) for PCBs, PCDDs, PCDFs for humans and wildlife. *Environ. Health Perspect*, Volume 106, p. 775–792.
- Van den Berg, M., Birnbaum, L., Denison, M. & al, e., 2006. The 2005 World Health Organization reevaluation of human and Mammalian toxic equivalency factors for dioxins and dioxin-like compounds. *Toxicol. Sci.* , Volume 93, p. 223–241.

- Van der Voort, M. et al., 2016. Impact of soil heat on reassembly of bacterial communities in the rhizosphere microbiome and plant disease suppression.. *Ecol Lett* , Volume 19, pp. 375-382.
- Vandecasteele, C., Billen, P. & Block, C., 2014. How to chose between recycling, incineration and landfilling and LCA perspective. In: *Energy and Materials from Waste..* Amsterdam, s.n., pp. 22-23.
- Vehlow, J., 2015. Air pollution control systems in WtE units: an overview.. *Waste Manag.*, Volume 37, p. 58–74.
- Vidonish, J. et al., 2016a. Pyrolytic treatment and fertility enhancement of soils contaminated with heavy hydrocarbons.. *Environ Sci Technol*, Volume 50, pp. 2498-2506.
- Vidonish, J. et al., 2016b. Thermal treatment of hydrocarbon-impacted soils: a review of technology innovation for sustainable remediation.. *Engineering*, Volume 2, p. 426–437.
- Vilavert, L., Nadal, M., Schuhmacher, M. & Domingo, J., 2015. Two decades of environmental surveillance in the vicinity of a waste incinerator: human health risks associated with metals and PCDD/Fs. *Arch. Environ. Contam. Toxicol.* , Volume 69, p. 241–253.
- Wakefield, M. e. a., 2014. Time series analysis of the impact of tobacco control policies on smoking prevalence among australian adults, 2001–2011. *Bull. World Health Organ*, 92(6), p. 413–422.
- Wang, J., Zhan, X., Zhou, L. & Lin, Y., 2010. Biological indicators capable of assessing thermal treatment efficiency of hydrocarbon mixturecontaminated soil.. *Chemosphere*, Volume 80, pp. 837-844.
- Wang, L., Gao, H., Wang, M. & Xue, J., 2022a. Remediation of petroleum contaminated soil by ball milling and reuse as heavy metal adsorbent. *J Hazard Mater*, Volume 424, p. 127305.
- Wang, Q. et al., 2022b. Thermally enhanced bioremediation: a review of the fundamentals and applications in soil and groundwater remediation.. *J Hazard Mater* , Volume 433, p. 128749..
- Wan, X., . Lei, M., Yang, J. & Chen, T., 2020. Three-year field experiment on the risk reduction, environmental merit, and cost assessment of four in situ remediation technologies for metal(loid)-contaminated agricultural soil.. *Environ Pollut.*, 266(3), p. 115193.
- Weishi, L. et al., 2021. Evaluation of low-medium temperature pretreatment on the removal efficiency of organic toxic pollutants from pesticide waste salts: characteristics, regularity, and key factors. *Journal of Cleaner Production* , Volume 316, p. 128118.
- Weiss, G. & Carver, P., 2018. Role of divalent metals in infectious disease susceptibility and outcome.. *Clin. Microbiol. Infect.* , Volume 24, p. 16–23.
- Wuana, R. A. & Okieimen, F. E., 2011. Heavy metals in contaminated soils: a review of sources, chemistry, risks and best available strategies for remediation. *International Scholarly Research Notices*.

- Wu, B. et al., 2019. Fast reaction of aluminum nanoparticles promoted by oxide shell. *J. Appl. Phys.*, Volume 126, p. 144305..
- Wu, P. et al., 2022. Boosting extraction of Pb in contaminated soil via interfacial solar evaporation of multifunctional sponge.. *Green Energy Environ.*, 8(5), pp. 1459-1468..
- Xiao, F., Li, J., Zhou, X. & Yang, R., 2018. Preparation of mechanically activated aluminium rich Al-Co<sub>3</sub>O<sub>4</sub> powders and their thermal properties and reactivity with water steam at high temperature.. *Combust Sci Technol*, Volume 190, pp. 1-15.
- Yagodnikov, D. A., Andreev, E. A., Vorob'ev, V. S. & Glotov, O., 2006. Ignition, combustion, and agglomeration of encapsulated aluminium particles in a composite solid propellant. I. Theoretical study of the ignition and combustion of aluminium with fluorine-containing coatings. *Combust Explos Shock Waves*, Volume 42, pp. 534-42.
- Yan, J. et al., 2009. Analysis of volatile species kinetics during typical medical waste materials pyrolysis using a distributed activation energy model. *J. Hazard Mater.*, 162 (2–3), p. 646–651.
- Yasutaka, T. et al., 2016. Development of a green remediation tool in Japan.. *Sci Total Environ*, Volume 563, p. 813.
- Yi, Y. et al., 2016. Changes in ecological properties of petroleum oil-contaminated soil after lowtemperature thermal desorption treatment.. *Water Air Soil Pollut*, Volume 227, p. 108..
- Yoshimura, H. et al., 2008. Evaluation of aluminium dross waste as raw material for refractories.. *Ceram. Int.*, Volume 34, p. 581–591..
- Yuan, S., Tian, M. & Lu, X., 2006. Microwave remediation of soil contaminated with hexachlorobenzene.. *J Hazard Mater*, 137(2), pp. 878-885.
- Yu, H. et al., 2013. Assessment of organochlorine pesticide contamination in relation to soil properties in the Pearl River Delta, China.. *Sci. Total Environ.* , Volume 447, p. 160e168.
- Zabaleta, I. et al., 2018. Biodegradation and uptake of the pesticide sulfluramid in a soil-carrot mesocosm.. *Environ Sci Technol*, 52(5), p. 2603–2611.
- Zhang, A. et al., 2012. Residues of currently and never used organochlorine pesticides in agricultural soils from Zhejiang province, China.. *J. Agr Food Chem*, Volume 60, pp. 2982-2988.
- Zhang, A. et al., 2011. Spatial distribution of hexachlorocyclohexanes in agricultural soils in Zhejiang province, China, and correlations with elevation and temperature. *Environ. Sci. Technol.*, Volume 45, pp. 6303-6308.
- Zhang, Y., Liu, Y. & Zhai, K., 2021. Identifying the Predictors of Community Acceptance of Waste Incineration Plants in Urban China: A Qualitative Analysis from a Public Perspective. *International Journal of Environmental Research and Public Health*, 18(19), p. 10189.
- Zhao, L. et al., 2012. Formation pathways of polychlorinated dibenzofurans (PCDFs) in sediments contaminated with PCBs during the thermal desorption process.. *Chemosphere*, Volume 88, pp. 1368-1374.

Zhao, Z. et al., 2017. PCDD/F formation during thermal desorption of p, p'-DDT contaminated soil.. *Environmental Science and Pollution Research*, Volume 24, pp. 13659-13665..

Zhou, X. et al., 2017. Effect of organic fluoride on combustion agglomerates of aluminized HTPB solid propellant.. *Propellants, Explos Pyrotech*, Volume 42, pp. 417-422.

Zhu, B. et al., 2019. Enhancing ignition and combustion characteristics of micron-sized aluminium powder in steam by adding sodium fluoride.. *Combustion and Flame*, Volume 205, pp. 68-79. .

Zhu, B. et al., 2022. Promotional effect of silica on the combustion of nano-sized aluminium powder in carbon dioxide.. *Chinese Journal of Aeronautics*, 35(4), pp. 245-252.